EARTH OBSERVING SYSTEM
Volume IIb

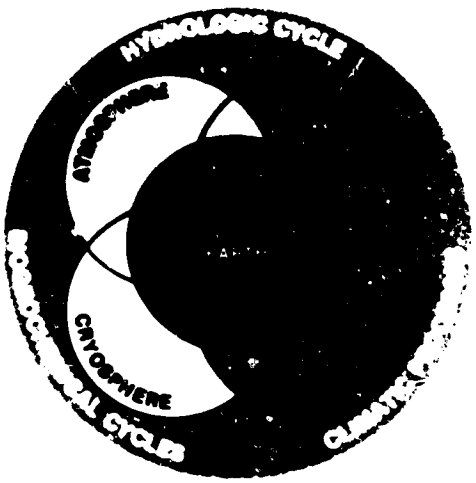

INSTRUMENT PANEL REPORT

National Aeronautics and
Space Administration

1986

EARTH OBSERVING SYSTEM REPORTS

Volume I	Science and Mission Requirements Working Group Report
Volume II	From Pattern to Process: The Strategy of the Earth Observing System Science Steering Committee Report
Volume IIa	Data and Information System Data Panel Report
Volume IIb	MODIS Moderate-Resolution Imaging Spectrometer Instrument Panel Report
Volume IIc	HIRIS & SISEX High-Resolution Imaging Spectrometry: Science Opportunities for the 1990s Instrument Panel Report
Volume IId	LASA Lidar Atmospheric Sounder and Altimeter Instrument Panel Report
Volume IIe	HMMR High-Resolution Multifrequency Microwave Radiometer Instrument Panel Report
Volume IIf	SAR Synthetic Aperture Radar Instrument Panel Report
Volume IIg	LAWS Laser Atmospheric Wind Sounder Instrument Panel Report
Volume IIh	Altimetric System Panel Report

MODERATE-RESOLUTION IMAGING SPECTROMETER INSTRUMENT PANEL FOR THE EARTH OBSERVING SYSTEM

Wayne Esaias, Chairman
William Barnes, Executive Secretary
Mark Abbott
Steve Cox
Robert Evans
Robert Fraser
Alexander Goetz
Christopher Justice
E. Paul McClain
Marvin Maxwell
Robert Murphy
Joseph Prospero
Barrett Rock
Steven Running
Raymond Smith
Jerry Solomon
Joel Susskind

Howard Gordon, Ex-officio Member
Michael Spanner, Ex-officio Member

COVER PHOTOGRAPH:

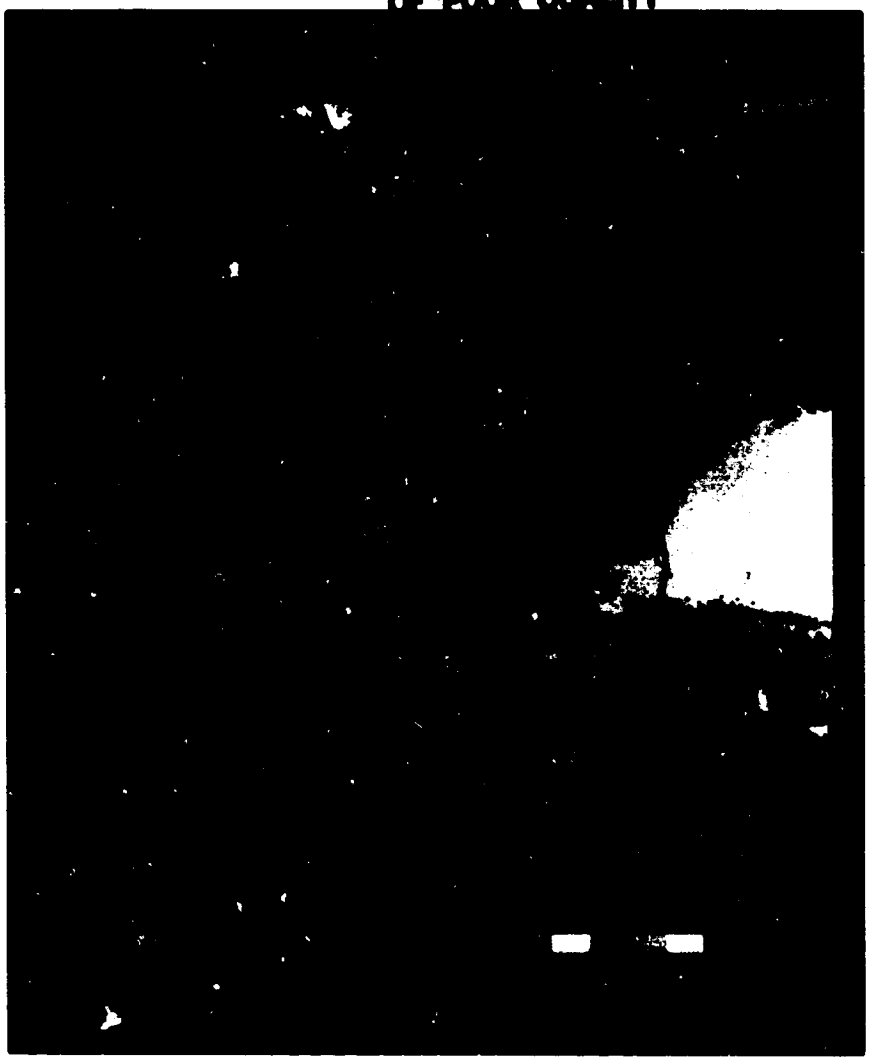

The figure above and on the cover shows the average plant abundance and distribution for a fifth of the Earth's surface in May. Different scales are used for land and water. For land areas, the Vegetation Index is derived from the NOAA-6 Advanced Very High Resolution Radiometer (AVHRR) for May 1982 (dark green is the highest density of green vegetation – right color bar). For oceans and lakes the amount of phytoplankton in terms of chlorophyll pigment density (red is highest – left color bar) is derived from the Coastal Zone Color Scanner (CZCS) on NASA's Nimbus-7 for May 1979.

The Sahara Desert, tropical rainforests, and spring greening of temperate forests and fields are evident on land. The corn and wheat belt south of the Great Lakes is less green because crops are just beginning to grow. In the oceans, productive upwelling areas along the coast (especially off N.W. Africa) and the "spring bloom" in the North Sea and northern North Atlantic are very evident. CZCS data do not distinguish between high sediment and pigments, and values in coastal and lake waters can be ambiguous.

This composite includes all daylight data collected by the two sensors during the periods in this region (10°S to 80°N, and 10°E to 100°W). For the land, this is but a part of a multiyear global data set. For the oceans, this is the first view of biological activity on a basin scale. Black areas in the ocean indicate no observations, white indicates that clouds or sea ice was present during every observation. Striping also indicates undersampling of oceanic variability with the limited duty CZCS.

This image illustrates current sensor capability, and the need for MODIS. The AVHRR is a weather sensor not optimized for vegetation sensing, and the CZCS collected limited data as a proof-of-concept mission. MODIS will provide comprehensive and simultaneous observations of variable land, ocean, and atmosphere properties on a global basis. Better spectral resolution and temporal coverage will provide less ambiguous and more accurate data on variations of plant abundance, and many additional properties essential for understanding and quantifying global change.

G. Feldman and C. Tucker, GSFC

EXECUTIVE SUMMARY

Over the last few years there has developed within the scientific community the conviction that the Earth must be treated as a single interacting ecosystem if major advances in our knowledge of the Earth and of man's impact are to be achieved. This has resulted in numerous integrated research programs having as a common theme the need for long-term global data bases to establish the Earth's present state and to delineate trends. These data bases are vital for the initialization and testing of a variety of models currently under development. The natural variations are such that the Earth's surface must be viewed every few days in order that dynamic events can be observed, and a minimum 10-year data base is required if we are to separate long-term trends from short-term natural variations.

In the spring of 1983 the Earth Observing System (Eos) Science and Mission Requirements Working Group was formed by NASA (National Aeronautics and Space Administration) with representatives from the various disciplines of Earth science to define critical questions for the 1990s and to delineate low Earth orbit observables that would materially address these questions. Eos has since become the anticipated payload(s) for the Space Station polar platforms. The results of this group's deliberations included requirements for a multispectral radiometer capable of frequent global surveys at a 1 kilometer spatial resolution for terrestrial, oceanic, and atmospheric properties. This system was designated the Moderate-Resolution Imaging Spectrometer (MODIS). The MODIS Instrument Panel was formed in mid-1984 to further define the scientific requirements and generate a set of sensor parameters that would ensure achievement of the scientific goals. The Panel was composed of representatives from the land, ocean, and atmospheric scientific communities, including representatives from NOAA (National Oceanic and Atmospheric Administration) and NASA. This document is a compilation of the recommendations of the MODIS Instrument Panel.

Terrestrial studies amenable to being addressed via low-resolution imaging radiometry include rate of tropical deforestation and type and rate of regrowth; areal distribution and effect of acid rain on the boreal forests of Europe and North America; rate and extent of desertification at the edge of the world's deserts; update of global vegetation maps; extent of freeze or drought damage in croplands and natural communities; land cover change and its effect on terrestrial biophysical systems; continental changes in snow cover with associated changes in albedo; and derived products including standing green biomass, intercepted photosynthetically active radiation, and net primary productivity. Computer simulation models that will depend on data from a sensor of this type include global surface climate models, carbon cycle models, hydrologic cycle/energy models, and comprehensive biogeochemical cycling models.

Oceanographers will utilize MODIS-visible data to characterize the global distribution of phytoplankton biomass and its temporal and spatial variability. Using *in situ* data together with regional scale models, it is possible to convert biomass to primary productivity. Thus oceanic and global measurements of primary productivity and their temporal variation will be possible. Thermal infrared (TIR) data will be used to study variability in sea surface temperature (SST) as related to physical processes on the climatological and physical dynamic scales. In addition, mesoscale ocean circulation features, such as warm and cold core rings and jets, can be observed and their development followed for months or years using ocean color and thermal infrared data. The effects of riverine fluxes and other forms of sediment transport can be observed and quantified, demonstrating their importance to ocean productivity and global biogeochemical cycles. Important phytoplankton subgroups, such as cyanobacteria and coccolithophores, will be identifiable.

Atmospheric constituents that will be monitored directly by MODIS include global distributions of clouds and aerosols, both of which have a direct impact on climate as well as on the geochemical and hydrological cycles.

Sensor requirements generated by the terrestrial studies subgroup include a spatial resolution of 500 meters based on a need for adequate discrimination of agricultural and forestry features, experience with National Oceanic and Atmospheric Administration/Advanced Very High Resolution Radiometer (NOAA/AVHRR) 1 kilometer data, and practical data volumes. Required spectral channels are essentially the same as those for Thematic Mapper with the possible addition of one or more channels in both the near infrared and shortwave infrared. Since thermal data is potentially quite useful in studies of soil moisture and evapotranspiration, a total of seven bands in the 3.5 to 4.0 and 8.5 to 12.0 micrometer window regions is also recommended. There is also a requirement for viewing fore and aft of nadir at several angles up to 60° in order to study the bidirectional reflectance distribution function (BRDF) of plant canopies. It was determined that an equatorial crossing time between 1:00 and 2:00 p.m. was acceptable and that a revisit time of two or three days was sufficient to measure vegetation dynamics.

Requirements generated by the oceanographer members of the MODIS Panel are based on experience with the Nimbus-7 Coastal Zone Color

Scanner (CZCS) and NOAA/AVHRR data. This has resulted in a need for at least 17 spectral bands in the wavelength region from 0.4 to 1.0 micrometer with the visible bands having bandwidths less than 20 nanometers and signal-to-noise in excess of 600:1. The near-infrared bandwidth and signal-to-noise requirements are less restrictive since those channels are principally used for aerosol corrections. The ocean color requirement having the greatest impact on the system is the requirement to point up to 20° fore or aft of nadir to avoid specular reflection (sunglint) from the ocean surface. Another ocean color requirement is the need for periodic solar-referenced calibrations. This is unique to oceans but will benefit all other disciplines. Additional ocean color requirements include one or more polarized channels in the visible to enhance atmospheric corrections; an equatorial crossing time as near noon as possible; spatial resolution of 1 kilometer in coastal regions with acceptable averaging to 4 kilometers in open oceans; minimal sensitivity to incoming polarized radiance at all viewing angles (with the exception of the polarized channels); a continuous, 10-year global data base; and two-day revisit.

Ocean thermal infrared requirements are aimed at obtaining SST retrievals accurate to within ± 0.5 K. This results in a need for "split" window channels in the 3.5 to 4.0 and 10.5 to 12.0 micrometer spectral regions.

Atmospheric science sensor requirements for MODIS are driven to a large extent by the terrestrial and oceanic requirements. The most demanding is a set of narrow spectral channels located in the oxygen A-band near 0.76 micrometer to measure cloud altitude. Other channels required for atmospheric and ice observations are readily accommodated within the constraints established by the terrestrial and oceanic requirements.

The MODIS requirements for (a) a view of 20° to 60° fore and aft of nadir for ocean observations and land bidirectional reflectance studies, (b) uninterrupted long-term global ocean surveys, and (c) minimum atmospheric path radiance for routine terrestrial sensing (i.e., nadir view) are incompatible with a single sensor package. Therefore, it was proposed that the optical component of the MODIS system be divided into two packages to be designated MODIS-T (tilt) and MODIS-N (nadir); the former containing the visible and near-infrared channels requiring fore or aft of nadir viewing, and the latter containing those channels with no requirement for off-nadir pointing, including all of the infrared (IR) channels requiring cooled detectors. Conceptual systems for the two sensors are discussed below.

The MODIS-T component will address those requirements that call for viewing the surface at predetermined angles fore and aft the subsatellite point (nadir). These include: (a) minimizing the amount of specular reflectance from the surface, (b) examining the BRDF from large homogeneous targets, and (c) performing atmospheric studies by examining the spectral signal as a function of optical depth. The MODIS-T requirements can be satisfied by any of several types of imaging radiometers. A practical system in terms of size, complexity, available technology, and overall utility is that of the imaging spectrometer. The version discussed in this report includes a crosstrack scan motor, collecting optics, spectrometer, and a 64×64 element silicon detector array. The optical aperture is on the order of 5 centimeters. This results in a very compact system capable of $\pm 60°$ rotation about the optical axis to give the required fore-aft tilt. The 1,500 kilometer (90°) swath is scanned in 9.5 seconds, the time required for the subsatellite point to advance 64 kilometers. The image of the spectrometer slit on the surface consists of 64 pixels along-track with each pixel being dispersed within the sensor into 64 perfectly registered contiguous spectral bands of approximately 10 nanometers width covering the range from 400 to 1,000 nanometers.

The MODIS-N (nadir) component will address those scientific tasks that do not require off-nadir pointing. The requirements cover the spectral range from 0.4 to 12.0 micrometers and include a requirement for 500-meter resolution in 12 channels in the region from 0.4 to 2.5 micrometers. Spectral width requirements vary from 1.2 to 500 nanometers. These requirements result in a system with at least 35 spectral bands. Due to the range of spectral widths, a requirement to measure polarization, and cooling requirements, it is impractical to use the imaging spectrometer concept of MODIS-T. Instead, a more conventional imaging radiometer concept is considered. This system consists of a crosstrack scan mirror and collecting optics and a dichroic filter that divides the incoming energy onto a cryogenically cooled focal plane (18 channels, 1 to 12 micrometers) and an ambient temperature focal plane (18 channels, 0.4 to 1.0 micrometer). The focal planes each have 36 detector elements. The required optics aperture diameter is 40 centimeters.

Data from both optical components will be of interest to many, if not all, users and should be considered as a single data set. The data rates from the instrument are about 8.8 megabits per second during the daylight and 1.2 megabits per second during night. Some redundancy of channels in the 400 to 1,000 nanometer range will enable complete spatial coverage during fore-aft tilt operations, which is especially useful along coastal lines for both terrestrial and oceanic applications and will aid in the required intercalibration of the T and N components. Accurate ($< \pm 1$ percent relative to the solar spectrum) calibrations are essential, and several scenarios utilizing Shuttle servicing capabilities are envisioned to monitor changes in instrument spectral sensitivity over the mission life of more than ten years.

In summary, MODIS, as presently conceived, is a system of two imaging spectroradiometer components designed for the widest possible applicability to research tasks that require long-term (5 to 10 years), low-resolution (0.5 to 1.0 kilometer), global, multispectral (52 channels between 0.4 and 12.0 micrometers) data sets. The system described is preliminary and subject to scientific and technological review and modification, and it is anticipated that both will occur prior to selection of a final system configuration; however, the basic concept outlined above is likely to remain unchanged.

CONTENTS

LIST OF TABLES

LIST OF FIGURES

ACRONYMS AND ABBREVIATIONS

AIS	Airborne Imaging Spectrometer
AMSU	Advanced Microwave Sounding Unit
AMTS	Advanced Moisture and Temperature Sounder
AO	Announcement of Opportunity
AVHRR	Advanced Very High Resolution Radiometer
BPI	Bits Per Inch
BRDF	Bidirectional Reflectance Distribution Function
CCT	Computer Compatible Tapes
CWR	Clear Water Reflectance
CZCS	Coastal Zone Color Scanner
DMSP	Defense Meteorological Satellite Program
DOMSAT	Domestic Communications Satellite
DOM	Dissolved Organic Material
EBB	Equivalent Black Body
Eos	Earth Observing System
ERS-1	European Space Agency Remote Sensing Satellite-1
FOV	Field-of-View
GAC	Global Area Coverage
gC	Grams Carbon
GIMMS	Global Inventory, Monitoring, and Modeling Studies
GOES	Geostationary Operational Environmental Satellite
GOFS	Global Ocean Flux Study
GSFC	Goddard Space Flight Center
GVI	Global Vegetation Index
HIRIS	High-Resolution Imaging Spectrometer
HIRS-2	High-Resolution Infrared Radiometric Sounder Model-2
HMMR	High-Resolution Multifrequency Microwave Radiometer
IFOV	Instantaneous Field-of-View
IPAR	Intercepted Photosynthetically Active Radiation
IR	Infrared
ISLSCP	International Satellite Land Surface Climatology Project
JPL/PODS	Jet Propulsion Laboratory/Pilot Ocean Data System
LAC	Local Area Coverage
LAI	Leaf Area Index
LASA	Lidar Atmospheric Sounder and Altimeter
LED	Light Emitting Diode
LFMR	Low Frequency Microwave Radiometer
Mbs	Megabits Per Second
MIZ	Marginal Ice Zone
MLA	Multispectral Linear Array
MODIS	Moderate-Resolution Imaging Spectrometer
MODIS-N	MODIS Nadir

ACRONYMS AND ABBREVIATIONS (continued)

MODIS-T	MODIS Tilt
MOS/LOS	Marine Observation Satellite/Land Observation Satellite (Japan)
MSS	Multispectral Scanner
MSU	Microwave Sounding Unit
N	Nadir
NASA	National Aeronautics and Space Administration
NESDIS	National Environmental Satellite, Data and Information Service
nm	Nanometer = 10^{-9} meter
NOAA	National Oceanic and Atmospheric Administration
NOSS	National Oceanic Satellite System
NPP	Net Primary Productivity
NROSS	Navy Remote Ocean Sensing System
OCI	Ocean Color Imager
PBL	Planetary Boundary Layer
PEC	Particulate Elemental Carbon
RMS	Root Mean Square
ROS	Research Optical Sensor
SAR	Synthetic Aperture Radar
SISEX	Shuttle Imaging Spectrometer Experiment
`R	Scanning Multifrequency Microwave Radiometer
:WG	Science and Mission Requirements Working Group
S/N	Signal-to-Noise
SPOT	Systeme Probatoire d'Observation de la Terre
SSM/I	Special Sensor Microwave/Imager
SST	Sea Surface Temperature
SSU	Stratospheric Sounding Unit
STS	Space Transportation System
SW	Shortwave
T	Tilt
TCSM	Tropospheric Chemistry Systems Model
TIMS	Thermal Infrared Multispectral Scanner
TIR	Thermal Infrared
TIROS	TV Infrared Operational Satellite
TM	Thematic Mapper
TOGA	Tropical Oceans and Global Atmosphere
TOMS	Total Ozone Mapping Spectrometer
μm	Micrometer = 10^{-6} meter
VIS	Visible
VIS/NIR	Visible and Near Infrared
WCRP	World Climate Research Program
WOCE	World Ocean Circulation Experiment

I. INTRODUCTION

In the spring of 1983, the Earth Observing System (Eos) Science and Mission Requirements Working Group was formed by NASA with representatives from the various disciplines of Earth science to define major questions for the 1990s and to delineate low Earth orbit observables that would materially address these questions. Eos has since become the anticipated payload(s) for the polar platform portion of the Space Station. The results of this group's deliberations (Butler *et al.*, 1984) included requirements for a multispectral radiometer capable of frequent global surveys at a 1 km spatial resolution. This system was designated the Moderate-Resolution Imaging Spectrometer (MODIS). The MODIS Instrument Panel was formed in mid-1984 to further define the scientific goals and observational requirements and generate a set of sensor parameters that would ensure achievement of these scientific goals. The MODIS statement of work is given in Appendix C.

This document is a report of the findings of the MODIS Instrument Panel. It includes a set of scientific objectives; ocean, atmosphere, terrestrial, and snow and ice research tasks requiring MODIS data; and a set of sensor requirements for each of these disciplines. These requirements have been combined and a preliminary sensor system that addresses most of the requirements has been generated. Owing to the diversity of these requirements, it has been necessary to divide MODIS into two sensor packages, which have been designated MODIS-N (nadir) and MODIS-T (tilt), and to include within the former several channels having 500 m resolution. A description of the system, including calculated performance parameters, is given in Chapter IV.

It is assumed that the Eos payload will include the High-Resolution Imaging Spectrometer (HIRIS), which will consist of 192 spectral channels between 0.4 and 2.5 μm with 30 m resolution over a 48 km swath, and that HIRIS will be on the same platform as MODIS. A discussion of the synergism that will ensue from this scenario is given in Chapter VII.

Additional topics covered include mission operations requirements (Chapter V), ground system processing and archiving requirements (Chapter VI), MODIS/HIRIS unique opportunities for synergism (Chapter VII), and algorithms (Appendices A and B). Results from the Phase-A studies of MODIS-N and MODIS-T that were completed during the preparation of this document are not included.

II. MODIS OBJECTIVES

Eos MISSION OBJECTIVES

The primary objective of the MODIS instrument is to provide a comprehensive series of global observations of the Earth (land, oceans, and atmosphere) in the visible and infrared regions, at sufficient spatial resolution to permit complete global coverage within a few days. The word "comprehensive" has several implications. First, it refers to the spectral as well as the continuous temporal coverage required to resolve the major frequencies of observed variability ranging from the synoptic-scale storm event (three to five days) to the climatic-scale event (a month to a decade or longer). Second, it refers to the unified nature of the observations, which is necessary for multidisciplinary studies of land, ocean, and atmospheric processes and their interactions and exchanges. The observations, made with an optimized set of sensors, will be nearly simultaneous, and thus will eliminate many of the higher-frequency geophysical variabilities and biases that must be removed from observations taken at slightly different times of day (or even within a few days) prior to various scientific analyses. Many of these biases have sources and variabilities that are themselves the subject of investigation as factors affecting large-scale biogeochemical fluxes, for example. Third, the word "comprehensive" refers to the fact that the observations encompass bands that have been measured with past and contemporary visible and infrared imagers and scanners, so as to provide for a longer-term record while permitting improved spectral sensitivity and hence better information content.

The heritage of the MODIS instrument includes the Landsat Multispectral Scanner (MSS) and Thematic Mapper (TM), used for Earth resources; the Advanced Very High Resolution Radiometer (AVHRR), used for meteorology, sea surface temperature, sea ice, and vegetation indices; the Coastal Zone Color Scanner (CZCS) used for oceanic biomass measurements and ocean circulation patterns; and a variety of experimental instrumentation including the Thermal Infrared Multispectral Scanner (TIMS), Shuttle Imaging Spectrometer Experiment (SISEX), etc.

MODIS will provide a continuing series of observations complementary to those obtained with the above instruments. It is included as part of an Eos research observation strategy that would augment the capability of the predecessor instruments considerably, both in terms of frequency of coverage (at reduced resolution, for the MSS and TM), and in terms of comprehensive spectral coverage. The added capability in the spectral domain serves to permit advanced algorithm development with a consistent data set, which contains the full range of global variability and richness, and will enable such advanced algorithms to be easily applied retrospectively to study linkages between biogeochemical components.

The MODIS instrument requirements are defined by the large spatial-scale ($\geq$1 km) observational requirements within the atmospheric, terrestrial, and oceanic sciences. These requirements are based on present (realized) capabilities and requirements as well as those for which a firm foundation has been established (e.g., near infrared for improved ocean atmospheric correction). The resulting matrices of spectral, temporal, and spatial coverage requirements, together with specific instrumental capabilities and characteristics, have been resolved into a unified set of requirements.

If spatial resolution of 1 km precludes the possibility of obtaining narrow enough spectral bands in the infrared necessary to have an atmospheric sounding capability on MODIS, then it is extremely important to have atmospheric temperature-humidity sounding capability provided alongside MODIS. This is needed both to correct MODIS observations for atmospheric effects and to permit thorough studies of atmospheric phenomena and their interaction with surface processes. We are assuming that, at a very minimum, a sounding instrument of the quality of the High-Resolution Infrared Radiometric Sounder 2 (HIRS-2), the current operational infrared sounder, will accompany MODIS. To obtain the most from MODIS capabilities, as well as to obtain an improved understanding of surface atmospheric interactions, we recommend that an advanced high spectral resolution infrared sounder with 10 km horizontal spatial resolution be developed to accompany MODIS.

MODIS COMPLEMENTS OPERATIONAL SYSTEMS

It is expected that MODIS will complement preexisting and concurrent capabilities on operational satellites, chiefly the slightly modified AVHRR on NOAA-K, L, M spacecraft. One of the two operational NOAA payloads (one morning, one afternoon) will be in an orbit similar to that of MODIS or will be onboard the same platform. These two payloads together will provide more frequent global thermal infrared coverage (twice daily). The five-channel AVHRR, however, will be constrained to two longwave and one shortwave infrared window channels at night and two longwave infrared channels and three reflected radiation channels (two in the near-infrared and one in the visible spectrum) during the day, and will have no ocean color capabilities. It is not known whether there will be an

operational Ocean Color Imager (OCI) in orbit, especially on a U.S. satellite, during the time frame in question.

Thus the U.S. concurrent operational satellites (including Defense Meteorological Satellite Program (DMSP) and Geostationary Operational Environmental Satellite (GOES-Next)) will form an incomplete basis for an adequate and integrated Earth Observing System, even if complemented by somewhat similar foreign systems such as Systeme Probatoire d'Observation de la Terre (SPOT), Marine Observation Satellite/Land Observation Satellite (Japan) (MOS/LOS), and European Space Agency Remote Sensing Satellite-1 (ERS-1). MODIS can provide the basis, from both an instrument development and an integrated data base management standpoint, for follow-on operational satellite data collection, processing, archiving, and dissemination. Research with the more advanced and more comprehensive (both spectral and temporal) measurements to be available from the total MODIS system should demonstrate conclusively the value of providing the more comprehensive data on an operational basis.

III. SCIENCE OBJECTIVES AND INSTRUMENT REQUIREMENTS

TERRESTRIAL STUDIES

The anticipated contribution of MODIS to terrestrial studies is to provide regular, high temporal frequency coverage potentially of the entire land surface. This moderate spatial resolution, global coverage sensor will be complemented by the high spatial/spectral resolution capability of HIRIS for detailed study of limited areas of the Earth's surface. MODIS is conceived as being an essential component of an integrated multisensor system, and from the terrestrial studies point of view, it is this simultaneous coverage by MODIS and HIRIS that would provide a unique capability of the proposed Eos system.

The MODIS sensor will be the primary tool for global ecological research on the Eos platform. Because of critical global issues facing mankind, such as climate change, desertification, resource depletion, and region-wide pollution, the science community is being directed toward the problems of global ecological research. Existing data bases to support such research on a global scale are at best limited and quite often completely unavailable. As a consequence, much of the existing global ecological research has been through computer simulation modeling based on small and often unrepresentative sample data sets. Although these models are currently providing insight into the scale and dynamic nature of global biogeochemical cycles, and focus attention on rate-limiting processes, the models are often constructed from fabricated and temporally static global data bases in which we have little statistical confidence. As part of the Earth Observing System, the MODIS instruments proposed in this document will provide a long-term data base giving a view of the dynamic changes of the Earth's surface. This will permit phenological changes in terrestrial vegetation to be quantitatively assessed at regional, continental, and global scales.

Our present understanding of the utility of low-resolution satellite data for terrestrial studies is, for a large part, based on the results of a small number of recent vegetation studies using NOAA AVHRR data (Hayes, 1985). These studies give us an indication of the potential usefulness of MODIS data for vegetation inventory and monitoring at regional and continental scales, but have only just started to reveal the full potential of 1 km resolution multitemporal satellite data.

Recent developments using 1 km resolution multispectral sensors have shown that it is possible to provide reliable continental- and global-scale data sets of sufficient precision to supplement and improve upon existing inputs for global models (Tucker *et al.*, 1985a and b). Existing small-scale vegetation maps are inadequate for providing a comprehensive and up-to-date estimate of the distribution and areal extent of the major vegetation formations of the world. Low-resolution, remotely-sensed data provide the means by which global vegetation maps can be updated and improved (Tucker *et al.*, 1985a).

At both regional and global scales there is a lack of baseline information on such environmental issues as the rate of tropical deforestation and the type and rate of regrowth, the areal distribution and effect of acid rain on the boreal forests of Europe and North America, and the rate and extent of desertification at the margins of the world's deserts and arid regions. These examples illustrate a diversity of environmental issues that will require careful, sustained measurement through and beyond the next decade to understand fully their effect on the biosphere.

Monitoring long-term changes in the boundaries of selected natural and man-altered ecosystems will undoubtedly provide us with direct evidence of the effects of climatic change on the biosphere. Most perturbations of the biosphere will be evidenced first by subtle vegetation responses that may reflect both the nature and severity of the perturbation. Vegetation response to stress varies with both the type and degree of stress. As a general rule, chronic agents such as geochemical stress (Goetz *et al.*, 1983) affect vegetation in the following ways. Low levels of stress generate biochemical changes at the cellular and leaf level, which have an influence on pigment systems and canopy moisture levels (Labovitz *et al.*, 1983; Chang and Collins, 1983). Increasing stress may result in phenological changes such as delayed leaf flush and/or premature senescence (Labovitz *et al.*, 1983). Alteration of canopy structure and the resulting reduced percent cover, canopy closure, or biomass may also result from increasing stress levels. At higher levels of stress, community composition will change, with less tolerant species being replaced by more tolerant species (Rock and Vogelmann, 1985a; Abrams *et al.*, 1985). Incipient water stress will have a dominant effect on the canopy moisture content, which in turn influences the canopy reflectance and emittance. A wide variety of vegetation responses to stress as well as some causes of stress may be monitored by remote sensing, and the repetitive coverage by MODIS should permit regular measurement of vegetation stress conditions worldwide. For example, information on the areal extent of freeze or drought damage to vegetation, for both cropland and natural communities, would be economically and ecologically useful and technically feasible through analysis of MODIS data. Air pollution or toxic chemical damage may also be measurable.

Spatially comprehensive and timely information on the phenology of natural vegetation and the status of agricultural crops through the growing season are unavailable for all but a few localized areas, yet such information is essential for modeling global food resources. Present resource models are hampered by the absence of reliable and quantitative data on agricultural and pastoral conditions at a regional scale. Such data can be obtained through analysis of daily low-resolution multispectral satellite data (Justice *et al.*, 1985).

Daily measuring of surface climate and atmospheric conditions will be among the more important functions of Eos. An example of global mean surface temperature measurements currently available from HIRS-2 and Microwave Sounding Unit (MSU) data is given in Figure 1. Surface climatic variables of interest to land processes include temperature, radiation balance, humidity, and precipitation. These data can be used to drive computer simulation models of important biogeochemical processes in order to interpret changes in surface features and elemental exchange rates. Surface climate data can be used to calculate crop phenology and growth rates, stress events, nitrogen and sulfur fluxes, carbon dioxide exchange, and numerous other process rates. Surface albedo changes have been associated with long-term changes in surface climate (Charney *et al.*, 1977). Several studies have shown the utility of monitoring albedo by satellite remote sensing (Otterman, 1981; Courel, 1985). MODIS, for the first time, will provide a means by which to monitor spectral albedo changes simultaneously with biologically important parameters on a regional and global scale in support of climate-related environmental studies.

MODIS will also provide a number of useful products for surface hydrology. Changes in land cover must be monitored because they significantly affect most of the major terrestrial biophysical systems. Among the most important influences are changes in runoff, infiltration, and evapotranspiration rates affecting the hydrological system; changes in evapotranspiration rates affecting the global energy balance; changes in erodibility of surface materials affecting sediment transport systems and the distribution of areas of net erosion-deposition.

Monitoring continental changes in snow cover and associated changes of albedo will also be possible. Watershed to basin-level snowmelt estimates can provide prediction of the temporal dynamics of river discharge rates, of importance for calculating elemental exchange between land and oceans for flood warning, and for irrigation management. In conjunction with precipitation rates sampled by other Eos sensors, large area estimates of soil moisture will provide critical input into assessments of vegetation growth and water stress. Regional evaporation and transpiration rates may be modeled from surface wetness and surface climate. These processes have implications as surface feedbacks to global climate models and as controls of vegetation stress and changes in primary production.

Beyond a basic inventory of global vegetation, MODIS spectral data should be able to provide measures of some important derived products, such as standing green biomass, intercepted photosynthetically active radiation (IPAR), and net primary productivity (NPP), dependent on growth in our understanding of spectral information in the next five to seven years. For example, vegetation leaf area index (LAI) is an important structural variable that can be used to calculate mass and energy exchange from vegetated surfaces. Global estimates of LAI would allow computation of carbon exchange rates based on measured data, instead of the guesses that must be used today. Estimates of global storage in terrestrial plant biomass vary from 400 to $1,200 \times 10^{15}$ gC (grams carbon). This uncertainty could be considerably reduced with a MODIS survey of plant biomass, and this would help significantly in understanding the balance of the global carbon budget.

For many uses, the MODIS data stream may be fed through global geographic information systems to facilitate implementation of computer simulation models. Global surface climate models, carbon cycle models, hydrologic cycle/energy models, and comprehensive biogeochemical cycling models will all require this data stream. It is recognized that very few of the complex global ecological issues are addressable with satellite imagery alone. Global models that integrate various data sources and calculate rates of fundamental processes such as photosynthesis will be necessary for a dynamic view of the global ecosystem (Figure 2). MODIS data will provide a direct, timely global measurement of the current conditions of the land surface for these models.

A brief description of the NOAA/AVHRR system, indicating the range of data products currently being used (Schneider *et al.*, 1981), will give the background for the present perception of what will be possible from improved moderate spatial resolution instruments such as MODIS. The NOAA/AVHRR system was first launched in 1978 (Kidwell, 1984) and has provided data since that time at a nominal spatial resolution of 1.1 km at the subsatellite point (Table 1). The standard NOAA/AVHRR product, collected worldwide on a daily basis, is the global area coverage (GAC) data with a 5 km × 3 km resolution element (Schwalb, 1982; Gatlin *et al.*, 1984). This is produced by onboard processing of the raw 1.1 km × 1.1 km local area coverage (LAC) data, which, for sample areas, may be transmitted to Earth by special request. Since April 1982 GAC products have been used to generate a third product, called the global vegetation index (GVI) (NOAA, 1986; Tarpley *et al.*, 1984). The GVI product is resampled from the GAC data to give a polar

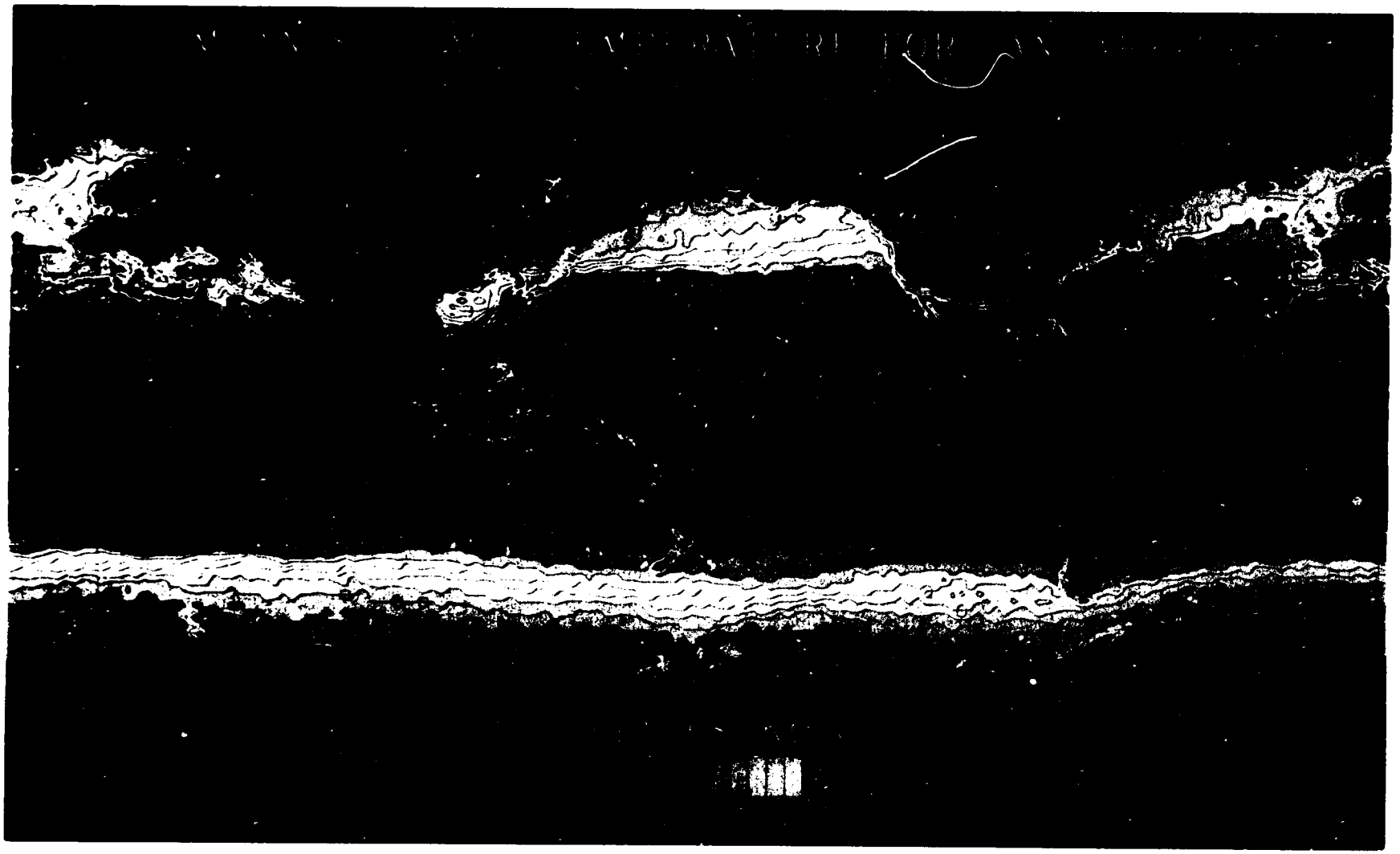

Figure 1. Global map of the Earth's mean monthly surface skin temperature for January 1979, from the High-Resolution Infrared Sounder 2 and the Microwave Sounding Unit. Skin surface temperature was derived from the 3.4 and 4.0 μm window channels on HIRS-2 in combination with additional microwave and infrared data from two microwave sounding units.

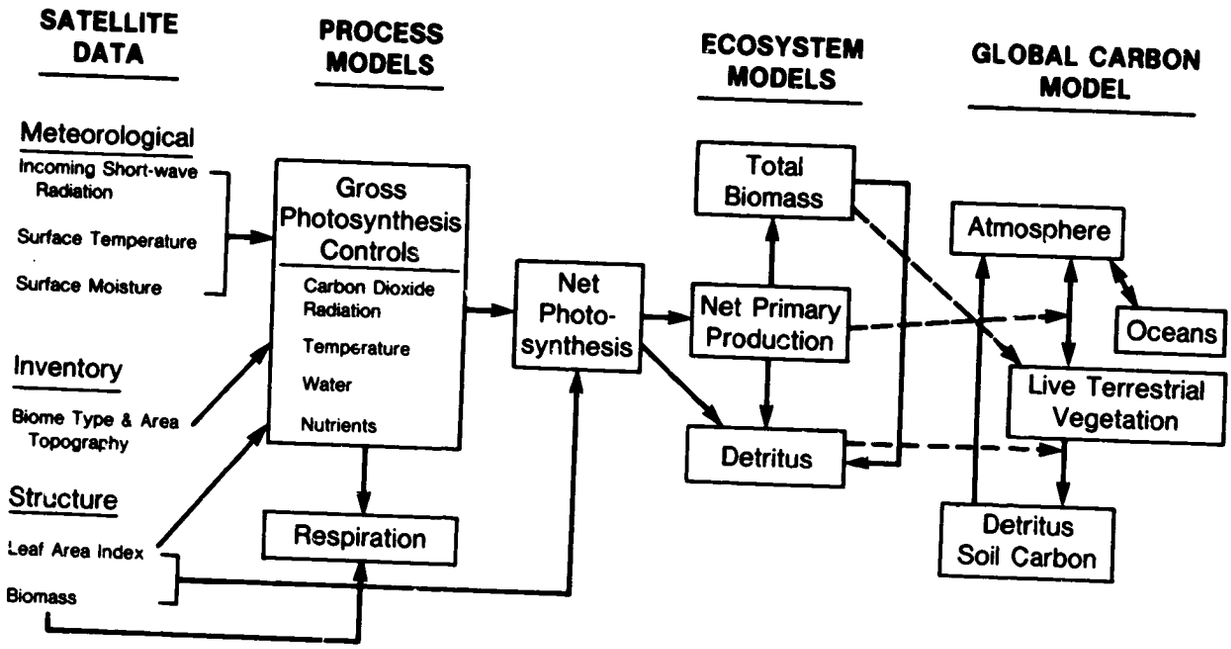

Figure 2. Organizational diagram of a proposed model of net primary production for a coniferous forest. All driving variables are derived from satellite data. Potential linkages to a global carbon model are shown by dashed lines (Running, 1984).

Table 1. Characteristics and Status of the NOAA/AVHRR Systems

TIROS-N, launched October 1978, NASA funded protoflight
NOAA-6, launched June 1979, NOAA funded
NOAA-7, launched June 1981, NOAA funded
NOAA-8, launched March 1983, NOAA funded
NOAA-9, launched December 1984, NOAA funded
Orbit inclination: 98.8°
Orbital height: 820-870 km
Orbital period: ~ 102 min
Scan angle range ±55.4°
Ground swath coverage: 2,700 km
IFOV 1.39 to 1.51 mrad
Ground resolution 1.1 km (nadir); 2.4 km (max. scan-angle along track); 6.9 km (max. scan-angle crosstrack)
Quantization 10 bit
Equatorial crossing

	Descending		Ascending	
	07:30 14:30		19:30 (NOAA-6 and NOAA-8) 02:30 (NOAA-7 and NOAA-9)	
Spectral channel	1	2	3	4	5
Spectral range (μm):	0.58-0.68*	0.725-1.1	3.5-3.93	10.3-11.3	11.5-12.5**

Status as of May 1985

NOAA-6	Taken out of operational service 5 March 1983. Reinstated 22 June 1984.
NOAA-7	Taken out of operational service March 1985.
NOAA-8	Taken out of operational service 12 June 1984.
NOAA-9	Operational.

*Channel 1 range on TIROS-N: 0.55 to 0.90.
**Not on TIROS-N, NOAA-6, or NOAA-8.

stereographic projection with 15 km resolution at the equator.

Examples of the NOAA GVI, GAC, and LAC data produced by the Global Inventory, Monitoring, and Modeling Studies (GIMMS) group at NASA/GSFC are presented as Figures 3, 4, and 5, respectively. Figure 4 is an example of 8 km resampled GAC produced by the GIMMS group for the purposes of African continental vegetation inventory and regional drought monitoring. The range of current activities using AVHRR data includes continental land cover mapping (Tucker *et al.*, 1983; Townshend and Tucker, 1984); rangeland monitoring and grassland productivity estimation (Tucker *et al.*, 1983); tropical forest inventory and deforestation monitoring (Tucker *et al.*, 1984a; Justice *et al.*, 1985); agricultural crop and drought monitoring (Justice *et al.*, 1984; Tucker *et al.*, 1984b; Justice *et al.*, 1985); ecological modeling (Norwine and Greegor, 1983; Goward *et al.*, 1985); desert locust monitoring (Tucker *et al.*, 1985b); and forest fire monitoring (Malingreau *et al.*, 1985; Matson *et al.*, 1984).

The methodologies for analyzing high temporal frequency, low spatial resolution data are currently being developed and can be expected to continue to substantially improve over the next few years. Of particular interest is the establishment of long-term data bases showing trends in vegetation response over a number of years. These can be used to examine the effects of long-term climatic change and altered land use practices.

The NOAA/AVHRR systems are assumed to be funded through the 1990s with slight modifications planned for the NOAA-K, L, and M satellites starting in 1989 (McElroy and Schneider, 1984 (see Table 2)). There is thus the exciting possibility of contemporaneous orbiting of the AVHRR and MODIS systems. With the sensor system characteristics outlined in Chapter IV, MODIS will represent a substantial improvement over the existing and planned AVHRR systems, especially in terms of the number of spectral bands designed to derive land and ocean parameters. The AVHRR system was designed as an operational meteorological sensor and has several characteristics dictated by this mission objective (Table 1) that are inconsistent with land and ocean science objectives. The present 7:30 a.m. and 2:30 p.m. overpass times result in problems of low light levels at high latitudes and cloud cover over equatorial zones. The amount of 1 km data (LAC) coverage possible has been and will continue to be severely limited by the capacity of the onboard tape recording system. The locational accuracy requirements of meteorological applications are considerably less severe than those for surface mapping and measurement. Similarly, the pre-launch and onboard sensor calibration procedures currently associated with the AVHRR leave much to be desired.

MODIS-N is being designed with terrestrial monitoring as a major mission objective, with Eos orbital characteristics, sensor calibration and configuration, locational accuracy, and data requirements specified accordingly (see Chapter IV). With the projected improvements in present data processing and archiving technology, global coverage at 500 m every two days will give an enhanced monitoring capability over the present and planned AVHRR systems. This improved spatial resolution will permit the detection of loud transformations undetectable using the current daily 4 km AVHRR data. Beyond that capability, a unique contribution of MODIS for terrestrial observations lies in the Eos concept of an integrated, multilevel sensing system. The capability for monitoring surface conditions will

Table 2. Proposed AVHRR Characteristics on NOAA-K, L, M

Channel	Spectral Band	S/N
1*	0.55 – 0.65 μm	
2*	0.84 – 0.87 μm	9:1 at 0.5% reflectance
3a (day)*	1.58 – 1.64 μm	20:1 at 0.5% reflectance
3b (night)	3.63 – 3.9 μm	
4**	10.3 – 11.3 μm	
5**	11.5 – 12.5 μm	

*It is also proposed that either the digitization be increased from 10 bit to 12 bit or that sampling of the dynamic range be changed to:

Channel	Reflective Range (%)	Counts Range
1	0–25	0–500
	26–100	500–1,000
2	0–25	0–500
	26–100	500–1,000
3a	0–12.5	0–500
	12.6–100	500–1,000

**It has been proposed that the maximum brightness temperature in channels 4 and 5 be increased from 320 K to 340 K.

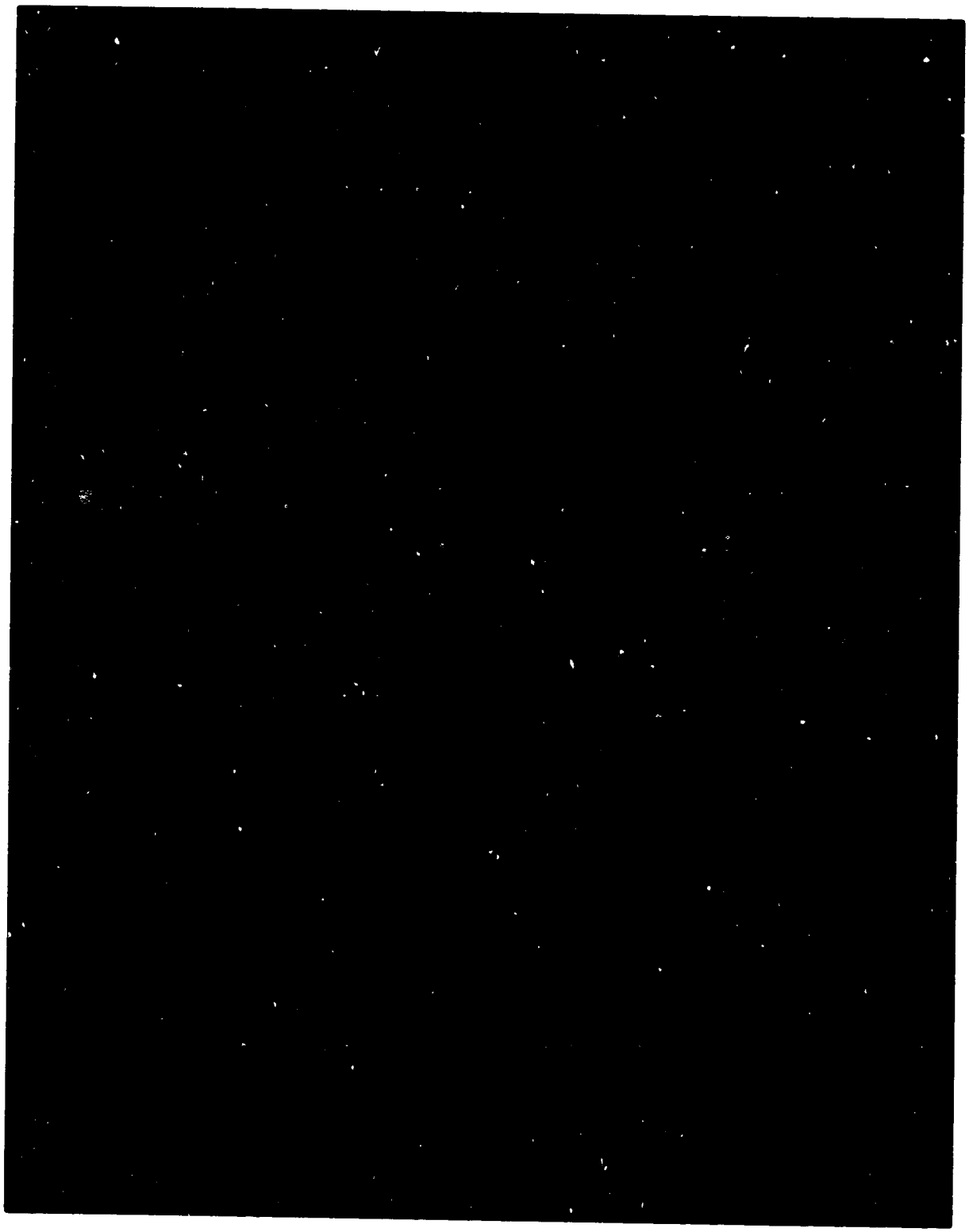

Figure 3. AVHRR global vegetation index for July 1982.

ORIGINAL PAGE
COLOR PHOTOGRAPH

Figure 4. Normalized difference vegetation index derived from AVHRR GAC data resampled to 8 kilometers.

NOAA-7 AVHRR LAC data (channels 1, 2)
1 km resolution (1.5× enlargement)
November 27, 1981

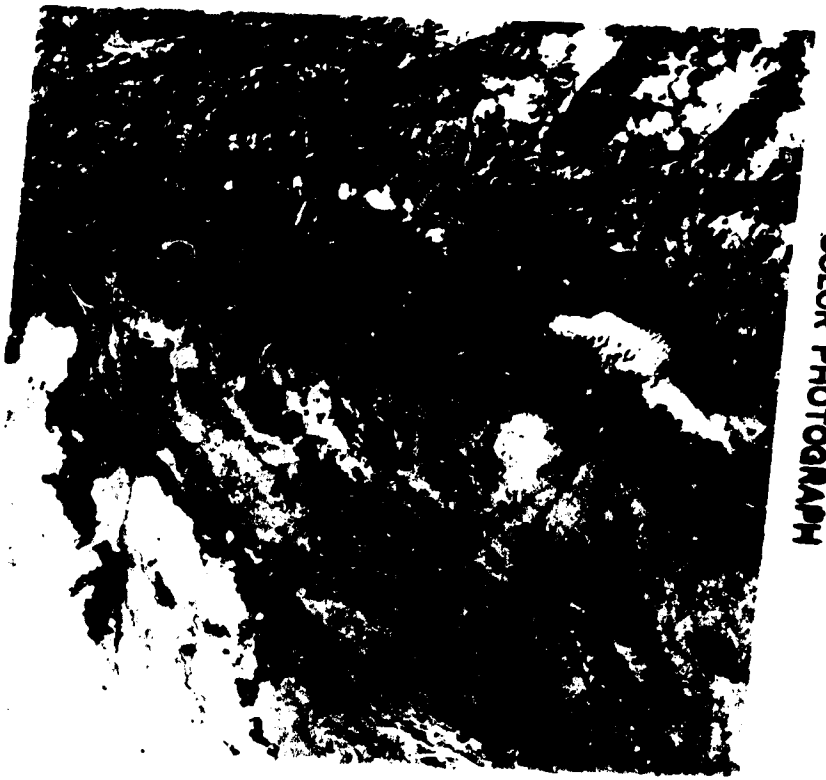

Landsat 3 MSS data (channels 4, 5, 7)
80 m resolution (full frame)
November 11, 1981

ORIGINAL PAGE
COLOR PHOTOGRAPH

Figure 5. Comparison of AVHRR local area coverage with MSS false color composites.

increase considerably when it becomes possible to simultaneously and selectively sample complete 500 m resolution coverage with a high resolution (30 m) limited swath. This is the conceptual basis for an integrated MODIS/HIRIS sensor configuration as proposed for Eos. The possible results from such a system would include cloud identification, atmospheric correction, and inferred rainfall in support of terrestrial studies. The practical problems of integrating high- and low-resolution data from different satellite systems in terms of data acquisition, temporal and spatial registration, and calibration prohibit this approach with existing satellites. The MODIS/HIRIS combination is one of the unique opportunities of the Eos polar platform approach.

Instrument Requirements for Terrestrial Studies

The instrument requirements for MODIS are determined by the applications for which the system is intended. The prime function of MODIS for terrestrial studies is the monitoring of vegetation dynamics and land transformations for a wide variety of research studies. One example of such studies that is receiving considerable attention at present is global CO_2 modeling (Hansen *et al.*, 1981; Fung *et al.*, 1986). The MODIS contribution to this research would include measures of the contribution from the vegetation component of the biosphere to the CO_2 cycle. Such measures would require a reliable map of the distribution of the major vegetation formations, the timing of their major phenological events, and the associated variations in photosynthetic activity and biomass production. Such objectives would necessitate a sufficiently high temporal frequency monitoring to detect phenological events such as green-up and senescence and to monitor variations in the timing of such changes over a number of years. To undertake such a measurement program will require consistent and reliable data sets over a number of years, which implies the need for a continuous coverage policy and a dependable operating status. In support of such a study, the HIRIS system would provide greater precision in our understanding of the relative contribution of the different components of the vegetation canopy to the measured reflectance, to the observed green-up, and to CO_2 exchange. The above example is just one of several potential uses of data from a MODIS system designed for measuring vegetation dynamics. In the following subsections we examine some of the required sensor characteristics in more detail.

Spatial Resolution

The proposed MODIS resolution for terrestrial studies is 500 m, an improvement by a factor of 2 over the AVHRR (1 km) spatial resolution for regional monitoring. A 500 m resolution at the edge of the swath will afford improved location of ground features for detailed calibration and complex scene radiation studies while permitting resampling for those continental studies requiring a lower spatial resolution (i.e., >500 m). Similarly, a resolution of 500 m will facilitate integration with the HIRIS 30 m resolution data. Agriculture and forestry practices frequently subdivide land on 50 to 100 acre blocks, or 0.2 km^2. The 500 m resolution should allow adequate discrimination of these features, which would be lost at lower resolutions.

High-frequency monitoring of large areas involves a trade-off between spatial resolution and the quantity of data that can be practically handled. The data stream from MODIS will be over 3×10^4 times less than HIRIS per unit of land area. Even so, the predicted data flow from the MODIS system (see Chapter IV, Data Rates) will require considerable improvements in data handling and storage over the existing Landsat and AVHRR systems.

Revisit Time (Temporal Resolution)

The required revisit time of the system and, indirectly, the orbital altitude are determined by the highest temporal frequency changes in the surface phenomenon that is to be measured. It is often the periods of rapid change in the vegetation that trigger other important processes within the ecosystem. The temporal resolution of the system should be sufficient to resolve such events. Vegetation research by remote sensing does not normally require daily data, as the development and senescence of plant communities is a relatively continuous process. However, it does require reliable and usable coverage within a week to 10 days, which, owing to cloud cover problems, necessitates a higher frequency of acquisition. Occasional threshold events, such as catastrophic subtropical freezes, are instantaneous; however, the resulting damage to the vegetation is best evaluated days after the event. Many vegetation stress responses, such as water or pollution stress damage, accumulate over periods of weeks to even years (Running, 1984). In contrast, semi-arid grassland species can germinate and fruit within a two- to three-week period. At present, the highest possible temporal coverage for the AVHRR LAC (within $\pm 30°$ off-nadir viewing limits) of three passes every nine days is required to produce acceptable cloud-free coverage of semi-arid areas, where such vegetation flushes are of major ecological importance. Even so, for areas of persistent cloud cover and haze, cloud-free coverage will remain unobtainable and, for such areas, emphasis must be placed on the Eos active and passive microwave sensors, Synthetic Aperture Radar (SAR) and High-Resolution Multifrequency Microwave Radiometer (HMMR), respectively. Some land surface hydrological events are sufficiently transient in nature that daily coverage is required, e.g., flooding and surface wetness. Seasonal snow accumulation and melt could be monitored at less frequent time intervals.

One of the most compelling reasons for a high temporal frequency for MODIS coverage is to provide estimates of surface climate conditions. The most important surface climate variables include air temperature, incoming shortwave radiation, humidity, and precipitation. MODIS, accompanied by a sounder, will be able to provide estimates of temperature and radiation, with inferences of humidity and precipitation through estimation of the dew point, cloud monitoring, and measurement of surface wetness. Important vegetation processes such as photosynthesis and transpiration respond to daily changes in surface climate. Remote sensing cannot always directly monitor such continuous vegetation processes; however, they can often be inferred by computer simulation of plant responses to other measurable environmental parameters (Running, 1984). For example, integration of vegetation structural features, such as leaf area index, with daily surface climate parameters derived from the satellite, may provide the best means of estimating CO_2 and H_2O flux from vegetated surfaces.

Based on understanding of the measurement studies that will be performed using MODIS data, the terrestrial studies group recommends as close to daily coverage as possible within a 30° sensor viewing angle limit.

Spectral Resolution

Present requirements for vegetation remote sensing from MODIS could be met by an approximation of the spectral channels used on the Thematic Mapper (TM) that were selected for this purpose. There has been little change in understanding of spectral requirements for vegetation monitoring since the launch of TM; however, refinements resulting from current TM studies (Barker, 1985) could easily be incorporated within the MODIS design and construction time frame.

Table 3 lists the major spectral regions of value for vegetation analysis (Cox, 1983). It cites specific wavelength regions of value for vegetation stress detection, species discrimination and mapping, and biomass estimation. Without sufficient scientific justification for high spectral resolution at the proposed moderate spatial resolution of MODIS, broader spectral bands have been kept than those recommended for HIRIS. For terrestrial studies in general, the MODIS channels should not encompass

Table 3. Spectral Regions for Remote Sensing of Vegetation*

Wavelength (μm)	Type of Feature	Value
0.440–0.500	Absorptance	Detection of changes in chlorophyll/carotenoid ratios (related to stress).
0.650–0.700	Absorptance	Detection of chlorophyll states as well as tannin and anthocyanin content. Initial stress detection.
0.700–0.750	Reflectance	Senescence detection. Detection of dead or dormant vegetation.
0.800–0.840	Absorptance	Possibly related to leaf anatomy and/or state of hydration.
0.865	Reflectance	Height of feature may be useful in species discrimination.
0.940–0.980	Absorptance	Shifts in this minor water absorption band may be useful in species discrimination and determination of hydration state.
1.060–1.100	Reflectance	Shifts in peaks may be related to leaf anatomy and/or morphology. May be useful for species discrimination.
1.140–1.220	Absorptance	Shifts in this minor water absorption band may be useful in species discrimination and determination of hydration state.
1.250–1.290	Reflectance	Height of this feature very useful for species discrimination of senescent forest species. A ratio of this feature with the one at 1.645 offers a good indication of moisture content and thus stress.
1.630–1.660	Reflectance	An indication of moisture content of leaf. May also be an indicator of variation in leaf anatomy. May be useful for species discrimination. An indicator of leaf moisture content when used as a ratio with the 1.270 data above.
2.190–2.300	Reflectance	An indicator of moisture content. May also be of value in species discrimination.
3.000–5.000; 8.000–14.000	Emittance	Little is known concerning the optimal thermal wavelengths for studying different vegetation parameters. This is an area that needs further study.

* Cox, 1983

atmospheric water absorption bands. Where possible, sufficiently narrow bands should be selected to minimize atmospheric effects, allowing a trade-off between bandwidth and radiometric sensitivity. The following paragraphs highlight some of the more critical wavebands for vegetation studies.

For detection of changes in chlorophyll/carotenoid ratios which provide a measure of plant stress, a channel in the 440 to 500 nm region is required. A spectral channel near TM channel 2 (520 to 600 nm) is necessary because of the increased reflectance of green vegetation in this portion of the spectrum. In addition, Richardson *et al.* (1983) found that reflectance in the near-infrared region (0.76 to 0.90 μm) was closely related to canopy nitrogen, an important parameter in biogeochemical cycling research.

For biomass estimation, spectral channels at 630 to 690, 660 to 680, and 760 to 900 nm are required. A channel close to TM3 (630 to 690 nm) is extremely important owing to its sensitivity to the chlorophyll concentration in vegetation, as well as tannin and anthocyanin content. A channel at 700 to 750 nm would provide useful information relating to senescence of vegetation, which would allow the monitoring of translocation of nutrients from the foliage. The 760 to 900 nm region, where infrared reflectance is at a maximum, is essential for vegetation monitoring and is directly sensitive to foliage biomass. A ratio of near infrared (760 to 900 nm) and red (630 to 690 nm) has been shown to be well correlated with foliage biomass for crops, rangeland, and forests (Tucker, 1980; Spanner *et al.*, 1984; Running *et al.*, 1985).

The spectral wavelength channel from 1.25 to 1.29 μm has been shown to be useful for discrimination of forest species (Rock, 1982, 1985b). A channel comparable to TM5 (1.53 to 1.73 μm), specifically 1.63 to 1.66 μm, is sensitive to the moisture content of leaves and may be indicative of variations in leaf anatomy. This channel, when ratioed with the 1.25 to 1.29 μm channel, is an indicator of leaf moisture content. Two channels within the 2.0 to 2.4 μm region will be useful for examining canopy chemical composition. A channel centered at 2.18 μm is useful for observing a protein absorption feature and may allow for determination of the nitrogen content of foliage (Peterson *et al.*, 1985).

Relatively little is known regarding the value of thermal data in the study of vegetation as compared to the visible and near-infrared portions of the spectrum. However, such studies as presented by Gurney *et al.* (1983); Heimburg *et al.* (1982); and Soer (1980) have demonstrated the potential and utility of thermal data for regional soil moisture and evapotranspiration studies. While it is not possible at present to identify the optimum thermal band selection for MODIS, future results from analysis of Thematic Mapper (channel 6), AVHRR (channels 3, 4, 5) and the airborne TIMS data will permit an informed band selection in the future.

Infrared atmospheric windows, that is, spectral regions in which the atmosphere is relatively transparent to infrared radiation, are found primarily in the regions between 8 and 12 μm (longwave window) and 3.5 to 4.2 μm (shortwave window). The regions each have advantages and disadvantages for monitoring surface temperature. The shortwave window observations are much less sensitive to water vapor absorption, especially water vapor continuum absorption, which becomes very large at longer wavelengths in humid atmospheres. The shortwave observations are also roughly three times more sensitive to variations in surface temperature and one-third as sensitive to variations in surface emissivity. On the other hand, shortwave observations are strongly affected by reflected solar radiation during the day and the surface emissivity over land is more variable than at longer wavelengths (see Figure 6).

AVHRR currently has two longwave window channels and one shortwave window channel (see Table 1). At night, observations in all these channels are used to help correct the temperature observations for atmospheric effects. During the day, only the two longwave window channels are used. HIRS-2, on the other hand, has one longwave (10.9 to 11.3 μm) and two shortwave (3.95 to 4.0 μm and 3.70 to 3.83 μm) channels. The shortwave windows allow for the simultaneous determination of daytime surface temperature and reflected solar radiation (by assuming the surface reflectivity is the same in both shortwave channels).

MODIS technology allows for spectral resolution comparable to that of HIRS-2 while keeping the 1 km spatial resolution of AVHRR. The main improvement from this will come from the ability to make split windows in the shortwave region, allowing for the daytime use of those channels that are less sensitive to water vapor absorption. Several options exist and one of these is outlined below.

Table 4 shows the central wavelength (λ) and channel widths ($\Delta\lambda$) for the thermal infrared (TIR) considered for MODIS. Also shown in the Table are the transmittance to the surface, τ_s; the transmittance excluding water vapor continuum absorption, τ_{w_cont}; and the difference between the computed brightness temperature T_B, and the sea surface temperature T_s, for both July (0°N) and April (40°N) climatological profiles. This difference shows the effect of atmospheric absorption and the correction needed to obtain the surface temperature. The computations assume that the surface temperature is identical to the surface air temperature and that the surface emissivity is unity. Effects of clouds or reflected solar radiation are not included.

This leads to a recommendation for four channels in the 8 to 12 μm region and three channels in

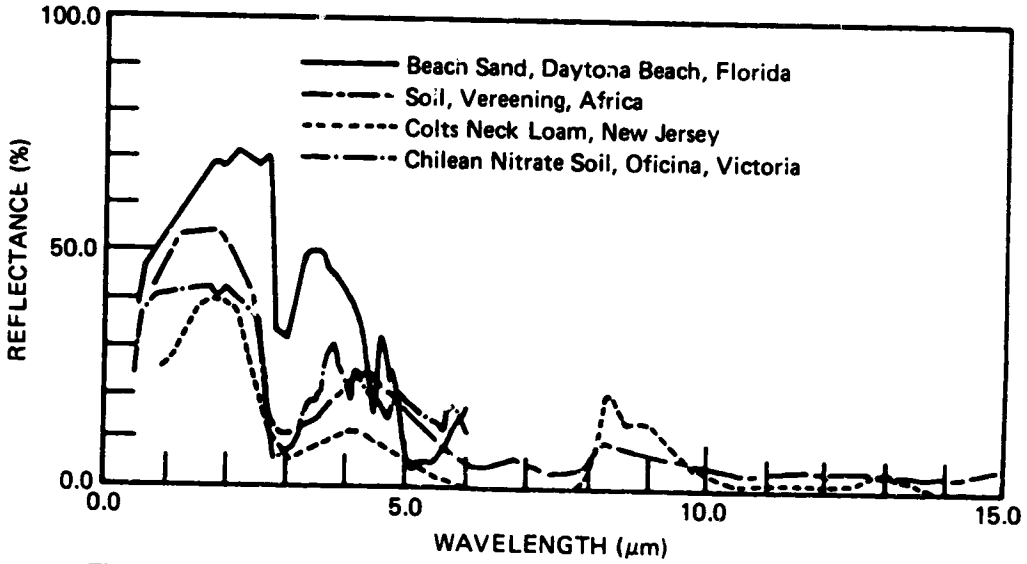

Figure 6. Reflectance vs. wavelength for a variety of soils (Wolfe and Zissis, 1978).

the 3.6 to 4.1 μm region. The channels at 11 and 12 and 3.75 μm are the most similar to those on AVHRR. In addition, there are three longwave channels that may help in identification of aerosols, such as those put into the atmosphere by the El Chichon eruption, and two shortwave channels that will help account for reflected solar radiation and that are quite insensitive to atmospheric water vapor variation, N_2 being the absorbing gas.

The channels at 8.55 μm and 10.15 μm were selected to help identify sulfuric acid aerosols, which have a maximum absorption at 8.55 μm and a minimum near 10.45 μm. Water aerosols have nearly the same transmissivity at these two wavelengths. Thus, for an atmosphere where only aerosol type was different, the difference in equivalent black body (EBB) temperature between the two channels should be almost as constant as aerosol optical thickness changes for water particles, but should change noticeably with changes in optical thickness of sulfuric acid particles. As seen in Table 4, by comparing atmospheric absorption for the two profiles, all shortwave channels are much less sensitive to water vapor absorption than the longwave channels, for which absorption is so great in tropical atmospheres that they become relatively insensitive to the surface temperature. Observations at the longer wavelengths are less affected by absorption by fixed gases (see April 40°N in Table 4) than are the observations at shorter wavelengths. As a result of these relative advantages, observations in the two wavelength regions really complement each other. In the higher latitudes, where water vapor amounts are less and where atmospheric temperature is variable, the long wavelength channels perform well because of the greater sensitivity to water vapor and the lesser sensitivity to gases other than water vapor. In the tropics, where moisture content is high and atmospheric temperatures are nearly constant, the shorter wavelengths perform better because of the greater contribution of the surface, and because the almost constant temperatures allow for compensation for the larger absorption by the gases with constant mixing ratios.

Table 4 also includes calculations for high spectral resolution infrared window channels ($\lambda/\Delta \sim 1,200, 600$) to demonstrate what can be achieved if narrow-band channels can be used to sound the surface at frequencies between absorption lines. It is clear that much cleaner windows can be obtained in the 3.7 to 4.0 μm region, which give atmospheric effects of less than 2° even in tropical atmospheres. Moreover, three clean windows in the shortwave region will allow for simultaneous determination of ground temperature, reflected solar radiation, and surface emissivity. The last factor becomes very important when attempting to measure land temperatures. High spectral resolution does not reduce broadband effects such as those due to the N_2 continuum around 4.0 μm and the water vapor continuum in the 8 to 12 μm region. N_2 absorption is easily accounted for, however, because the N_2 concentration is well known. The high-resolution, longwave channels are good windows in dry atmospheres but exhibit considerable absorption due to the water vapor continuum (but not water lines) in humid atmospheres. This makes these channels particularly good for determining low-level water vapor once the ground temperature is determined from the shortwave channels.

The need for a supplemental infrared sounding instrument at higher spectral resolution but lower spatial resolution than MODIS will be discussed in Chapter III, on Complementary Atmospheric

Table 4. Effect of Atmospheric Absorption on Surface Temperature Retrievals

λ (μm)	Δλ (nm)	July (0°N) τ_s	July (0°N) $\tau_s/\tau_{w\ cont}$	July (0°N) T_B-T_S (K)	April (40°N) τ_s	April (40°N) $\tau_s/\tau_{w\ cont}$	April (40°N) T_B-T_S (K)
MODIS Windows							
3.750	90	0.763	0.768	2.87	0.874	0.876	1.58
3.989*	50	0.845	–	2.42	0.869	–	2.14
4.05*	50	0.738	–	4.12	0.741	–	3.92
8.55	500	0.375	0.623	8.09	0.725	0.782	3.78
10.45**	500	0.423	0.868	5.48	0.837	0.932	7.92
11.03	500	0.405	0.879	5.34	0.845	0.948	1.44
12.02	500	0.221	0.815	8.08	0.749	0.906	2.25
High-Resolution Windows							
3.723	3.2	0.911	0.915	1.08	0.966	0.967	0.73
	6.4	0.905	0.909	1.23	0.957	0.958	0.86
3.822	3.2	0.958	0.961	0.74	0.976	0.977	0.70
	6.4	0.926	0.929	1.07	0.960	0.961	0.84
3.955*	3.2	0.885	–	1.85	0.894	–	1.77
	6.4	0.879	–	1.91	0.891	–	1.80
8.866	7.5	0.553	0.933	4.39	0.876	0.947	2.43
	15.0	0.552	0.929	4.33	0.878	0.949	2.34
10.914	9.0	0.460	0.981	4.29	0.887	0.993	1.03
	18.0	0.460	0.981	4.29	0.887	0.993	1.03
11.994	9.0	0.269	0.985	6.30	0.825	0.996	1.33
	18.0	0.269	0.983	6.31	0.824	0.995	1.33

* N_2 continuum absorption is significant
** O_3 absorption is significant

Sounding Data. This sensor would provide atmospheric sounding capability as well as the high spectral resolution windows needed to improve surface temperature determination. Spectral bands suitable for atmospheric correction and cloud detection are considered to be essential components of the MODIS terrestrial monitoring system. Specific band selection for these purposes is discussed in Chapter III. on Oceanographic Studies.

To summarize the spectral requirements for MODIS land studies, 13 to 19 fixed spectral channels should be distributed through the spectrum in the following way:

- Visible-near IR 4-8 channels
- Shortwave IR 2-4 channels
- Midwave IR 3 channels
- Longwave IR 4 channels

} a provisional list of the bands is provided in Table 16

Orbital Overpass Time

The decision concerning the orbital overpass time for terrestrial studies will inevitably be a compromise of several conflicting requirements. Vegetation monitoring requires cloud-free coverage, which for tropical areas would indicate the need for an early- to mid-morning overpass. Quantitative analysis of the diurnal variations in cloud cover and atmospheric haze as a function of latitude would permit a more precise indication of the factors in selecting different orbital overpass times. Vegetation stress studies ideally would require an afternoon overpass around 2:30 to 3:00 p.m. In contrast, detection of plant stress through stomatal resistance can best be performed between 9:30 and 10:00 a.m. (Waring, 1983). Studies of soil moisture using the thermal bands will require an overpass time around 1:30 p.m. Another constraining factor concerns low light levels at high latitudes associated with an early morning or late afternoon overpass during the winter season.

Based on current understanding of the potential terrestrial applications of MODIS, an overpass time between 1:00 and 2:00 p.m. solar time would provide an acceptable compromise between the different requirements.

Discussions of MODIS radiometric accuracy, sensor calibration, and registration requirements

are incorporated in Chapter IV, along with a more detailed description of the proposed sensor characteristics.

OCEANOGRAPHIC STUDIES

Biological Oceanography

The fixation of carbon in the ocean by photosynthesis is roughly of the same order of magnitude as that occurring in terrestrial ecosystems. However, there are large differences in the turnover rates and reservoirs in the two systems. Terrestrial systems are dominated by plants with large amounts of structural material and that have turnover times of a few decades; marine systems are dominated by unicellular plants that have turnover times of days. Soil humus is another large reservoir, and it has a turnover time of a few centuries. Dissolved organic carbon in the ocean has a similar size and turnover time. However, the largest reservoir in the global carbon cycle is the carbon in marine sediments, and it has a turnover time of millions of years.

It is necessary to know the processes regulating the growth of phytoplankton in the ocean as well as the processes influencing the fate of this organically-fixed carbon in order to understand the role of the ocean in the global carbon cycle (Eppley and Peterson, 1979). Specifically, we wish to understand how changes in the relevant forcing functions affect the fixation of atmospheric carbon dioxide by phytoplankton and its transfer rate to the deep marine sediments. Along with the carbon cycle, we also wish to understand the role of the ocean in the cycling of other important elements: nitrogen, phosphorous, and sulfur. As with carbon, the uptake and fate of these nutrients are strongly affected by (as well as influenced by) the growth rate of phytoplankton (National Academy of Sciences, 1984).

Although primary productivity and phytoplankton biomass are the initial variables of interest, we emphasize that other processes are equally important in carbon cycling. Physical processes such as solar radiation, vertical and horizontal transport and mixing strongly affect phytoplankton dynamics and transport (Mackas *et al.*, 1985). Biological processes such as species composition of the producer and grazer communities affect uptake and cycling rates as well as the fates of various materials.

Shipboard measurement of primary productivity has improved significantly in the last decade (McCarthy, 1984 and references cited therein). However, there is still a fair amount of controversy concerning the accuracy of these measurements. A variety of processes may affect these measurements, such as incubation duration, bottle effects, photoinhibition, micrograzers, trace metal contamination, and species composition changes. Although there have been several estimates of global primary productivity (Steeman-Nielsen, 1952; Ryther, 1969; Koblentz-Mishke, *et al.*, 1970; Platt and Subba Rao, 1975), these have been based on C^{14} measurements which may severely underestimate true primary production. Revised estimates by DeVooys (1979) and Eppley (1980) suggest that primary production may be as much as three times larger than earlier estimates.

Leaving aside such methodological considerations, the sampling limitations of shipboard measurements are more important to the accuracy of any global maps of primary productivity. Numerous studies have shown that the characteristic time and space scales (as well as intensity) of phytoplankton variability make shipboard estimates extremely difficult (e.g., Esaias, 1980; Denman and Powell, 1984). Ship sampling is limited in its ability to sample in both the temporal and spatial domains. Thus, the global estimates of productivity described earlier are based on composites of measurements over several decades and are therefore suspect. More importantly, we wish to describe and understand the fluctuations in productivity as much as we wish to have an accurate map of the mean field: such sampling cannot be accomplished with ship measurements alone.

The last decade has shown that fluctuations in the temporal and spatial distributions of phytoplankton are largely the result of variations in physical processes. We need to understand the nonlinear coupling between these physical and biological processes if we are to understand the production and fate of biogenic materials on a broad range of time and space scales. The episodic nature of these processes is of particular importance. For example, coastal upwelling tends to be very irregular in eastern boundary currents. These events tend to stimulate the growth of rapidly sinking diatoms, which may result in high rates of carbon transport out of near-surface waters. The biological response to this type of variable forcing, on both mesoscales and large scales (as well as the global scale) need to be understood.

The estimation of near-surface phytoplankton biomass from satellite measurements of ocean color has been shown to be accurate to within about ± 35 to 40 percent for a large range of pigment concentrations (Brown *et al.*, 1985) in Case 1 waters (Morel and Prieur, 1977) where the primary materials affecting light absorption and scattering are phytoplankton pigment and other co-varying detrital materials, and within a factor of 2 generally. Preliminary work has begun on the use of near-surface phytoplankton concentrations to estimate water column primary productivity (Hayward and Venrick, 1982; Platt and Herman, 1983; O'Reilly and Busch, 1984; Eppley *et al.*, 1985). There is considerable scatter in this relationship, and it is unlikely that a simple, constant relationship will work for the world ocean. Use of ancillary data such as

sea surface temperature, daylength, and winds will improve regional models (Eppley *et al.*, 1985). However, this uncertainty points to the need for continued work on the factors and processes affecting water column production. Despite the relative inaccuracy of satellite estimates of water column productivity, it is likely that the improved sampling characteristics of satellite data will help reduce these errors. It is also clear that any program that intends to study global biological processes in the ocean will need to employ a variety of sampling methods (Smith *et al.*, 1982).

A program to monitor global primary productivity would be a key component in any study of global biogeochemistry (National Academy of Sciences 1984; Butler *et al.*, 1984). Such a program would consist of both long-term global monitoring by satellites of physical and biological processes, and a range of detailed *in situ* process studies. The primary satellite measurement would be ocean color as an estimate of near-surface phytoplankton biomass. Given the long term scales of variability (such as El Niño-Southern Oscillation events), it is essential that these measurements be made for at least one decade. Additional data could be collected on chlorophyll fluorescence and pigment group abundance by the same satellite sensor. The monitoring and mapping studies by the satellite need to be developed in parallel with *in situ* process studies. These measurements would be used to complement the sampling characteristics of the satellite as well as to document subsurface and other processes not directly observable by the satellite. These studies would consist of the traditional shipboard sampling programs as well as long-term moorings and drifters equipped with both biological and physical sampling gear. A specific task will be to improve our understanding of the relationship of near-surface phytoplankton biomass to water column productivity. Other studies are obviously important: grazing, vertical mixing, and sinking rates are examples of such processes that will depend on *in situ* measurements.

The Coastal Zone Color Scanner has been making useful measurements of near-surface phytoplankton pigment concentrations since late 1978 (Hovis, 1981). Much work has been directed towards development of processing algorithms (e.g., Gordon and Morel, 1983), and initial uses of CZCS in oceanographic research have been described (Smith *et al.*, 1982; Abbott and Zion, 1985; Brown *et al.*, 1985). The basic CZCS algorithm (after calibration and removal of atmospheric effects) relies on the basic fact that the reflectance spectrum of water carries information on all of the constituents that are suspended in the water.

Although the number of bands available on the CZCS is small, it has been shown that information on coccolithophore presence can be extracted from the satellite data as well as chlorophyll pigment concentrations (Holligan *et al.*, 1983).

The MODIS instrument as described in this report will be able to recover the entire reflectance spectrum. Aside from the fact that the increased number of spectral bands will greatly improve atmospheric correction, this instrument will allow a number of new and important measurements to be made from space. First, we will be able to resolve the chlorophyll fluorescence peak at 685 nm (at least for chlorophyll concentrations >4mg/m^3). The fluorescence/chlorophyll ratio is known to vary for a variety of reasons, including species composition, light history, nutrient status, and growth rate (Kiefer, 1973; Harris, 1980; Abbott *et al.*, 1982). Basically, the amount of light-absorbed solar radiation that goes into fluorescence rather than into the photosynthetic system depends on the physiological state of the phytoplankton. Although fluorescence has been used in many studies as a measure of biomass (e.g., Denman, 1976), we will be able to obtain an independent measurement f biomass using the shift in ocean color (Gordon and Morel, 1983). Thus, we will be able to investigate the patterns of the fluorescence/chlorophyll ratio. Such information may be extremely useful in estimating productivity.

Second, we may be able to separate the presence of other pigments in addition to chlorophyll. This will be very useful information, as many of the major groups of phytoplankton play different roles in nutrient cycling (e.g., nitrogen fixation by cyanobacteria). Although little *in situ* work has been done on this measurement, there is at least some promise that it can be done (e.g., Mitchell and Kiefer, 1984; Campbell and Esaias, 1985). Finally, more detailed information on the reflectance spectrum will allow quantitative measurements to be made in turbid coastal waters. Thus, we might be not only able to measure pigment concentrations in such conditions, but also to obtain quantitative estimates of sediment concentrations. This would be valuable in studies of transport of materials from the land to the coastal ocean.

There are certainly many other uses of such information besides support for multidisciplinary studies of biogeochemical cycles. For example, MODIS imagery would be valuable for studies of mesoscale processes (10 to 200 km, 2 to 20 days) which are very difficult to sample adequately using ships. Imagery can also be used to track identifiable features over several days in order to infer near-surface water velocities. Imagery of phytoplankton biomass has also been shown to be useful in fisheries research (Laurs *et al.*, 1984). Finally, real time broadcast of color imagery is extremely useful for ship-based investigations in order to increase sampling efficiency. There are many other discipline-oriented studies in which satellite imagery of phytoplankton biomass, fluorescence, pigment groups, and sediment concentrations would be valuable.

The characteristic length and time scales of phytoplankton biomass distributions are generally in the range of 1 to 5 days and 1 to 10 km (Steele, 1978; Denman and Powell, 1984). Thus, the spatial resolution of MODIS should be on the order of 1 km in the coastal region and 4 km in the open ocean. The temporal resolution (or revisit time) should be nearly one day, given the average cloudiness over the ocean (about 50 percent). This means that on average a particular portion of the ocean will be sampled 3 to 4 times per week. However, we note that this is an optimistic estimate; some regions and seasons are more likely to be cloudy than others. The result is a space and time series that is irregularly sampled temporally and spatially. For example, on the west coast of North America, clear periods tend to be associated with equatorward (or upwelling-favorable) winds. These events are episodic, lasting for about 4 to 6 days (Huyer, 1983). Between events, the winds are less or are even upwelling unfavorable, and the ocean is obscured by clouds. Also, the ocean west of about 130° W tends to be much cloudier than the area closer to the coast. Thus, the coverage of 130° W is limited and the coverage along the coast biased towards upwelling conditions. This is a fundamental limitation of visible and infrared remote sensing that must be dealt with. There will be other processes that will result in gaps in the time series: specular reflection from the sea surface (which cannot be avoided entirely) and low solar radiance at high latitudes (especially outside of summer) will cause gaps. However, traditional ship sampling is even more irregular: or as long as we are careful with our statistical estimates, we can cope with the satellite series that are basically oversampled in space and undersampled in time (and irregular as well), and still greatly improve our estimates of phytoplankton, chlorophyll, global ocean productivity, and other parameters.

Spectral Band Requirements

During the last several years, considerable effort, both theoretical and experimental, has gone into the interpretation of images of the color of the ocean acquired with the Nimbus-7 CZCS. The goal of the CZCS was to provide estimates of the near-surface concentration of phytoplankton pigments, principally chlorophyll-α. These estimates are based on measurements of the amount of solar radiation diffusely backscattered out of the ocean. Phytoplankton pigments are strongly absorbing in the blue and blue-green regions of the spectrum, in contrast to the green-yellow region. Thus, waters low in phytoplankton pigments reflect more blue light than green, while waters high in pigments appear to reflect more green light owing to the selective absorption of the pigments. The amount of radiation backscattered out of the water and reaching MODIS also depends on factors other than the pigment concentration: the absorption by the water itself, which is weak in the blue but strongly increases at longer wavelengths toward the red; the amount of solar radiation incident on the sea surface in the particular spectral band under consideration; and the amount of radiance backscattered from the atmosphere. In fact, the radiance backscattered from the atmosphere can contribute from 80 to 90 percent of the total radiance received by the sensor, and must be removed to determine the radiance backscattered out of the ocean that contains the information concerning the near-surface constituents of the water. The removal procedure is referred to as atmospheric correction.

The success of the CZCS program led to proposals for follow-on sensors such as CZCS-II proposed for National Oceanic Satellite System (NOSS), the Ocean Color Imager (OCI) proposed for the NOAA series of polar orbiting satellites, and the OCI proposed to fly on the French space platform SPOT-3. Much of the following discussion is based on information generated during those studies.

Choices of the spectral bands for these instruments were guided by seven years of experience with the CZCS. The CZCS had only four spectral bands for atmospheric correction and the subsequent estimation of the pigment concentration: 443, 520, 550, and 670 nm. The bands at 443 and 670 nm are in regions of absorption maxima of chlorophyll-α; 550 nm is in a region where the phytoplankton contributes little to the optical characteristics of the water. At 670 nm the water is also strongly absorbing, so the radiant signal at this wavelength originates, for the most part, from the atmosphere, and hence this band is used for atmospheric corrections. Starting from these highly successful CZCS spectral bands, fine tuning was carried out to try to achieve a better sensitivity in the pigment determinations, and new spectral bands were added to overcome difficulties encountered in situations with very high pigment concentrations. The latest proposed sensor, the SPOT-3 Ocean Color Imager, like the present Coastal Zone Color Scanner (CZCS), is an imaging radiometer that will view the ocean in six to eight co-registered spectral bands: 443, 490, 520, 565, 620, 665, 765, and 867 nm. These spectral bands are chosen to optimize the accuracy of estimating the near-surface concentration of phytoplankton pigments on a global scale. For maximum sensitivity to the presence of phytoplankton, spectral bands centered at the wavelengths of the maximum and minimum of phytoplankton absorption are desirable; however, a Fraunhofer absorption line (G) falls near the maximum of pigment absorption (435 nm), and the absorption coefficient of water itself varies rapidly with increasing wavelength in the region of minimum pigment absorption (565 to 610 nm). To avoid problems associated with these spectral regions, i.e., a reduction of extraterrestrial solar

irradiance because of the Fraunhofer line and difficulty in interpretation because of the rapid spectral variation in the absorption of water, bands of 20 nm width centered at 443 nm (the original CZCS blue band) and 565 nm have been chosen. The CZCS red band has been moved from 670 nm to 665 nm to avoid strong overlap with the *in vivo* sunlight-induced fluorescence feature of chlorophyll-α, centered at 685 nm. The CZCS band at 520 nm, which seems ideally suited for the detection of very low concentrations of suspended material in water, remains unchanged. At high concentrations of suspended material this band will saturate and so a new band centered at 620 nm, where water is more strongly absorbing, has been introduced to overcome this effect.

Dissolved organic material (DOM) (or yellow substances) in moderate to high concentrations interferes with the detection of phytoplankton because of its increasing absorption toward the blue region of the spectrum but is found only in low-salinity estuaries, the outflow from principal rivers, and low-salinity seas like the Baltic. Separation of the effects of phytoplankton pigments and DOM requires very accurate measurements of the reflection spectrum of the ocean at wavelengths smaller than 443 nm. Bands in this spectral region are not included in the OCI because design constraints would have made the addition very expensive, and their absence will not have a serious impact on the proposed mission of the project.

Finally, two difficulties have been encountered with the operation of the CZCS: (1) At high concentrations of pigments or surface suspended sediments, atmospheric correction is difficult because significant amounts of radiance can emerge from the ocean in the red band. (2) At high pigment concentrations the radiance backscattered out of the water in the blue is very small, requiring use of the green and yellow bands (520 to 550 nm), which are rather insensitive to phytoplankton pigments, to estimate the concentration. To overcome the first problem, two new spectral bands in the near infrared (765 and 867 nm) are planned for the OCI, whereas the CZCS has only one broad 700 to 800 nm channel. These bands have been positioned in windows between strong atmospheric water vapor absorption features (the band centered at 765 nm actually consists of two bands, 745 to 759 nm, and 770 to 785 nm illuminating a single detector). At these infrared wavelengths sea water is approximately an order of magnitude more absorbing than at 670 nm, hence, the ocean can be considered totally absorbing at much higher pigment and suspended sediment concentrations. The second problem is overcome by an additional spectral band at 490 nm, i.e., on the shoulder of the phytoplankton blue absorption feature. This band will be available for use at pigment concentrations above those for which the 443 nm band fails.

The choice of these spectral bands was made with the assumption that the OCI would be flown on a platform with an AVHRR to provide estimates of sea surface temperature in the split window 10.5 to 11.5 μm and 11.5 to 12.5 μm. In the event that the OCI platform does not contain an AVHRR, these thermal infrared spectra were to be added to the OCI. Finally, if data rate considerations limited the total number of bands to eight, the OCI bands at 520 and 620 nm, being least critical to the primary mission of OCI, could be eliminated, and the band at 490 nm moved to 500 nm to provide more sensitivity at high pigment concentrations. Thus, the resulting spectral band choice would be 443 nm, 500 nm, 565 nm, 665 nm, 765 nm, 867 nm, 10.5 to 11.5 μm, and 11.5 to 12.5 μm.

By greatly expanding the number and range of the spectral bands available, the MODIS design can remove many of the constraints on the design of the systems described above, providing an opportunity to observe the complete spectrum of the oceans from 400 nm to the thermal infrared. This is important because it will no longer be necessary to limit the choice of individual spectral bands for a specific function, e.g., 443 nm for estimation of pigments at the lower concentrations. Now it will be possible to address the problem of recovering the constituents of surface water analytically through the recognized fact that the information regarding the constituents is contained in the entire reflectance spectrum–its shape and mean reflectance. Through a judicious choice of a few bands it is clearly possible to obtain limited, although valuable, information, as with CZCS; however, the full potential of ocean color remote sensing can be realized only when the entire reflectance spectrum is measured. The choice of spectral bands for MODIS, with this in mind, is made based on two criteria:

1. Spectral bands should be placed at obvious absorption features, e.g., the maximum (435 nm) and the minimum (565 nm) of phytoplankton absorption or the sunlight *in vivo* fluorescence peak of chlorophyll at 685 nm.
2. Additional bands are required to "fill-in" the remaining spectrum throughout the visible region such that the information content of the spectrum is preserved.

One obvious addition of spectral bands over those described for the instruments above is for the separation of phytoplankton pigments and DOM in coastal and estuarine waters. This requires bands in the 400 to 440 nm spectral region. A spectral band centered at 405 nm with a bandwidth of 10 nm would suffice for this purpose and would satisfy the criteria above; however, it should be pointed out that good atmospheric correction for this band will be critical and is subject to research both pre-launch and post-launch. As mentioned above, the maximum of the

phytoplankton absorption in the blue occurs at 435 nm, but this wavelength is not used in present designs owing to the presence of a Fraunhofer absorption line in the solar spectrum. Since a state-of-the-art sensor could be expected to have considerably more sensitivity than conventional sensors, there would be no reason to avoid Fraunhofer lines, so a band should be added at 435 nm with a bandwidth of 10 nm. Again, atmospheric correction will be somewhat more difficult with this band than with that at 443 nm.

Other spectral bands that should be added for specific purposes include 490 nm for estimation of pigments at medium concentration; 520 nm for estimation of pigments at high concentrations and detection of inorganic suspended material at low concentrations; 620 nm for detection of inorganic suspended material at moderate concentrations; 680 nm to observe the chlorophyll-α fluorescence peak centered at 685 nm (placing this band at 680 nm rather than 685 nm avoids interference from the atmospheric water vapor band near 690 nm); and 665 nm, 765 nm, 867 nm, and 1,060 nm for atmospheric corrections. To fill-in the remaining spectrum, the following bands are suggested (in order of decreasing importance): 460 nm, 535 nm, 590 nm, 450 nm, 415 nm, and 640 nm. All bands, except those in the near infrared, have a total bandwidth of 10 nm. With these bands, the largest inter-band gap is 20 nm. A complete listing of these bands is presented in Table 5.

Radiometric Sensitivity

The radiometric sensitivity of these bands should be determined based on the minimum detectable water-leaving radiance desired and the maximum total signal expected. The radiometric sensitivity and digitization should be determined by the requirement that the sensor noise level be significantly less than the signal produced by the minimum water-leaving radiance of interest, and that the noise correspond to one-to-two digital counts. Or, equivalently, the signal-to-noise ratio based on the water-leaving radiance divided by the sensor noise should be the basis of deriving the radiometric sensitivity. It is reasonable to expect that this ratio should exceed 50 under typical conditions. For those bands for which the water radiance is not insignificant under typical conditions (wavelengths less than 600 nm), this corresponds to a much higher than conventional signal-to-noise ratio; e.g., at 520 nm under typical conditions the conventional signal-to-noise ratio is 300 to 500. The saturation radiance should correspond to approximately 1.3 times the maximum radiance expected in each band under typical atmospheric and oceanic conditions. These sensitivity and saturation criteria can be easily determined through simulations.

Table 5. Proposed MODIS Spectral Bands and Priority for the Oceans in the Visible and Near-Infrared Regions

Band	Wave-Length (nm)	Band-Width (Total nm)	Priority
1	405	10	1
2	420	10	4
3	435	10	1
4	450	10	3
5	460	10	2
6	490	10	1
7	520	10	1
8	535	10	2
9	565	10	1
10	590	10	2
11	620	10	1
12	640	10	4
13	665	10	1
14	680	10	1
15	765	40*	1
16	865	47	1
17	1,060	100	1

* This band is "notched" to prevent interference from the oxygen band between 760 and 770 r.n.

Additional Considerations

Additional considerations for the MODIS design:

1. Co-register channels
2. Active calibration (e.g., diffuser plate)
3. Depolarize incoming visible radiation
4. Aerosol measurements
   Other Eos instruments will need to measure aerosols for use in MODIS corrections. This information probably can be stated as concentration versus latitude band. Current visible correction calculations use a "standard" concentration and therefore a nominal absorption for gases such as ozone. This concern is also relevant for infrared work in the 3.5 to 4 μm band where aerosol absorption is a consideration. CO_2 and sulfur aerosols such as those from El Chichon are important. Others should be checked. Again, since these are effects governing the rms error terms, knowledge of their concentration is necessary over relatively large areas.
5. Infrared corrections
   Infrared corrections can benefit from the relatively large space scales for atmospheric variation, and can derive atmospheric temperature and water vapor profiles over scales

of tens of kilometers for inclusion in infrared calculations for sea surface temperature (SST) frontal variability where scales from 1 through 4 km should be resolved.

6. Spatial resolution
MODIS visible resolution should be on the order of 1 km for correction, but can be degraded in stored sample space, if onboard tape recording is a limitation, to the order of 4 km, as is done for the AVHRR instruments.

Sea Surface Temperature

Use of AVHRR-derived estimates of SST and CZCS-derived estimates of pigment concentration has been useful in several studies of mesoscale processes (e.g., Brown *et al.*, 1985; Abbott and Zion, 1985). However, as the CZCS and AVHRR measurements are not simultaneous, there are some severe constraints imposed on studies such as those of cloud and ocean-feature movement between the satellite overpasses, and the necessity to access two separate data archives.

There would be many improvements in both data processing and the scientific quality of the data if SST and pigment measurements were made simultaneously using MODIS. Both SST and phytoplankton pigment are nonconservative tracers: SST can change as a result of heating and cooling, and phytoplankton can grow, die, and sink. However, phytoplankton pigment is a passive tracer whereas SST is intimately linked to the dynamics of the flow field. In addition, pigment concentrations are related nonlinearly to the flow (Denman, 1983). Examination of the differences in the behavior of these two tracers in mesoscale flow may allow us to separate the effects of phytoplankton growth (and death) from fluid flow (Bennett and Denman, 1985). Initial studies of SST and pigment have shown that the evolution of the relationship between these two tracers can be used to elucidate many features of the flow field (Abbott and Zion, 1985).

As SST can be used as an indicator of physical processes, simultaneous measurements of SST may improve estimates of productivity derived from pigment concentrations such as detection of upwelling. Finally, information on SST and the diffuse attenuation coefficient (closely related to the pigment concentration) may be useful in studying mixed layer dynamics and surface transport mechanisms.

In processing, it would be far simpler to obtain both data sets for a given study if the measurements were in the same data stream. Both variables will be used for studies of mesoscale processes: most studies will want access to both data sets rather than just one. As both clouds and ocean features move (clouds typically move several 10s of kilometers in an hour; ocean features can move a few kilometers in an hour), studies that require direct comparisons of both data sets will benefit by having simultaneous measurements. Finally, it will be possible to use information on atmospheric aerosols as derived from the visible imagery to correct for atmospheric effects in the infrared imagery. This should result in improved SST retrievals.

The most stringent requirement for global SST appears to be that stipulated by the World Climate Research Program (WCRP) (see Table 6 from Harries *et al.*, 1983). It is not clear that the needed accuracy for "large-scale processes" can be achieved by either the slightly modified AVHRR on NOAA-K, L, and M or by the Low Frequency Microwave Radiometer (LFMR) on the Navy Remote Ocean Sensing System (NROSS). The MODIS, with its better and more numerous windows in the 8.5 to 12.5 μm and 3.6 to 4.3 μm bands, and with bands in the visible and reflective infrared for better cloud/aerosol detection and correction, is expected to enable satellite SST retrievals that meet the WCRP requirements.

Oceanographic experiments in the WCRP are categorized in three streams of differing time scales (Woods, 1983): stream (1) extended range weather forecasting (several weeks); stream (2) short-term climate prediction (several years); and stream (3) longer term climate prediction (several decades). For the studies in stream (1), updating SST charts with satellite data collected during the previous week or month is considered useful if the interannual thermal anomalies can be resolved. Stream (2) experiments include the investigation of oceanic "teleconnections" to the atmosphere that are thought to be related to oceanic thermal anomalies. A major international project called TOGA (Tropical Ocean and Global Atmosphere) will focus on such processes over a period of 10 years or longer, and a recent TOGA Workshop (Bernstein, 1984) recommended a satellite SST accuracy of 0.3°C for monthly means over 200 × 200 km areas. Another WCRP document (ICSU/WMO/IOC, 1983) listed estimates of satellite SST accuracies required for heat flux investigations, the most stringent being ±0.5°C over 5° × 5° areas. Stream (3) investigations require consistent long-term global times series of highly accurate SSTs, since on decadal time scales it appears quite certain that atmospheric temperature and precipitation changes will be linked inextricably to changes in sea surface temperature, related in turn to CO_2 increases in the atmosphere. The above requirements for "mesoscale processes" or "small-scale processes" can be met by either MODIS- or AVHRR-based (see Tables 1 and 2) infrared measurements, although the more frequent coverage by the AVHRR gives it some advantage over the MODIS for the dynamic "small-scale" processes.

Table 6. Accuracies of Measurements of Sea Surface Temperature For the World Climate Research Program

Large-Scale Processes	
Absolute temperature accuracy	0.2 K
Spatial averaging interval	200-300 km
Temporal averaging interval	20-40 days
Type of data product	isotherm contours in map coordinates
Mesoscale Processes	
Absolute temperature accuracy	1.0 K
Spatial averaging interval	5-10 km
Temporal averaging interval	3.5 days
Type of data product	isotherm contours in map coordinates
Small-Scale Processes	
Absolute temperature accuracy	2.0 K
Spatial averaging interval	1.0 km
Temporal averaging interval	instantaneous
Horizontal gradient accuracy	0.5 K/1.0 km
Type of data product	gridded images located to 10 km

The basic instrument requirements (Tables 13 and 15) for such measurements can be stated as follows:

1. Sufficient number of bands in the visible portion of the spectrum (400 to 1,000 nm) to characterize the shape of the reflectance spectrum
2. Sufficiently narrow spectral bands so as to detect (and in some cases avoid) features that have a narrow spectral signature
3. Sufficient digitization and signal-to-noise ratio to be able to measure small changes in the level of the reflectance spectrum, given the low albedo of the ocean
4. At least one polarized channel to improve atmospheric correction
5. Regular calibration of the entire instrument system to ensure long-term stability of the measurements

To address the scientific questions briefly described earlier, there are observational requirements as well:

1. Given the constraints imposed by cloudiness (about 50 percent of the ocean is obscured by clouds at any one time) and by the time scale of phytoplankton growth, it is essential that global measurements be obtained on the order of once every two days in order to resolve important temporal fluctuations and avoid aliasing.
2. The spatial resolution of these measurements should be 1 km in the coastal zone and 4 km in the open ocean, given the characteristic spatial scale of phytoplankton variability.
3. These measurements should be continued for time scales on the order of 10 years in order to resolve synoptic-scale fluctuations (time scales of months to a few years).
4. The visible radiance field observed by MODIS will include contributions from atmospheric scattering (aerosol and Rayleigh scattering) that account for 50 to 90 percent of the total radiance; observations should be made near local solar noon to minimize errors in the separation of the aerosol scattering, Rayleigh scattering, and water-leaving radiance components, as well as to minimize the amount of specular reflection (glint) from the ocean surface and the amount of surface obscured by afternoon cumulus clouds and low level morning stratus.
5. The sensor should be able to view either fore or aft of the spacecraft (as well as at nadir) to avoid areas of glint.

6. Methods are needed to calibrate the sensor system periodically, using both internal sources and reflected solar radiance sufficient to ensure accurate measurements of ocean reflectance.

Data from other satellite sensors as well as *in situ* measurements will also be necessary if we are to understand the mean and fluctuating components of ocean primary productivity. These needs are discussed in later sections.

ATMOSPHERE STUDIES

Clouds

There are two atmospheric phenomena that can be monitored directly by MODIS: clouds and aerosols. Both play a major role in climate. In addition, they affect other important Earth processes; for example, the geochemical and hydrological cycles. The following section presents some of the physical and distributional characteristics of these constituents and their temporal variations as they relate to MODIS objectives. Atmospheric temperature and humidity fields should be monitored by a sounder accompanying MODIS: this will also help in cloud field determination as well as sea and land surface temperature determination. This is described in Chapter III, Terrestrial Studies.

Impact of Clouds on Weather and Climate

Clouds have a major impact on the radiation balance of the Earth's atmosphere system. Most clouds are both excellent absorbers of infrared terrestrial radiation and reflectors of solar radiation. Clouds reduce the amount of outgoing radiation from the Earth's surface to space. Also, clouds are a major factor in determining the amount of solar radiation reflected back into space. Because of the importance of clouds, they are a crucial component in all meteorological and climate models. In order to model clouds, information is required on a number of cloud properties. Important characteristics are the areal distribution, cloud-droplet size distribution, cloud-top altitude, cloud temperature, and optical thickness. Many of these characteristics can be determined on the basis of multispectral measurement studies in the visible, near-infrared, infrared, and microwave regions to be supplied by MODIS and other Eos sensors. On the basis of such studies, it should be possible to develop a cloud-characteristic climatology and to monitor rainfall over land and oceans. These data are important in understanding the interrelationships of parameters such as sea surface temperature, soil moisture, and vegetation index with cloudiness and rainfall.

Also, these studies should, together with supplemental sounding data, be useful in operational weather applications, rainfall forecasts in particular. Because of the global coverage of MODIS, such forecasts would be extremely important for hydrological monitoring in areas where rainfall measurements are unavailable, i.e., in remote areas and over the oceans. The Eos sun-synchronous polar orbit will, however, result in a temporal bias that will make interpretation of this data a challenge.

Relation of Clouds to Atmospheric Chemical Cycles

The measurement of cloud characteristics on a global scale will also be important from the standpoint of understanding global chemical cycles. Clouds play a very important role in the transport, transformation, and removal of chemical species in the atmosphere. For example, clouds are the dominant mechanism for the removal of the oxides of sulfur and nitrogen that are important in the acid deposition problem, and for removal of soil dust, radioactive particles, and particles produced in combustion processes (soot). It is estimated that on a global scale 80 to 90 percent of these species are removed by precipitation. In addition, the cloud droplets themselves play a major role in the atmospheric chemistry of many gaseous species. The total surface area of cloud droplets is very large and, consequently, gases can be rapidly absorbed once they enter a cloud. Once absorbed, the chemistry of many species will be dominated by aqueous-phase processes. With regard to the acid deposition problem, important species such as SO_2, N_2O_5, and NO_3 may go through fast aqueous transformation in cloud droplets; ultimately, the end products of such reactions are SO_4 and NO_3, the species that are primarily responsible for the pH of precipitation. However, most clouds do not precipitate; they simply evaporate. In doing so the reaction products in the cloud droplets are converted to solid or liquid aerosol particles. Thus, clouds serve as chemical reaction vessels that efficiently convert gaseous species to other chemical and physical forms; they also are efficient in cleansing the atmosphere.

Clouds are also an important contributor to the transportation and mixing of materials in the atmosphere. For example, most chemical species of interest, both natural and anthropogenic, are emitted from the Earth's surface into the planetary boundary layer (PBL), the top of which is usually defined by an inversion that restricts exchange with the free troposphere. Consequently, the concentration of these species and their reaction products is much higher in the PBL. The PBL is disrupted by strong convective activity, which is usually manifested by characteristic cloud types.

Because of the importance of clouds in such processes, a recent NAS report (Global Tropospheric Chemistry: A Plan for Action, 1984) recommends that a major effort be made to understand the role of clouds in tropospheric chemistry. This

effort would be but one component of a major program to develop a Tropospheric Chemistry Systems Model (TCSM). An important component of the TCSM is a cloud transport-transformation-removal model that includes detailed treatments of the physical and chemical mechanisms involved.

The physical aspects of the model would include the parameterization of radiation, condensation, evaporation, stochastic coalescence and breakup, and precipitation development. It is clear that the development of such a model and its implementation will require an extensive knowledge of cloud distribution and characteristics on a global scale. Such information can be obtained only by remote sensing techniques.

Aerosols

An aerosol is defined as a gaseous suspension of liquid and/or solid particles. The aerosol particles found in the atmosphere are formed by two primary processes: by direct injection (e.g., sea salt particles, dust, soot) and as a product of the atmospheric reaction and transformation of gaseous materials (e.g., conversion of SO_2 to H_2SO_4 droplets or to SO_4 salts in particles).

Aerosols can be broadly classified on the basis of their production processes or their composition, and their distribution in the atmosphere. On this basis, the major aerosol types are classified as described in Table 7.

The major issues in the field of aerosol science today, featuring those aspects that might be addressed in a remote sensing program, are as follows: climate, geochemical cycles, anthropogenic impacts, temporal trends in aerosol concentrations, characteristics of aerosol distributions, and volcanic aerosols.

Climate

Aerosols can affect climate in two ways. First, the particles can alter the radiative properties of the atmosphere directly by absorbing or scattering radiation. In order to assess the role of aerosols in climate, the following are required: the size distribution of the aerosols, the composition and/or optical properties as a function of size, the vertical distribution in the atmosphere, and the global distribution. Second, aerosols serve as condensation and freezing nuclei in the atmosphere, and they play a critical role in the cloud formation process.

Current understanding of the climatic role and impact of aerosols on a global (or even a regional) scale is very poor. A major problem is that few data on the distribution and composition of aerosols for vast regions of the Earth are available. This is especially true for the oceanic areas and for most areas of the southern hemisphere.

Table 7. Aerosol Types

Defined on the Basis of Composition or Sources:
Natural
Sea spray residue
Windblown mineral dust
Volcanic effluvia (includes both direct particle emissions and products derived from the subsequent reactions of emitted gases)
Biogenic materials – particles emitted directly and particles produced from the condensation of volatile organic compounds emitted by plants and trees (e.g., terpenes) or the reaction products of these gases
Smoke from the burning of land biota
Natural gas-to-particle conversion products (e.g., sulfates derived from reduced sulfur emitted from the ocean surface)
Man-Made
Direct anthropogenic particle emissions (e.g., soot, smoke, road dust, etc.)
Products from the conversion of anthropogenic gases
Defined on the Basis of Distribution:
Tropospheric background aerosols – a residue of aerosols in remote locations; also includes aerosol produced continuously from a large-area source such as the ocean
Stratospheric aerosols – primarily volcanic effluvia

Geochemical Cycles

Aerosols play an important role in many geochemical cycles and processes. Examples include: (1) The dominant aerosol in the atmosphere on a mass basis is sea salt: sea spray is important in the exchange of a number of substances between the atmosphere and the ocean; (2) Wind-transported soil dust, another major aerosol species on a mass basis, is the major non-biological component in deep sea sediments in most open ocean regions around the Earth; and (3) The aerosol phase of the sulfur and nitrogen cycles is the dominant mechanism by which these species are removed from the atmosphere; indeed, the acid rain problem (discussed below) to a large degree is concerned with the aerosol-related aspects of these cycles.

Quantitative assessment of the geochemical aspects of aerosols is very difficult because of the limited data we have on the concentration and distribution of these species over the Earth. This is particularly the case for remote areas. In the case of soil aerosols, the major sources are located in arid regions, which are typically located in remote, sparsely inhabited regions.

Anthropogenic Impacts

Man is a prolific producer of aerosols and of gases that are aerosol precursors. Estimates vary, but it is generally agreed that about one-third to one-half of the atmospheric flux of oxidized sulfur and nitrogen species can be attributed to anthropogenic sources. This is the cause of the acid rain phenomenon. There is also reason to believe that a substantial portion of the soil aerosols in the atmosphere is derived from human activity, primarily poor land use practices compounded with variations in climate.

Another major aerosol constituent is particulate elemental carbon (PEC) that is emitted by combustion processes. PEC can play an important role in climate because the particles are highly absorbing throughout much of the radiation spectrum. Because of the small size of PEC particles and their unreactive character, PEC can have a long residence time in the atmosphere and it can be transported great distances. The global budget of PEC is essentially unknown, primarily because of the unknown impact of the burning of vegetation in remote regions where it is a common agricultural practice.

A major problem is that of assessing the extent of anthropogenic impacts. This statement applies not only to the problem of determining the quantities of materials involved, but also to gauging the areal extent and degree of these impacts.

The ultimate example of the climatic impact of anthropogenic materials in general and of PEC (and, to a lesser extent, soil aerosol) in particular is provided by the nuclear winter scenario (Turco *et al.*, 1983). To a major extent, the assessment of the climatic impact of nuclear war will depend on the ability to understand and model the production of PEC and soil aerosols, their subsequent transport and distribution in the atmosphere, and their ultimate disposition on the Earth's surface.

Temporal Trends in Aerosol Concentrations

The residence time of aerosol particles in the troposphere is of the order of 10 days. This lifetime is about the same as that of water vapor in the troposphere. The similarity in lifetimes reflects the fact that clouds and precipitation processes play the dominant role in the removal of aerosols from the atmosphere. Because of this short lifetime, it is difficult to develop a synoptic knowledge of aerosol distributions using conventional techniques. Consequently, remote sensing provides the only hope of obtaining a large-scale, integrated picture of aerosol distributions.

The temporal time scales of aerosol-related phenomena range from minutes to years. However, on the larger geographical scale, aerosol distributions are governed by meteorological processes that have lifetimes of days (i.e., individual synoptic events). Individual parcels of pollution-derived aerosols can be followed by satellite as they move off the northeast coast of the U.S. Also, individual dust storms can be followed as they emerge from the Sahara and Gobi deserts. Twice in 20 years the concentration of dust over the Atlantic has increased by a factor of three in response to drought in Africa. Over the long term, the output of particles will vary with climate or with human activity. Continuous and extended global measurements of aerosol concentrations and distributions would enable discernment of trends and the identification of the time scales of these trends so as to relate them better to causes and effects.

Characteristics of Aerosol Distributions

It is difficult to obtain a coherent picture of aerosol distributions over the continents because of the great diversity of sources and because of their temporal variability. Over the oceans, the picture is somewhat clearer in a general, broad sense. The major conclusion is that the continents are the source for many classes of substances found in the marine atmosphere. Figure 7 shows the distribution of Aitken particles over the oceans. Aitken particles have sizes below 0.1 μm. They are produced primarily in combustion processes, having a very short residence time in the atmosphere, of the order of hours to tens of hours. It is clear that the major source of these particles is the continents. Figure 8 shows the distribution of haze at sea for the summer season; the numbers represent the percentage of meteorological reports that cite the occurrence of haze. Haze is caused primarily by particles in the size range between about 0.2 μm and 1 μm. Haze is often enhanced by the hygroscopic action of aerosols which serve as nuclei for the haze particles. When relative humidity is high, haze is considerably thicker. Even though these data were culled from meteorological reports collected before the 1930s, it is clear that anthropogenic sources are a major source of haze-producing aerosols. It is clear that deserts are also a major source of aerosols found over the oceans.

Volcanic Aerosols

Volcanic aerosols generally play a relatively small role in the global budget of aerosol species because of the sporadic nature of major events such as El Chichon. However, volcanoes can have a great impact on climate; only those aerosols that reach the stratosphere are important in this regard–the tropospheric particles have too short a residence

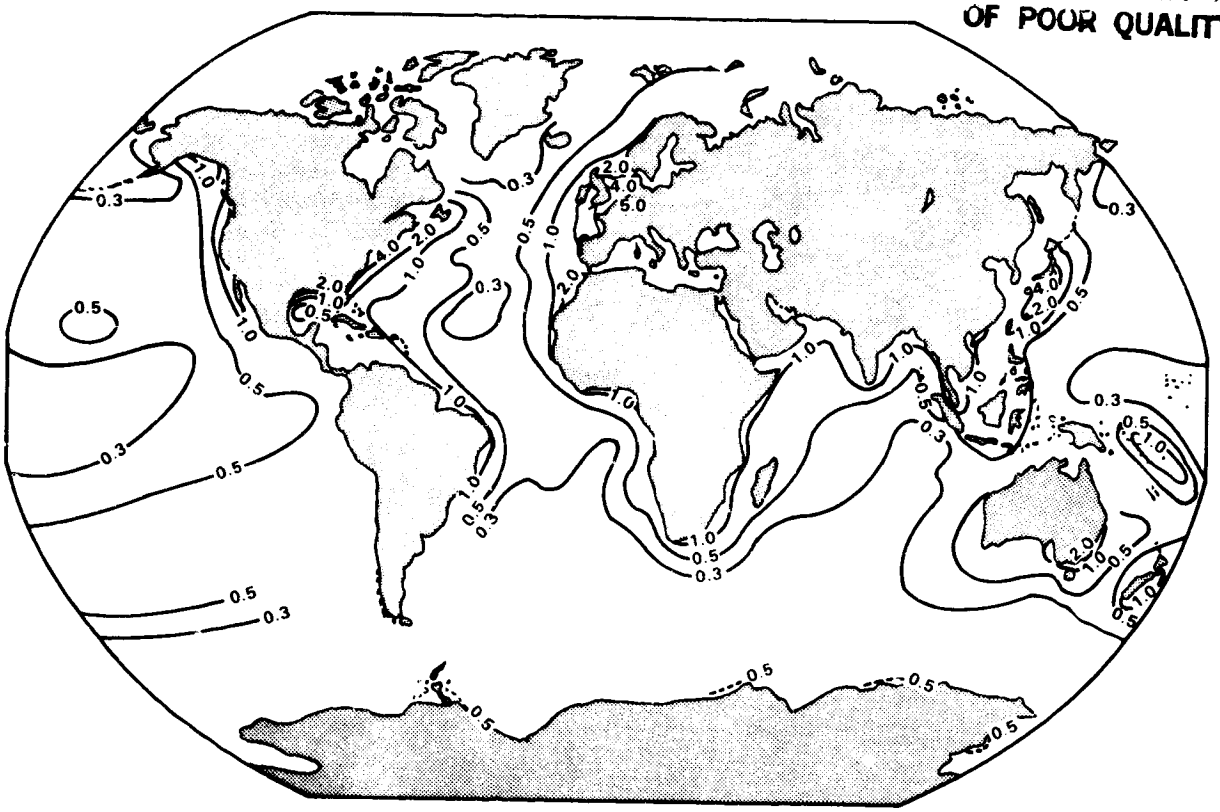

Figure 7. Aitken nuclei concentrations in 10^3 cm $^{-3}$.

time. The emissions that are most important are the sulfur gases that eventually become oxidized to sulfate particles. Over geological time scales, volcanoes have been a major determinant of climate. It is important to understand the behavior and transport of volcanic materials so that the mechanisms by which they affect climate can be better understood. Such studies also provide an insight into the mechanisms by which other types of aerosols affect climate. Because of the sporadic nature of volcanic events, remote sensing techniques are the only means by which systematic measurements of these emissions can be obtained.

Current Status of the Remote Sensing of Aerosols

Visible Imagery (qualitative)

There are many examples of images showing large-scale aerosol phenomena. These include large haze patches related to pollutant episodes, smoke plumes related to major fires, volcanic eruption plumes, and dust storms.

Infrared Imagery (qualitative)

Infrared imagery is used to locate dust storms over the deserts: the dust clouds being at a higher altitude than the surface, radiate at a lower temperature. This procedure has been useful for identifying in a precise manner the location of major areas of soil deflation and relating this knowledge to geology, geomorphology, soil characteristics, land use patterns, etc. Carried out in association with meteorological studies, this work also provides an insight into the mechanisms for larger scale dust storm generation.

Quantitative Measurements

Surface brightness values can be used to estimate aerosol optical thickness. Measurements over the ocean have been shown to have an accuracy of a few hundredths (Griggs and Stowe, 1984). Measurements over land are most difficult because of the non-uniformity of the surface; nonetheless, recent work has shown that the measurements of aerosol optical depth by satellite correlate quite well with ground measurements carried out simultaneously. Furthermore, the fine particle mass ($d<2.5$ μm) at low relative humidity correlates well with the dry scattering coefficient and, therefore, with the aerosol optical thickness.

Ultimately, it should be possible to measure aerosol mass concentrations from satellites. This will require some knowledge of the aerosol size distribution and optical properties. The size distribution over water could be determined by making optical thickness measurements as a function of wavelength. It should also be possible to estimate the

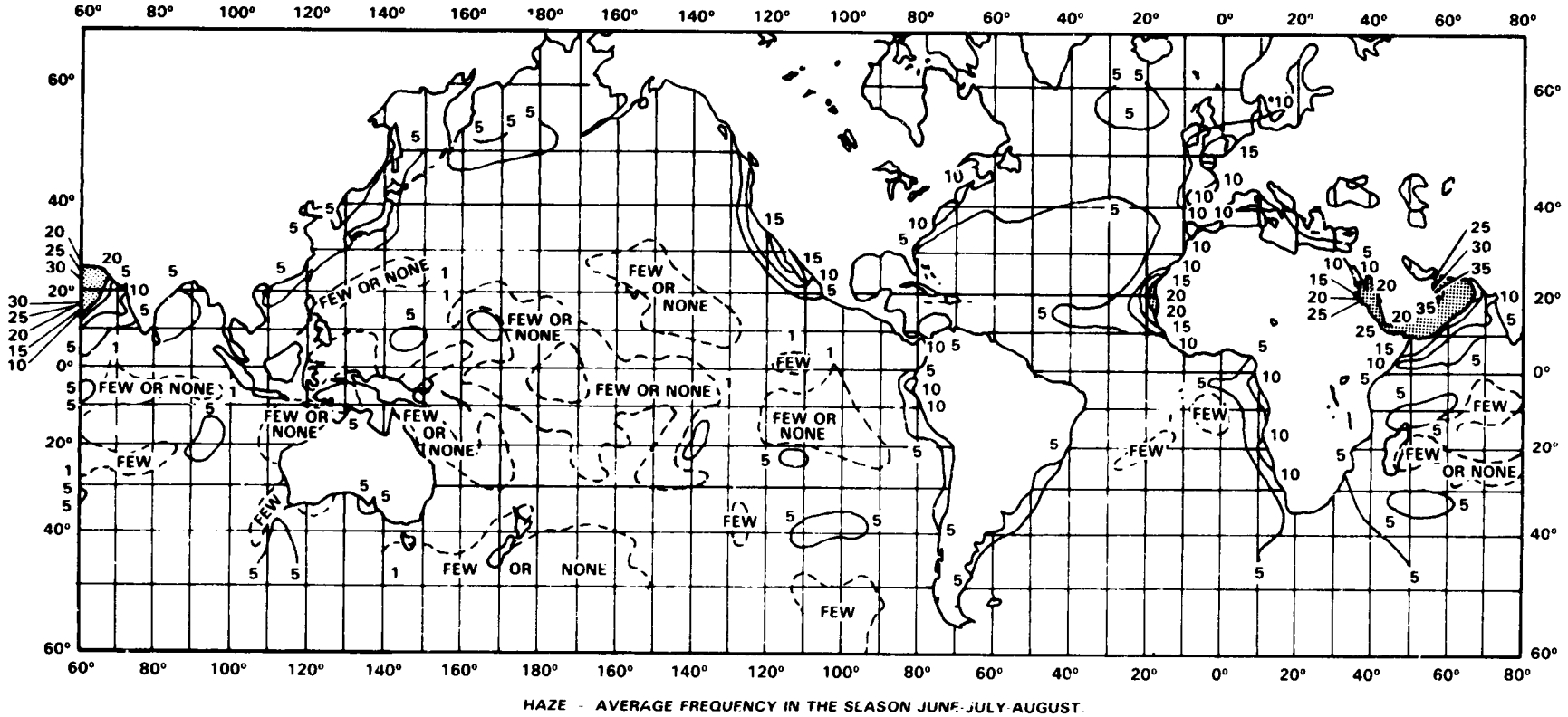

Figure 8. Average haze frequency for June, July, August time period.

absorptive properties of aerosols by making measurements over relatively bright and dark surfaces.

In order to attain MODIS objectives, it would be extremely helpful to have information on the vertical distribution of aerosols and the vertical distribution of relative humidity. It might be possible to obtain the vertical distribution of aerosols by lidar; however, there are major difficulties in interpreting lidar backscatter because the return is very much dependent on some of the same aerosol properties that we are seeking to measure.

Proposed Strategy for Remote Sensing of Aerosols

Aerosols are an important aspect of tropospheric chemistry research. Global-scale measurements of a number of important species are required. One of the major uses of these measurements will be to provide data for development and validation of large-scale atmospheric transport models. It is clear that a network of ground stations will provide a minimal data set for such purposes. Remote sensing of aerosols will complement the ground network and improve the efficiency of both the surface and Eos measuring systems. It can provide large-scale interpolation between the ground stations. The ground network could also make ancillary measurements that would serve as surface truth for the satellite measurements.

On a smaller scale, special emphasis should be placed on programs for sensing in the coastal areas. It is clear that these regions are the most heavily affected by continental sources of aerosol materials. Aerosol measurements in these regions would also be helpful to those studying the water surface color characteristics, whereas satellite measurements will provide estimates of the mass flux of aerosol materials to the coastal zone, these data will enable one to estimate the possible impacts on the marine environment.

Cloud Measurement Requirements

The requirements presented below have been compiled by dividing the interest in clouds and aerosols into four categories for removing data seriously contaminated by cloud and aerosol climatology and for detailed studies of cloud microphysical properties. In order to meet the goals of these categories, information in the form of measurements or assumptions will be required about the state of the atmosphere.

Table 8 summarizes specific measurements that will be applied to one or more of the categories outlined above. In the more detailed discussion below, other supportive observation products such as imagery, temperature, and moisture products will be identified.

MODIS Requirements for Detection of Clouds and Aerosol Editing

Perhaps the simplest treatment of clouds and aerosols in the MODIS concept is to identify their presence in a binary fashion for discarding all data that are so contaminated. This is an editing process, and while this task may sound relatively simple, it is not. Differentiating between snow, ice, or some desert surface and clouds requires more than simple single-channel visible imagery. Likewise, clouds whose spatial extent is less than 20 percent of the field-of-view (FOV) and low-concentration aerosol are difficult to discern. This becomes especially challenging over natural surfaces with relatively high albedos.

Table 9, from a NASA Goddard Proposal, "Cloud Radiation Experiment" (Curran, 1982), outlines the channels required to examine clouds and how each is used.

Table 10 is an initial attempt to define some specific spectral information that will lend itself to the cloud/aerosol identification task. Undoubtedly some revisions and additions will be necessary, particularly for the aerosol layers.

Table 8. Variables Required for MODIS Atmospheric Applications

	Cloud/ Aerosol Editing	Surface Parameter Correction	Cloud/ Aerosol Climatology	Cloud/ Aerosol Properties
Aerosol	X	X	X	X
Cloud	X	X	X	X
T(p), Q(p)		X		X
T_{sfc}	X	X	X	X
$Q_{bnd\ layer}$		X		X
Reflected SW			X	

Table 9. Spectral Channels for Detailed Observations of Clouds

Channel	Band Center (μm)	Bandwidth (μm)	Range (Reflectance)	S/N	IFOV
1	0.7540	0.0012	0.05–1.1	400	1 km
2	0.7607	0.0012	0.05–0.9	400	1 km
3	0.7632	0.0012	0.05–0.9	400	1 km
4	1.131	0.075	0.05–0.9	600	1 km
5	1.639	0.10	0.10–0.8	600	1 km
6	2.06	0.05	0.01–0.4	300	1 km
7	2.13	0.05	0.01–0.5	300	1 km
8	10.99	1.15	N/A	0.18 K*	1 km

NOTES:

Channel 1–0.7540 μm is non absorbing by both ice and water.
Channel 2–0.7607 μm–Oxygen A band 0.7619 μm.
Channel 3–0.7632 used for altitude–Oxygen A band 0.7619 μm.
Channel 4–1.133 μm used to infer mass density of water vapor near cloud top.
Channel 5–1.639 μm is less reflective for ice than water clouds. May also be used to separate snow ice from cloud.
Channel 6–yields correction for cloud penetration with channel 3.
Channel 7–yields correction for cloud penetration with channel 3. Also uses ratio, with 1.6 μm radiance to distinguish between snow and clouds as in channel 5.
Channel 8–*NEΔT @ 300 K

Channels 1, 5, and 9 should enable one to discriminate cloudiness in the field-of-view of the instrument using shortwave information only. Channel 5 is required to delineate high-albedo ice and snow from cloud features. Channels 8 and 10 will be used to discriminate clouds using their thermal radiation signature. Channel 10 will be useful for this purpose primarily during the night-side pass, while channel 8 will be useful both day and night. Channel 8 will be particularly useful for the detection of optically thin, high clouds during daylight hours; these clouds may otherwise escape detection from the short wavelength measurements.

Channels 1, 2, 5, and 9 may also yield an indication of the presence of aerosol in the atmosphere. Channel 9 lies in a spectral region associated with little aerosol absorption; channel 2 lies in a region associated with high reflectance by aerosol species containing iron, while channel 5, as well as channel 9, is relatively unaffected by water vapor absorption.

MODIS Requirements for Correcting Resource Data for Atmospheric Effects – Correction of MODIS surface data for atmospheric effects requires a knowledge of the atmospheric medium between the satellite and the surface. The variables required to make this correction are listed in Table 8. For the purpose of this discussion we will assume that all pixels including clouds have been edited out leaving only pixels with clear atmosphere or aerosol or haze-laden air with optical depths less than one.

One of two tactics for atmospheric correction can be adopted. First, one can attempt to obtain an independent measurement of the variables listed in Table 8 for each pixel, relying solely on simultaneous satellite observations; unfortunately, some of the variables may be difficult to observe in this manner. Second, one could attempt to rely on some average distribution of some or all of the variables to develop a correction based on these average distributions and any real-time observations that might be available. In the following comments it is assumed that

Table 10. Spectral Channels for Editing Cloud or Aerosol Pixels

Channel	Wavelength (μm)	Bandwidth (μm)	IFOV (m)
9	0.52	0.0100	500
2*	0.7607	0.0012	500
5*	1.639	1.10	500
10	3.70	0.20	500
8*	10.99	1.00	500

* See Table 9.

simultaneously observed distributions of the essential variables will be the primary basis for corrections.

Temperature and moisture profiles are observed using a complementary atmospheric sounder instrument. An open question at this time is whether such a set of observations needs to be boresighted with MODIS surface resource data or if some modest relaxation of time simultaneity and spatial resolution can be tolerated for the sounder observations. It is clear, however, that simultaneity is desirable.

Aerosol contamination and appropriate corrections therefore may require two sets of observations of differing spatial resolution. While the effects of aerosols may be monitored on the highest resolution MODIS measurements, it is likely that it will be necessary to look at larger-scale imagery to separate effects of sub-FOV-scale clouds, and aerosols and haze. One would look for spatial and temporal continuity of aerosol and haze, whereas small clouds would probably lack that continuity. This type of imagery could be observed by a complementary imaging instrument or by constructing an image from the MODIS high-resolution data. Once the presence of a dust layer is determined, one could then go back to the high-resolution data listed in Table 8 to make individual corrections. It should be noted that the probability of successfully detecting and correcting for the effects of aerosols is considerably higher over uniform, low-reflectance surfaces such as oceans than over highly variable surface features.

MODIS Requirements for Cloud Climatology Applications – Any cloud climatology developed from MODIS will necessarily be a component in a more comprehensive cloud climatology derived from several satellites. This is because of the limited sample time associated with a sun-synchronous satellite. Ideally, data products derived from MODIS will be compiled in a form suitable for merging with data from Earth-radiation-budget and operational meteorological satellites. With this viewpoint as a guide one can define a set of data products that MODIS might provide that would be useful in cloud climatology studies (Table 11).

MODIS Requirements for Detailed Studies of Clouds – While clouds represent an obstacle to viewing surface features from the satellite, they represent extremely important variables in the climate-weather system. Therefore it would seem prudent to utilize the opportunity when clouds dominate the scenes viewed by MODIS to gather detailed cloud property statistics for use in weather- and climate-related research, and ultimately, in operational applications. Table 12 summarizes the primary cloud property variables observable from visible, near-infrared, and infrared sensors. Table 12 was extracted from a NASA Proposal, "Cloud Climatology and Radiation Budget Experiment for Spacelab-2," (Curran, 1976).

Complementary Atmospheric Sounding Data

Knowledge of atmospheric temperature and humidity structure and cloud fields is important both for correcting MODIS surface observations for atmospheric effects, and for understanding the role of the atmosphere in the land-ocean-atmosphere system. The increased spectral resolution and resulting number of channels used by atmospheric sounders allow for more accurate determination of atmospheric and surface properties than is possible from broadband window channels. This improvement results from an ability to better correct for atmospheric effects and to utilize narrow spectral regions which are less affected by atmospheric absorption. In order to achieve the increased spectral resolution, one has to decrease spatial resolution to achieve similar signal-to-noise ratios. Currently, atmospheric temperature-humidity profiles are monitored operationally by NOAA using the combination of HIRS-2, SSU (Stratospheric Sounding Unit),

Table 11. Specification of Cloud Climatology Requirements

Data Product	Derivable From	Horizontal Scale	Comments
Fractional cloud cover	Cloud contamination algorithm	100 × 100 km	See spectral channels under cloud detection
Cloud height stratification	Cloud contamination algorithm + window radiance	100 × 100 km	
	0.76 μm/ 2.06 μm radiance	During day	
	11-14 μm sounder data	Day and night	
Integrated solar radiance (0.3-3 μm)	MODIS SW channels or measured directly		

and MSU infrared and microwave sounding instruments flying on the NOAA series meteorological satellites. NOAA-K, L, and M will include the Advanced Microwave Sounding Unit (AMSU) in place of the MSU and SSU.

Susskind *et al.* (1984) have developed a retrieval system based on finding solutions of the radiative transfer equation representing the observations in the channels of HIRS-2 and MSU. The retrieval system produces atmospheric temperature profiles, and in addition, provides sea and land surface temperatures, cloud heights and amounts, and ice and snow cover. The increased spectral information provides the possibility of producing improved surface soundings, even at the expense of losing high spatial resolution, once thought necessary for finding clear columns, because cloud effects can be treated as part of the analysis. Completely clear columns are not necessary with this technique.

A recently completed sea surface temperature workshop intercomparing monthly mean fields of sea surface temperature derived from AVHRR, HIRS-2/MSU, SMMR (Scanning Multifrequency Microwave Radiometer), and ships and buoys, shows the HIRS-2/MSU fields to be of comparable accuracy to those produced from AVHRR (in the rms sense) when compared to ship measurements. The errors in HIRS-2/MSU fields are more random spatially and do not give large areas of small (0.5°C) but significant anomalies as are observed in the AVHRR data, especially in the western tropical Pacific.

Land surface temperatures are harder to measure than ocean temperatures for a number of reasons. The land surface is highly variable with regard to both temperature and emissivity. In addition, land temperatures may have large and variable differences from the air in the PBL. Consequently, multi-channel regression approaches such as those used in operational analysis of AVHRR sea surface temperatures may not work as well over land. Even the physical approach of analysis of sounding data has limitations in the absolute accuracy of retrieved ground temperature due to uncertainty in the surface emissivity.

Ground temperatures over land are also hard to verify, or even define, because of high spatial and temporal variability. Their day-night difference does give a good measure of the thermal inertia of the ground, which is related to evapotranspiration rates and soil moisture. Monthly mean fields of the difference between the 3:00 p.m. and 3:00 a.m. ground temperatures derived from analysis of HIRS/MSU show good agreement with climatological temperature, moisture fields, and derived cloud fields. Mintz *et al.* (1985) have developed a theory relating the ground temperature differences to evapotranspiration and soil moisture and have derived reasonable fields for a number of months.

Table 12. Summary of Passive Techniques to Determine Cloud Physical Parameters

Parameter	Technique
Optical Thickness	Reflectance at 0.754 μm together with theoretical relationship
Thermodynamic Phase	Reflectance ratio R(1.61 μm)/R(0.754 μm) compared with theory
Particle Size	Reflectance ratio R(2.125 μm)/R(0.754 μm) as compared to theory
Cloud Top Altitude	Agreement in matching 0.763 μm altitude and 2.06 μm altitude from theory
Volume Scattering Coefficient	Agreement in comparison of 0.763 μm and 2.6 μm altitude determination
Temperature/Height	10-12 μm split window; 14 μm temperature inversion product

The HIRS-2 has channels in the ranges 14.96 to 13.37 μm, 11.1 to 6.73 μm, and 4.57 to 3.75 μm, with a resolving power ($\lambda/\Delta\lambda$) of about 100. The spatial resolution of the instrument is about 20 km at nadir and 50 km at 50° look angle. MSU has four channels, and a spatial resolution varying from 100 km to 300 km. Two of the channels, at 50.3 GHz and 53.7 GHz, are very important for optimized multispectral sounding capability. These channels enable the determination of ice and snow fields and, even more importantly, aid the accuracy of infrared soundings under partially cloudy conditions. Currently, retrievals are done on a 125 km grid, and the potential exists for going to a 50 km grid with the HIRS-2/MSU data.

Cloud height and fractional cloud-cover fields are derived from HIRS-2/MSU data primarily from the 14 μm HIRS-2 sounding channels and the 11 μm window. The ice and snow-cover fields are determined by a combination of surface temperature measurements from the window channels in HIRS-2 and the 50.3 GHz surface emissivity as determined from MSU. HIRS-2 also contains a channel in the near infrared and red. Monthly mean reflectance fields, derived from the visible channel, show good consistency with the infrared-derived cloud fields. In addition, other features are apparent, such as deserts and ice and snow effects, though the latter are difficult to distinguish from the clouds at high latitudes. Scenes are selected as clear or cloudy

based only on the thermal channels, so as to use the same cloud algorithms day and night and not bias the day-night cloud difference. To check the accuracy of this procedure, all scenes determined to be cloud contaminated were deleted before creating the monthly mean reflectance field. The resulting field showed no clouds but did have excellent reproduction of the deserts, as well as ice and snow fields that matched those determined from the surface emissivity and surface temperature. Thus, a multispectral sounding complement can not only give temperature humidity profiles necessary to correct MODIS measurements for atmospheric absorption, but also can provide accurate estimates of ground temperature and its day-night difference, ice and snow cover, surface reflectivity, and cloud cover.

While the HIRS-2/MSU, or HIRS-2/AMSU (an advanced 50 km to 150 km resolution microwave sounding unit with more stratospheric sounding channels and humidity sounding capability) will be flying on operational satellites at the time MODIS is launched, it is preferable to have a sounding capability either as part of MODIS, or at least on the same platform, because humidity and clouds are highly variable in space and time (even on scales of 5 to 10 minutes). The potential exists for significant improvement over the current sounding capability or that scheduled to fly on NOAA NEXT. In particular, a design exists for an advanced high spectral resolution ($\lambda/\Delta\lambda \cong 1{,}200$) infrared sounder with a spatial resolution of 10 km (Chahine *et al.*, 1984), which will significantly improve sounding capability, particularly in the lower troposphere and at the surface. As shown in Table 4, high spectral resolution enables the selection of very clean atmospheric windows, with atmospheric transmittance of the order of 0.95 even in very humid atmospheres. The presence of three clear windows also allows for the determination of surface emissivity. The high spectral resolution allows for a set of atmospheric temperature and humidity sounding channels with much sharper, lower tropospheric weighting functions than those of current systems or systems planned for the 1990s.

Simulation studies have shown atmospheric temperature retrieval accuracy to be of the order of 1 to 1.5°C in up to 90 percent cloud cover (Halem and Susskind, 1984). Retrieval accuracy in the lower troposphere will be considerably higher than that expected from the operational AMSU-HIRS system as currently configured. The accuracy of retrieved single-spot sea surface temperatures was shown to range from 0.2°C under clear conditions to 0.8°C under 90 percent cloud cover. Monthly mean sea surface temperature fields should have accuracies of at least 0.2°C at a 50 km scale. This would further increase MODIS's utility. In addition, ground temperatures and their diurnal variations should have accuracies of the order of 1°C. These simulation studies included the simultaneous use of a microwave instrument of the quality of MSU to aid in cloud filtering. The advanced infrared temperature sounder concept instrument would have 28 channels in the ranges 16.48 to 14.94, 11.43 to 8.12, 6.06 to 5.18, and 4.20 to 3.72 μm. The current design calls for 10 km spatial resolution with contiguous coverage on an 833 km orbit. Considerable cooling (detectors to 75 K, instrument to 160 K) is required to meet the signal-to-noise requirements for the small footprint and narrow bandpass.

Addition of such capabilities to Eos would greatly enhance the experiment. Accurate surface temperatures and day-night temperature differences can be retrieved at 10 km spatial resolution. The MODIS 1 km ground temperature measurements, which may have local biases because of uncertainty owing to humidity and emissivity effects, can be used to interpolate fine structure within the 10 km × 10 km box. The high-accuracy lower tropospheric temperature humidity structure determination will improve the ability to compute surface-atmospheric heat and moisture flux.

Two options exist for incorporation of temperature sounder-type capabilities data into the Eos system. It may be included either as a stand-alone instrument, as referred to above, or appropriate channels can be added to the MODIS instrument. While the intrinsic spatial resolution of MODIS is 1 km, it is unlikely that the appropriate signal-to-noise ratio for high spectral resolution sounding requirements can be met at that spatial resolution. Nevertheless, observations in a number of spots can be averaged to give accurate soundings on a degraded spatial resolution. In either event, it is desirable to have a complementary microwave sounding capability to aid in cloud filtering and determine ice and snow cover. In addition, a proper choice of microwave channels will also give rain indications, especially in conjunction with the temperature sounder channels. The temperature sounder can provide accurate estimates of cloud height and fraction on a 10 km scale. Such measurements have been shown to give good estimates of convective rainfall (Richards and Arkin, 1981). Concurrent measurements at 10 km resolution, at 37 GHz and 90 GHz, will give passive estimates of rainfall (Spencer *et al.*, 1983).

Ozone amount is another atmospheric property that affects surface imaging in the near infrared. Addition of a co-located total ozone monitoring capability such as the Total Ozone Mapping Spectrometer (TOMS) to the Eos platform is also desirable. A global total ozone field gives good indications of important circulation features such as the jet streams and tropopause heights. TOMS can be used to further improve the atmospheric sounding capability of the temperature sounder(s). While TOMS measures ozone only during the day, the temperature sounder has day and night ozone sounding capability. Comparisons with TOMS data during the

day will give an indication of the accuracy of the temperature sounder total ozone measurements and indicate whether the accuracy is good enough for nocturnal ozone monitoring. Two-dimensional total ozone measurements are essential for these applications. Nadir viewing instrumentation such as SBUV-2, which will fly operationally on the NOAA satellites, is not adequate for this purpose because of large gaps in coverage. Limb-viewing ozone sounders are not designed to give adequate horizontal resolution for this purpose and coverage and therefore do not satisfy this need.

The ultimate in vertical resolution and accuracy of atmospheric temperature-humidity profiles, as well as aerosol distribution, will come from lidar instruments, although lidar will not be able to give information about sea surface temperature, or ground temperature diurnal variations. Lidar, at least at first, will not provide the complete spatial coverage given by the passive sounders. Simultaneous analysis of spot lidar soundings, with their intrinsically high vertical resolution together with a field of passive temperature soundings, should provide a much more accurate field of temperature and humidity profiles than would be achievable by either instrument type alone. The high-accuracy lower tropospheric temperature-humidity soundings will improve the ability to compute surface-atmosphere heat and moisture flux.

SNOW AND ICE RESEARCH

Using 1 km visible and infrared imagery, the seasonal distribution of snow and ice can be documented both on land and oceans during cloud-free conditions. MODIS observations will be used directly to aid in assessment of snow cover and sea ice coverage, and will complement all-weather observations made with microwave radiometers (25 km resolution globally) and SAR (30 m resolution regionally). Knowledge of snow cover and thickness is important for terrestrial radiation budgets, meteorology, and hydrology, and is an important environmental parameter in ecosystem assessment. For the latter application, the availability of snow cover extent with measurements of green plant material provided by MODIS is of great importance.

Sea ice coverage has a major effect on air-sea heat flux calculations and is a sensitive indicator of climatic change. Furthermore, it has important operational considerations for shipping and fishing activities as well as for identifying locations of ice features for research expeditions. Areal coverage of open water within the ice pack and distributions of various types of sea ice are of prime concern to ice scientists. Distinguishing between sea water and pools of meltwater on the surface of the larger ice floes is one area where MODIS can contribute significantly to the elimination of ambiguities in microwave observations.

The marginal ice zone (MIZ) the area of active ice formation and melt, is a region of intense biological production resulting from ocean mixing processes associated with the MIZ and growth of algae on the bottom surface of the ice. Enhanced biological production associated with ice formation and melt leads to a very rich food web supporting large fish, mammal, and bird populations. There is a potentially opposite feedback mechanism operating here as well, namely, enhanced production causes solar heating to be confined to a shallower depth, leading to higher temperatures in the upper few meters of the ocean, which would temporarily serve to inhibit ice formation during the spring and fall. Availability of ocean color and surface temperature data along with ice extent on a continuing basis will enable these interdependences to be investigated to a much greater extent than is now possible.

The MIZ and polynyas are also sites of formation of the cold, dense, deep waters of the world's oceans. Better knowledge of seasonal and interannual variability in their regional extent and processes occurring in sites of deep water formation are critical for unravelling the role of the ocean in global heat flux and climate cycles. The chemical composition and radionuclide content of the deep water are used to trace its decadal-scale motion and mixing in the deep ocean basins. Since these properties are strongly influenced by biological processes operating in the upper layers at the sites of formation, better knowledge of the initial surface bio-optical properties of incipient deep water will be useful to the tracer effort.

The MODIS instrument requirements for snow and ice research are exceeded by the requirements for ocean color, SST, and land assessment. The 0.5 to 1.0 km resolution using visible and near-infrared bands, with daily coverage in the polar regions, is fully adequate to complement microwave sensors for distributional assessment. Research applications of the remaining infrared bands are also considered important. Depth of snow pack is not addressable with MODIS. Potentially, discrimination of sea ice thickness up to tens of centimeters may be possible based on spectrally dependent reflectance in the visible region. For obvious geographic and seasonal reasons, use of MODIS in snow and ice observation will require high radiometric sensitivity and near noon equatorial crossing to deal with the low-incident light levels (somewhat offset by the high albedo) and good atmospheric correction routines to deal with the long atmospheric incident path length and multiple scattering by the atmosphere. Since atmospheric scattering at high latitudes is strongly polarized, the polarization discrimination ability of MODIS will be quite useful in this regard.

OPERATIONAL NEEDS

The operational needs that could be met by MODIS measurements are largely those outlined in Chapter II, where complementary operational capabilities are discussed. Meeting the requirements for studying living marine-resource activities, in particular, would depend on MODIS if no Ocean Color Imager were carried on an operational spacecraft during this period. Aerosol distributions and aerosol corrections to satellite-derived sea surface temperatures are important for operational products. Plant growth-health indices derived from MODIS data are expected to be significant improvements over the rather crude vegetation index calculated from AVHRR measurements, and these could lay the basis for future operational products for agriculture and forestry. The scientific success of MODIS in the above research activities covering land, oceans, cryosphere, and atmosphere will make this instrument a prime candidate to replace the currently used NOAA/AVHRR.

IV. THE MODIS SENSOR SYSTEM

BACKGROUND

As discussed in the preceding chapter, MODIS must be capable of conducting global surveys to support terrestrial, oceanographic, snow and ice, and atmospheric science. The two attributes of MODIS that are crucial to its mission are its numerous spectral channels in the region between 0.4 and 12.0 μm, and its revisit time of two days for channels viewing reflected solar radiance and one day for thermal channels. The goal is to develop a sensor system that will address the widest possible variety of research tasks that further the science objectives of Chapter III, within the limitations of the available resources and consistent with the overall goals of the Earth Observing System.

Heritage for MODIS includes the Coastal Zone Color Scanner (CZCS) of Nimbus-7, the Ocean Color Imager (OCI) being planned as a follow-on to the CZCS, and the various models of the Advanced Very-High-Resolution Radiometer (AVHRR, AVHRR-2, and AVHRR-3) being used on the NOAA series of operational weather satellites. Each of these has demonstrated advances both in remote sensing technology and in the numerous scientific problems that can be addressed with frequently repeated, multispectral, 1 km resolution global surveys.

The CZCS is a six-channel imaging spectrometer that has demonstrated the ability to convert remotely-sensed data to maps of oceanic chlorophyll. The OCI is an eight-channel enhancement of the CZCS design. The AVHRR series of sensors has been utilized as the operational ocean temperature sensor and cloud imager during the last six years, and will continue as such into the mid-1990s through NOAA-K, L, and M. These sensors have fully demonstrated an ability to generate global surveys of a wide variety of ocean, land, and atmosphere parameters at a resolution of 1 to a few km on a daily to weekly basis. The experience gained from the AVHRR and CZCS in technology utilization, sensor and data calibration, space operations, and ground data processing is directly transferable to MODIS.

In developing the scientific requirements for MODIS, it was apparent that the requirements for (1) the ocean color sensing channels to view 20° fore or aft of nadir in order to avoid specular reflections of sunlight (glint) from the ocean surface, (2) the need for uninterrupted long-term surveys of ocean chlorophyll, and (3) the desire for the terrestrial viewing channels to have minimum atmospheric path radiance for most applications were incompatible with a single sensor package. This is especially true since the planned polar orbit and 1,500 km swath width would result in numerous passes along the United States coastlines that would include both ocean and terrestrial sites in each scan line. Therefore, it is proposed that MODIS be implemented in two packages to be designated MODIS-T (tilt) and MODIS-N (nadir), the former containing the required ocean color channels and to be pointable fore or aft of nadir, and the latter to contain those channels with no requirement for off-nadir pointing. The two packages are discussed in some detail in the following paragraphs. The sensors are not independent as they will require a joint data multiplexer so that the data from T and N can be transmitted jointly.

MODIS-T

MODIS-T (tilt) will address those science requirements that call for viewing the surface at predetermined angles forward or aft of the subsatellite point (nadir). These requirements include: (a) minimizing the amount of specular reflectance of solar radiance from the surface, (b) examining the BRDF of large homogeneous targets, and (c) performing atmospheric studies by examining the spectral signal at several optical depths. The high-priority ocean color requirements result in a need for both fore and aft pointing in 1° to 2° steps to a maximum of 20°, a set of 17 spectral channels in the visible and near-infrared region (0.4 to 1.0 μm) (see Table 5), a spectral width of approximately 10 nm for all channels, a signal-to-noise minimum of 600:1 for the visible channels, frequent revisits, and acquisition of long-term global data sets. The oceanographers on the Panel stated that spatial resolution of 1 km in the coastal regions is sufficient, and that the resolution in open oceans could be reduced to 4 to 10 km. It was decided, however, that any such reduction in resolution would best be done during ground processing. The BRDF requirements include viewing to angles as large as 60° both fore and aft. Other requirements, both for BRDF and for the proposed atmospheric studies, are less restrictive and therefore fit within those for ocean color.

Sensor Concept

The MODIS-T requirement for a minimum of 17 spectral bands with 10 nm width, and the desire for additional bands in the region from 0.4 to 1.0 μm, can be satisfied by any of several types of imaging radiometers. A practical system in terms of size, complexity, technology availability, and overall utility is that of the imaging spectrometer shown in Figures 9 and 10. The system consists of a crosstrack scan mirror, collecting optics, spectrometer, and a 64 × 64 element silicon detector array, with the

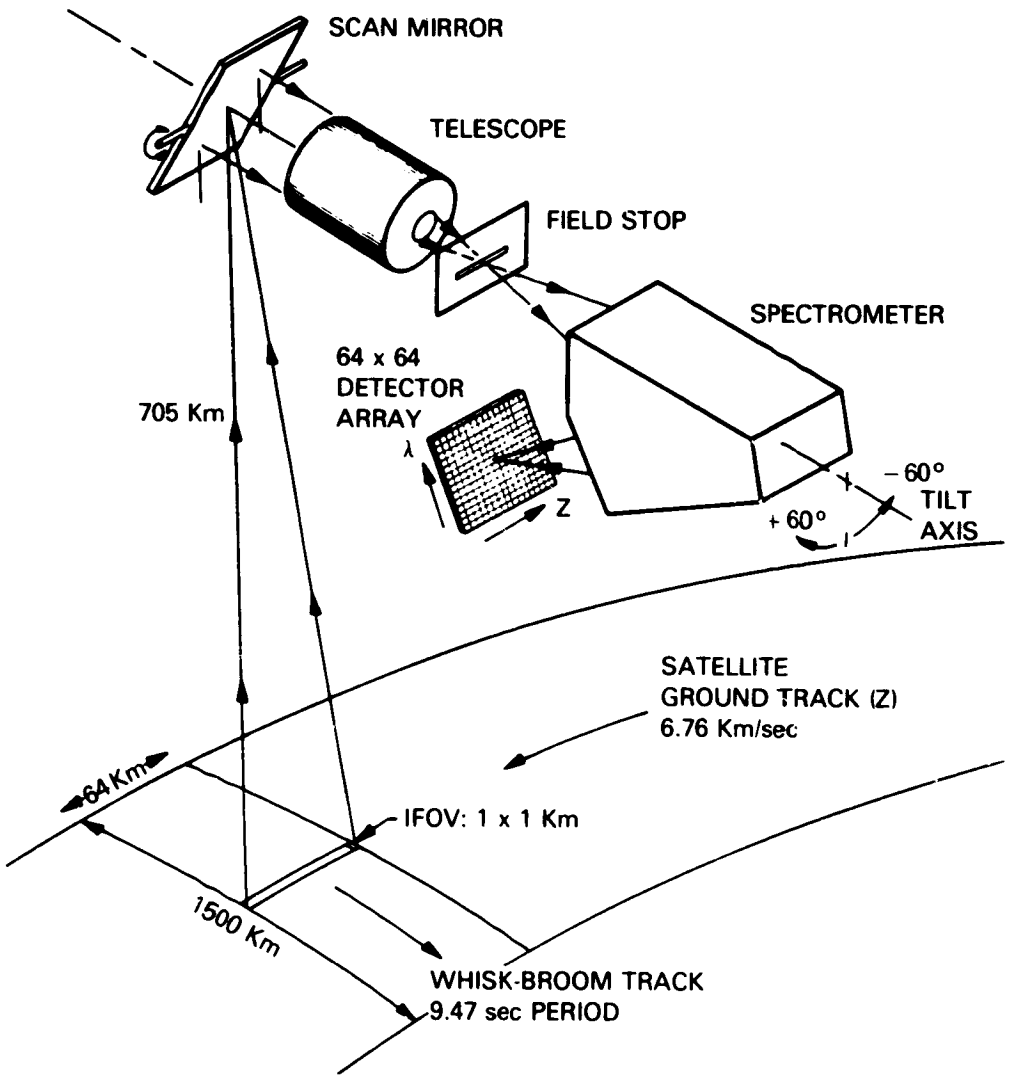

Figure 9. MODIS-T scan geometry and conceptual system layout.

entire system capable of ±60° rotation about the optics axis to give the required fore-aft tilt. The scan mirror views the 90° swath required for two-day global coverage in 9.5 seconds, the time required for the platform subsatellite point to advance 64 km. The collecting telescope can use either reflective or refractive optics or a combination of the two. The spectrometer disperses the beam from the entrance slit along one dimension of the detector array. Therefore, the image of the spectrometer slit on the surface consists of 64 elements along track, with each element being dispersed into 64 perfectly registered contiguous bands of approximately 10 nm width covering the range from 400 to 1,000 nm.

The parameters used to calculate the signal-to-noise anticipated for MODIS-T are listed in Table 13. It is worth noting that the entrance aperture (telescope diameter), which sizes the entire system, is only 5.0 cm. Also, note that the signal-to-noise calculations were made using a sensor look angle of 20° and an atmospheric model with total nadir optical thickness of 0.72.

The calculated signal-to-noise ratios for 25 of the 64 channels of MODIS-T, using the parameters listed in Table 13, are tabulated in Table 14. The resulting numbers are in excess of 1,000:1 from 400 through 540 nm and greater than 300:1 for wavelengths shorter than 900 nm.

MODIS-N

MODIS-N (nadir) will address those scientific tasks that do not require the system to be pointed. The requirements generated in Chapter III cover the spectral range from 0.4 to 12.0 μm and include a strong justification for 500 m nadir resolution in several channels in the visible, near-infrared, and shortwave infrared. MODIS-N spectral widths vary from 1.2 to 500 nm. These requirements result in a

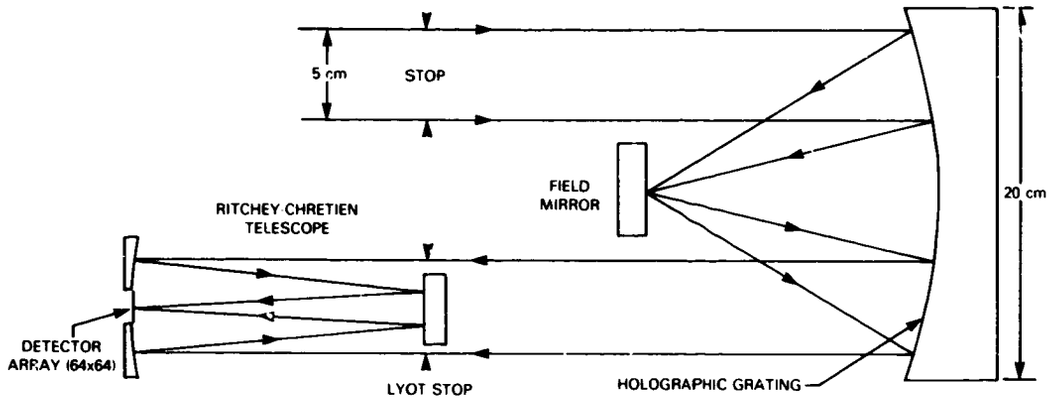

Figure 10. Conceptual optical system for MODIS-T (Shafer, 1981).

system that is more complex than MODIS-T but capable of solving a wide variety of problems in the areas of terrestrial ecosystems, climatology, and oceanography.

Sensor Concept

The requirements outlined above result in a system with at least 35 spectral bands. Owing to the range of spectral widths, and a requirement to measure polarization, it is impractical to use the imaging spectrometer concept of MODIS-T. Instead, a more conventional imaging radiometer is envisioned. This system consists of a crosstrack scan mirror and collecting optics similar to those shown in Figure 9 for MODIS-T and a set of individual detector elements with spectral interference filters located in the focal plane of the collector. The layout of the focal plane is illustrated schematically in Figure 11, which shows the detector/filter layout for 36 channels, 18 maintained at a temperature of 300 K and 18 at 80 K. Each of the 24 1,000 m resolution channels has a single filter/detector module, whereas each of the 12 500 m resolution channels has four detector elements with a single spectral filter over all of them. Since the platform advances only 1 km along track during the swath scan period (148 milliseconds), which is 64 times faster than that of MODIS-T, the optics for MODIS-N must be larger than those of MODIS-T in order for the system to collect the required number of photons in the limited time available.

Signal-to-noise calculations for MODIS-N were made using an optics diameter of 40 cm. This results in a scan mirror as large as 40 × 104 cm. The optics size could be reduced by increasing the number of detectors for each band and thereby scanning more than one line for each pass of the mirror. This, however, increases the mechanical and electrical complexity of the focal plane and the amount of testing and calibration required. This tradeoff must be examined.

Examples of the parameters used to calculate expected signal-to-noise are listed in Tables 15 and 17 for a shortwave infrared and thermal infrared channel, respectively. The results for these and the remainder of the MODIS-N channels are listed in Tables 16 and 18. Typical, but by no means complete, applications are also listed for each band.

Table 13. MODIS-T Parameters for Sensitivity Calculations

Satellite Height	705 km
Ground Resolution	1,000 m
Swath Width	1,513 km
Wavelength	See Table 14
Spectral Bandwidth	10 nm
Solar Zenith Angle	22°
Sensor Look Angle	20°
Optical Transmission	0.1
Detector Size	104 μm
Telescope Diameter	5.0 cm
Optical f-Number	1.5
Surface Reflectivity	See Table 14
Quantum Efficiency	See Table 14
Saturation Radiance	2.1 mw cm^{-2}-sr-μm
(Integration Time) (Dwell Time)	1.0
Time to Map the Earth	2 days
Number of Detectors Per Spectral Band	64
Scanning Efficiency	0.85
Expected NEDρ	See Table 14

Table 14. MODIS-T Twenty-Five of Sixty-Four Spectral Bands

Band	Wavelength (nm)	Detector Quantum Efficiency	Water Reflectance (%)	S/N	Comments
1	410	0.43	4.7	1,100	Dissolved organic material
2	420	0.44	5.0	1,120	Dissolved organic material
3	430	0.47	5.0	1,140	Dissolved organic material
4	440	0.50	5.1	1,170	Chlorophyll absorption maximum
5	450	0.51	5.1	1,180	
6	460	0.52	5.1	1,200	
9	490	0.57	3.5	1,180	High chlorophyll concentration
12	520	0.60	2.8	1,070	Low suspended sediment
14	540	0.63	2.1	1,030	
17	570	0.66	1.7	980	Chlorophyll minimum
19	590	0.67	1.0	~930	
22	620	0.67	1.0	~870	High suspended sediment
24	640	0.67	1.0	~840	
27	670	0.67	1.0	~790	Chlorophyll absorption maximum
28	680	0.67	1.0	~780	Chlorophyll fluorescence
30	700	0.66	1.0	~760	
34	750	0.64	1.0	~670	Atmospheric correction
37	780	0.59	1.0	~600	Atmospheric correction
40	800	0.57	1.0	~560	
44	840	0.43	1.0	~490	
47	870	0.39	1.0	~430	Atmospheric correction
50	900	0.29	1.0	~350	
55	950	0.16	1.0	~230	H_2O
60	1,000	0.07	1.0	~120	
64	1,040	0.00	1.0	~0*	

* Cover this row of detectors for dark current monitor. NOTE: Reflectance obtained from Wolfe and Zissis, 1978.

CALIBRATION

Conversion of digital counts to radiance entering the sensor requires complete characterization of the system prior to launch; including response to an extended standard source, in-flight system monitoring and response to known sources, and constant vigilance over the life of the mission to detect changes in the system and to interpret and compensate for these changes.

The principle standards for prelaunch radiometric calibration will be a visible and near-infrared integrating sphere similar to those used for MSS, TM, CZCS, and AVHRR, and a calibrated black body.

In-flight visible and near-infrared calibration has typically taken the form of monitoring system response to incandescent lamps and referring these changes to the prelaunch values. Thermal in-flight calibration usually is based on viewing a black body built into the backscan portion of the sensor and the near-zero temperature of space. Inclusion of an aperture filling visible and near-infrared sources that is external to the sensor is highly desirable for both

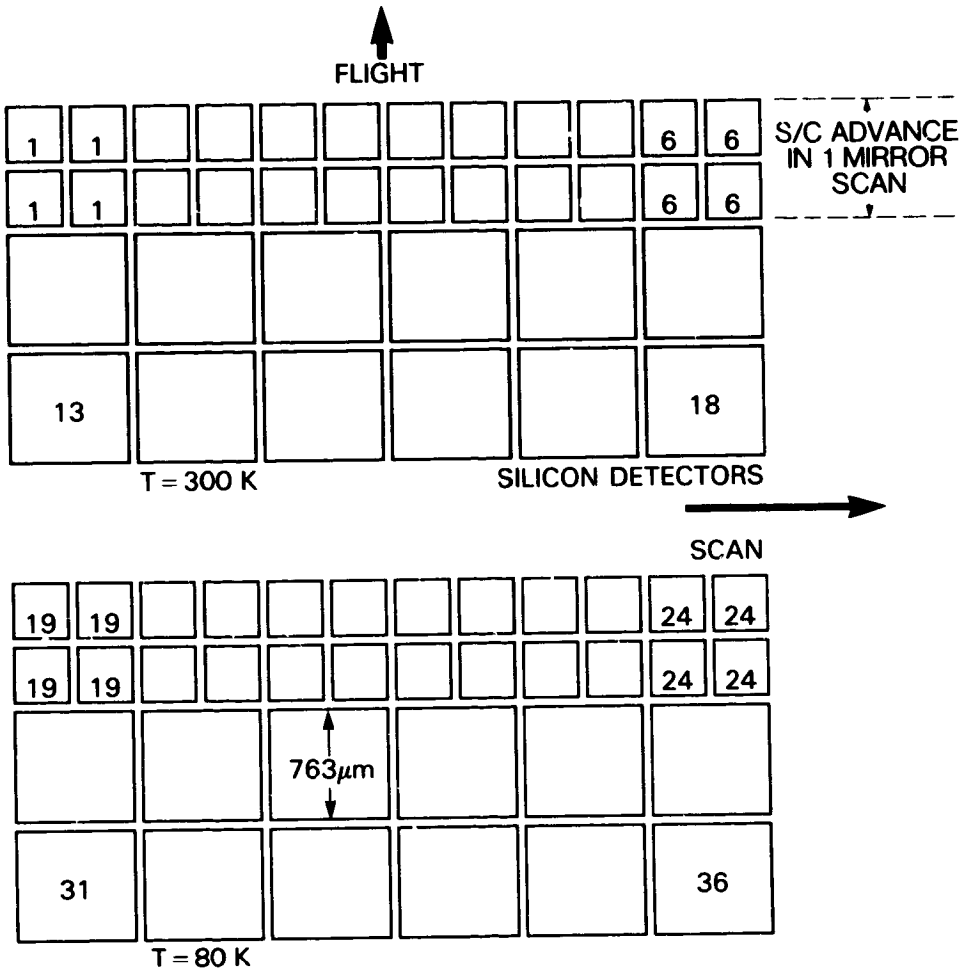

Figure 11. MODIS-N focal plane layout (conceptual) showing 18 cooled (80 K) and 18 uncooled (300 K) spectral channels – Channels 1-6 and 19-24 have 500 m spatial resolution.

MODIS-N and MODIS-T, but may be difficult for the former owing to aperture size. Inclusion of more than one blackbody in MODIS-N is also desirable.

For many of the planned applications of MODIS, the spectral radiance reflected from the surface is compared against the incoming solar spectral radiance. Direct measurement of the solar radiance using a calibrated diffuse reflector bypasses many of the difficulties inherent in radiometric calibration. Therefore, inclusion of a deployable calibrated diffuser is required for MODIS-T and highly desirable for MODIS-N. The 40 cm MODIS-N optics diameter will make the latter difficult.

The third type of in-flight radiometric calibration is accomplished using surface targets that are well characterized and located in areas with a generally clear atmosphere. Careful measurements of the surface and atmosphere at the time of spacecraft overpass coupled with radiative transfer modeling, can result in accurate sensor radiometric calibration.

In addition to in-flight radiometric calibration, it is imperative that any post-launch degradation in the spectral and spatial response of the system be known. Spatial response may best be measured using known surface targets; as with radiometric surface targets, atmospheric measurements and radiative transfer modeling must also be utilized. In-flight spectral characterization may be accomplished using absorption lines in rare Earth glasses or input from light emitting diodes (LEDs).

Precise cross-calibration of MODIS-T and -N is required since the science algorithms will use channels from both sensors. A single calibration source will be used prior to launch. Methodology for in-flight cross-calibration will be developed using simultaneous observations.

Use of as many of the calibration techniques described above as are practical for both MODIS-N and MODIS-T will ensure the greatest possible scientific return for the resources expended.

DATA RATES

Eos guidelines call for a 100 percent duty cycle for MODIS. This implies that the thermal channels

Table 15. MODIS-N – Example of Performance Calculations (Channel 25)

Satellite Height	705 km	Surface Reflectivity	0.10
Ground Resolution	500 m	Quantum Efficiency	0.40
Swath Width	1,513 km	Saturation Radiance	0.71 mw/cm^2-sr-μm
Wavelength	2.13 μm		
Spectral Bandwidth	20 nm	(Integration Time)/ (Dwell Time)	1.0
Solar Zenith Angle	22°	Time to Map the Earth	2 days
Sensor Look Angle	0°	Number of Detectors Per Spectral Band	2
Optical Transmission	0.35		
Detector Size	382 μm	Scanning Efficiency	0.25
Telescope Diameter	39.8 cm	Calculated	247
Optical f-Number	1.35		

Table 16. MODIS-N Visible/Near IR Channels (Preliminary)

Channel	λ (nm)	Δλ (nm)	IFOV (m)	Surface Reflectance (%)		S/N Calculated	Comments
1	470	20	500	3	(B)	740	Soil-Vegetation Differentiation
2	550	20	500	10	(B)	920	Green Peak Chlorophyll
3	670	20	500	6.5	(B)	770	Chlorophyll Absorption
4	710	20	500	9	(B)	830	RED-NIR Transition
5	880	20	500	25	(B)	850	Vegetation Max Reflectance
6	960	20	500	24	(B)	520	H_2O Peak
7	435	10	1,000	5.1	(C)	1,480	Low Chlorophyll
8	490	10	1,000	3.5	(C)	1,520	Nonlinear Chlorophyll
9	520	10	1,000	2.8	(C)	1,390	High Chlorophyll
10	565	10	1,000	1.8	(C)	1,290	Chlorophyll Baseline
11	590	10	1,000	0.6	(C)	1,160	Sediment
12	665	10	1,000	0.17	(C)	950	Atmosphere/Sediment
13	765	10	1,000	0.1	(C)	720	Atmosphere Correction
14	865	10	1,000	0.1	(C)	470	Atmosphere Correction
15	754	1.2	1,000	30	(D)	920	Cloud Altitude
16	761	1.2	1,000	90	(D)	1,550	Cloud Altitude
17	763	1.2	1,000	50	(D)	1,160	Cloud Altitude
18	500	100	1,000	2.5	(B)	2,880	Polarization
19	500	100	1,000	2.5	(B)	2,880	Polarization
20	1,080	20	500	25	(B)	1,120	Leaf Morphology
21	1,131	20	500	10	(A)	520	Cloud H_2O Absorption
22	1,240	20	500	10	(A)	750	Leaf H_2O Absorption
23	1,550	20	500	14	(B)	480	Leaf H_2O Absorption
24	1,640	20	500	10	(A)	375	Snow/Cloud Differentiation
25	2,130	50	500	10	(A)	250	Cloud Penetration

References: (A) Colwell, 1983 (B) Huck *et al.*, 1984 (C) Wolfe and Zissis, 1978 (D) Personal Communication, W.L. Barnes

Table 17. MODIS-N Thermal Channel S/N Calculation (Channel 35)

Satellite Height	705 km	Telescope Diameter	39.8 cm
Ground Resolution	1,000 m	Optical f-Number	1.35
Swath Width	1,513 km	Surface Temperature	270 K
Wavelength	12.0 μm	Responsivity	4.8 amps/watt
Spectral Bandwidth	0.5 μm	(Integration Time)/(Dwell Time)	1.0
Solar Zenith Angle	22°	Time to Map the Earth	2 days
Sensor Look Angle	0°	Number of Detectors Per Spectral Band	1
Optical Transmission	0.35		
Optical Depth of Atmosphere	0.10	Scanning Efficiency	0.25
Detector Size	763 μm	Expected NEΔT	0.011 K

Table 18. MODIS-N Thermal Channels (Preliminary)

Channel	λ (nm)	Δλ (nm)	IFOV (m)	NEΔT (K@ 270 K)	Comments
26	3,750	90	1,000	0.14	Clouds & Surface Temp*
27	3,959	50	1,000	0.14	Clouds & Surface Temp
28	4,050	50	1,000	0.13	Clouds & Surface Temp
30	8,550	500	1,000	0.01	Stratospheric Aerosol Detection
33	10,450	500	1,000	0.01	Stratospheric Aerosol Detection
34	11,030	500	1,000	0.01	Clouds & Surface Temp
35	12,020	500	1,000	0.02	Clouds & Surface Temp

* Temperature

will be on at all times and the reflected solar channels will be on for one-third of each orbit. Assuming 10-bit digitization, 40 percent over-sampling in the crosstrack direction, and contiguity at nadir, MODIS-N, with 24 channels having 1,000 m resolution and 12 channels with 500 m resolution, will output 7.6 Mbs (megabits per second) in daylight and 1.2 Mbs during the remainder of the orbit. MODIS-T, using the same assumptions and outputting 17 of its 64 spectral channels, has a data rate of 1.2 Mbs (day only). These rates result in a total of 3.4×10^{11} bits per day. This is equivalent to 200 CCT (computer compatible tapes) per day (at 6,250 bits per inch (BPI)).

V. MISSION OPERATIONS REQUIREMENTS

TILTS

The MODIS-T instrument will be capable of operation with a tilt of 60° fore and aft as well as nadir. The entire instrument will be tilted, not just the scan mirror, which will lead to a scan pattern different from that of the present instruments. The time to tilt from fore to aft of 20° over the ocean to avoid glint will be a few seconds, so as to minimize the data loss. Tilts in excess of 20° will be used over land for BRDF measurements.

The onboard processing system would know the position of the sunglint point, and could control the acquisition along the scan to acquire the data on the appropriate part of the scan, even near the glint.

GAINS

The required accuracies can be achieved with 10 to 12 bits digitization. If 12-bit digitization is achieved, there will be no need for commandable or programmable gain control within the data system. If 12-bit quantizing is not included, then it may be necessary to have some commandable gains to minimize the quantizing noise in the signal. These would be selected using the solar illumination angles and world map information to best use the available dynamic range of the analog-to-digital converter.

ONBOARD PROCESSING

The onboard processing system of MODIS will have information about the current and future positions of the spacecraft, the attitude of the spacecraft and the sensors, sun position, and surface illumination angles. The system will store a world map that identifies some essential characteristics of the Earth in regions varying in size from approximately 30 km × 30 km to 300 km × 300 km, depending on their location. Each region can identify between four and eight different surface cases, such as deep ocean, coastal water, estuaries, barren land, natural vegetation, cultivated land, nominally snow or ice, urban areas, special investigation region, etc. The specific bands selected for acquisition and any processing for bandwidth reduction can be optimized for each of the classes. This would primarily apply to the MODIS-T instrumentation, selecting which 17 of the 64 available bands would be acquired. It would also permit control of the resolution of the data acquired, i.e., 1 km in coastal areas and 4 km in the open ocean. Over land a few selected bands (or synthesized bands by summing selected channels) from the fore- and aft-looking instrument could be acquired to provide some bidirectional information.

The system would have a minimum solar illumination angle defined to identify Earth day or night and the solar reflectance channels would not be acquired at night. The world map could have an effect on the definition of acceptable angles since some very-low-angle data may be desired over the ice-covered regions.

CALIBRATION

The various applications of the data from MODIS will require very precise calibration of the system both before launch and in flight. Both the MODIS-N and -T instruments are scanners, and this will allow calibration of the total optical system by observing space before and after the Earth scan, and integration spheres and/or black body targets during the back scan. Occasional looks at a diffuse solar reflector or the lunar surface could provide additional useful calibration information (see Chapter IV, Calibration). Every two years, when Eos is visited by the Shuttle, a recalibration using STS-borne precision calibration systems should be done.

Electronic systems will be used to check the linearity of the signal processing electronics and step-size uniformity of the analog-to-digital converters.

OPERATIONS

The MODIS instrument will routinely acquire data over the world using a stored acquisition strategy that is a function of its world map. The strategy can be changed in-flight by loading new tables into the onboard processing system. In addition, there will be a limited number of investigations of specific test areas underway at any time. These will be identified in the world map with special identifiers, and data acquisition will be optimized for these investigations.

VI. GROUND SYSTEM PROCESSING AND ARCHIVING REQUIREMENTS

The processing requirements for MODIS are defined by considering both the volume of data that will be produced by the instrument and the wide range of investigations with their attendant differences in both spectral and spatial requirements. The diversity of applications, both for land and water, leads to the generalized case where each application can require a separate product tailored to the physics of the observables. Given the large volume of data that will be produced by such an instrument, a balance is needed between achieving a suitable breadth in product generation and restricting the computation to usable, e.g., cloud-free, observing periods.

OVERVIEW

The MODIS Panel recommends a multi-tiered approach to processing and analysis of the instrument data. A layered network should be established to meet the need for a limited number of widely used standard products. Simultaneously the low level (Level 0 or data 1) would be distributed to local or regional processing centers for generation of research or specialized products. This approach has the potential to make optimal use of the improved satellite data handling and analysis capability that is projected to exist within interested laboratories and institutions. Thus a central requirement necessary to implement this strategy is the definition and implementation of a network topology.

The network can serve multiple uses ranging from simple catalog searches to distribution of the low-level satellite data for further processing. While the network concept provides a flexible mechanism to generate a range of products, distributed access to supporting data bases (satellite management, sensor instruments, allied instruments) needs to be managed in a coherent manner. Data base coordination with respect to the sensors (MODIS, the platform, allied instruments) and the central and distributed processing centers is a prime concern. The range of science questions that will be addressed by MODIS requires provision for synergistic melding of Earth- and space-based observations. Studies addressing these concerns have been initiated by the Eos Data Panel.

LEVELS OF DATA PROCESSING

The MODIS Panel has formulated a set of level definitions that are used to provide a framework for discussion of data products (see Table 19).

MODIS ARCHIVAL AND DISTRIBUTION REQUIREMENTS

Level 1B data, together with the cloud and land/ocean masks, would be archived permanently. The routine Level 3 products given above would also be archived permanently.

The Eos Data and Information System would have the responsibility for producing user-specific products on request, and would utilize the Level 1B data for this. An example of such user-specific products are those for investigators who would like to develop improved algorithms, or algorithms for new properties, requiring the generation of data sets of particular regions over varying time periods. Storing the Level 1A data in geographically useful regions (Level 1B) would facilitate this, as well as requests for distribution of Level 1A data. Anticipated annual data requests are listed in Table 21.

A substantial application for MODIS data will stem from current practice of use for AVHRR and CZCS data where daily coverage of large geographical regions is used to study evolution of the physical and biological regimes of the ocean's upper mixed layer. Daily coverage is necessary for avoidance of clouds or other contaminating features and to resolve the space time variability inherent in the observables. This class of investigation is currently undertaken in a number of ocean-oriented research institutions. Daily coverage is also utilized for computation of LAI by National Aeronautics and Space Administration/Goddard Space Flight Center (NASA/GSFC). Basin-wide and global analyses are undertaken utilizing GAC data from the NOAA platforms for both terrestrial and oceanic applications. These studies are increasing in scope and number of investigators with the advent of low-cost high-coverage-frequency access based on data distributed by domestic communications satellites (DOMSAT). As global programs such as TOGA, WOCE (World Ocean Circulation Experiment), Global Flux, Eos, etc., enter the research arena, the need for rapid and varied access to satellite products increases and the use of large-scale, synoptic observations of a region or process becomes a routine and indispensable component of a complete observation program.

Data cost and access have been and probably will continue to be prime factors influencing the use of satellite observations. Since the user community spans an experience and capability range from those who need simple images of preprocessed data to those whose research requires large volumes of Level 1A data, the range of capabilities afforded by networking various processing organizations

Table 19. Definition of MODIS Data Products Levels

Level 0	Level 0 data represents the basic telemetry stream as received from the spacecraft for the MODIS instrument.
Level 1A	Level 1A data contains MODIS instrument data augmented with all ancillary data necessary to compute Earth-located, geophysical parameters. Potential ancillary parameters include calibration information, satellite ephemeris, attitude, time, sensor information (gain, tilt, channel selection). Sufficient information or pointers to easily accessible auxiliary data bases should be present within the data stream to allow subsequent processing at an appropriate center. These data would be available in orbit-sequential data bases.
Level 1B	The MODIS Panel reviewed existing and anticipated practice for processing satellite data and recommends that satellite swaths be ordered by region and then by time. This recommendation assumes large-volume, low-cost storage media are available in the MODIS time frame, but the total data volume will still be large. Segmenting the data regionally will permit ready access to that portion of the overall data archive that can be logically grouped. This regional-area data segmentation can be a function for either the central or regional center. Thus geographical blocks such as continents, ocean basins, polar regions, etc., should be established. Coastal zones represent an area where MODIS and HIRIS data can be used to address a range of problems over various space scales. Data should be flagged for presence of land or clouds.
Level 2	Level 2 data are derived geophysical parameters in orbital serial format. Atmospheric corrections and derived-product algorithms are applied here. This level is not reversible to Level 0. A minimal set of derived properties is computed routinely. The number of these properties is expected to be on the order of 25. Some examples are: 1. Terrestrial Leaf Area Index 2. Ocean Chlorophyll Pigment 3. Terrestrial Surface Temperature 4. Sea Surface Temperature 5. Aerosol Optical Depth (over oceans) Additional properties for which algorithms are expected to be well developed by launch: 6. Chlorophyll Fluorescence 7,8. Additional Terrestrial Vegetation Indices 9. Bioluminescence 10. Oceanic Cyanobacteria Index 11. Terrestrial Aerosol 12-15. Atmospheric Properties 16. Oceanic Particulate Calcium Carbonate Concentration (Coccoliths) Items 17-25 are reserved for new properties of general and routine interest for which algorithms are not presently under development.
Level 3	Level 3 data products are spatial and or temporal composites of Level 2 mapped to a fixed Earth grid. Sample time and space scales for compositing are given in Table 20. Each Level 3 grid point should contain the mean, number of pixels used to compute the mean, standard deviation, and skewness. Other Level 3 products may be requested and required to support AO investigators on the MODIS team.

permits the information needs to be met in a cost-effective manner as part of the Eos Data and Information System. These MODIS requirements recognize:

1. A need for some rapid data delivery, specifically in support of field programs and oceanic expeditions
2. The expected demand for standardized products of some basic derived properties, for global-scale interdisciplinary studies in particular

The MODIS Panel has therefore recommended that (near) real-time distribution of low-level data

Table 20. Compositing Scales

Property	Spatial Bins	Temporal Bins
LAI	0.5 km	week
Ocean Pigment	10 km	week, month, annual
Temperature Land	0.5 km	week
Sea Temperature	10 km	week
Ocean Aerosol	100 km	week

be provided as well as routine production and archiving of standard products. The real-time distribution could be effected in several ways, including:

1. Onboard processing to quick-look products with direct transmission
2. Some rapid data center processing and transmission to users via communication satellites
3. Distribution (possibly of selected channels) of Level 1A data to networked processing centers for the purposes of large-scale regional studies, algorithm development where such development requires substantial volumes of data, and global studies requiring specialized processing not compatible with standardized, central service-produced products

Table 21. MODIS Data Requirements–Expected Requests for Data

Requests	Users	Requests/Year	Comments
Access to Level 1B	1. Algorithm developers	50-75	all channels, regional time series (1,000 km)
	2. Field experiments anywhere	2-5, anytime	<1 day, level 3, 1,000 km
	3. Demand for special Level 3	10, up to 50	highest resolution, random regions
	4. Operational product improvement	10	1 month, all data, selected regions
	5. Reprocessing of Level 3 sets	once every 1 to 3 years	improved algorithms, data updates
	6. Regional distributed archives		rapid access to all storage limited, up to 50 centers
Level 2 cloud masks –every Level 1B special request –cloud statistics		2-3	regional requests/yr
Level 3 (No. of requests depends on success of regional centers) –surface temperature land ocean		60 75	(subset of chlorophyll pigment)
–vegetation indices land ocean		100s 250	
–aerosols		50-100	
–others–undefinable, less than above, potentially nearly equal			

VII. MODIS/HIRIS SYNERGISM

Simultaneous imaging by MODIS and HIRIS will present a unique and important capability for terrestrial remote sensing by the Eos system and will provide an invaluable data set for a wide range of studies. The justification for simultaneous high- and low-resolution coverage lies primarily in our need to fully understand the scene radiance of the low-resolution data. The spectral response from low spatial resolution pixels is produced by the reflectance from a diversity of surfaces. Our understanding of such complex spectral responses comes from spatial-spectral modeling studies. Simultaneous imaging by MODIS and HIRIS would produce the data sets necessary to address such scene radiation questions, to test our models of complex surface reflectance, and to calibrate the low-resolution data more accurately than has been possible to date. Calibration of low spatial resolution observations by surface measurements has been hampered by the low accuracy of location for surface sampling. Simultaneous high-resolution data would provide an important intermediate spatial and spectral link between ground measurements and the low-resolution data. The inter-diurnal variations in atmospheric conditions, ocean conditions, soil temperature, and moisture are sufficiently large to warrant simultaneous imaging from HIRIS and MODIS.

In addition to the scene radiation modeling studies, simultaneous high (30 m) and moderate (500 m) spatial resolution data will provide the basis for a multilevel sampling approach for a wide variety of applications, with detailed spatial information being made available in its regional context. Multilevel sampling by remote sensing has long been advocated for range and forest management, and has been used in such applications as desert locust monitoring and crop forecasting. However, difficulties in coordinating, obtaining, and registering contemporaneous coverage from different platforms have rendered such multilevel approaches problematic. MODIS will collect data in 1,000 m and 500 m pixels over a swath 1,500 km wide, while HIRIS acquires data over a 50 km swath with 30 m pixels over land and, by averaging, 150 m pixels over water (in order to attain adequate radiometric sensitivity).

The question of synergism can be understood in the context of phenomena and measurables to be addressed. The following four areas cover the major ways in which the two instruments could provide complementary data.

DYNAMIC PHENOMENA

HIRIS is a target-of-opportunity instrument, while MODIS acquires global coverage every two days. Dynamic surface phenomena such as insect infestation and red tide development, and episodic events such as volcanism and floods will be detected by MODIS. HIRIS can then be targeted to study the phenomena in detail. HIRIS can be pointed $\pm 20°$ crosstrack to reach any point on the globe in a maximum of six days.

CONTEXT AND PIXEL STRUCTURE

When simultaneous or near-simultaneous HIRIS/MODIS data are acquired, investigators for each instrument benefit in two ways. MODIS provides data for HIRIS investigators by developing the scene context. Therefore, mesoscale variability surrounding the HIRIS scene is provided and the effect of larger-scale forcing functions on smaller patterns is seen. Since MODIS is planned for a two-day repeat coverage, temporal interpolation between HIRIS data acquisitions is possible.

MODIS investigators will benefit from HIRIS data because the higher-resolution images will reveal the inhomogeneity and structure within MODIS pixels. Among others, this capability will aid in the study of coastal fronts due to tides or river plumes and the study of marine macrophytes such as Sargassum and kelp. To provide a high-resolution sampling for MODIS, the HIRIS design should include programmable pointing capability that will permit selectable coverage for specific locations within the MODIS scene.

SIGNATURE EXTENSION AND SPATIAL EXTRAPOLATION

Simultaneous MODIS and HIRIS data will make possible surface-reflectance signature extension using HIRIS-generated files of spectral endmembers (signatures) to generate the mixed-pixel signatures of MODIS. In addition, it will be possible to extrapolate processed information developed from HIRIS data to other areas. This will lead, for instance, to global maps of vegetation indices and a better understanding of the limits of MODIS for composition determination. Other examples are the determination of Trichodesmium Nitrogen fixation and sediment transport processes.

ATMOSPHERE

Understanding of the atmospheric spectral transmission and path radiance is a necessity for the

proper utilization of data from either HIRIS or MODIS. Intercomparison of results from both instruments, and from companion instruments such as LASA, will provide better atmospheric corrections, particularly over land-water interfaces. MODIS will provide information on cloud cover surrounding the areas imaged by HIRIS for analysis of adjacency effects.

APPENDIX A: ATMOSPHERIC CORRECTIONS OVER LAND

Satellite measurements of the characteristics of land surfaces depend significantly on the optical effects of the atmosphere. This section discusses such effects for a cloudless atmosphere and methods for correcting for the effects in the spectral range below 3 μm. The essence of the atmospheric effects can be discussed with the aid of the following accurate expression for the radiance (L) of the Earth-atmosphere system:

$$L = L_o + Tr$$

where L_o is the path radiance of the atmospheric column, T is the transmission of sunlight to the surface and then to a satellite, and r is the surface reflectance. All quantities are functions of wavelength, polar angles from the surface to both the sun and the satellite, location, and time. Since the radiance is nearly a linear function of the surface reflectance, if the latter is known for dark and bright surfaces, then the two atmospheric parameters L_o and T can be estimated from the satellite measurements of radiance. Although the method seems simple, it is difficult to apply because the surface reflectance is not usually known with enough accuracy.

The optical effects of the gaseous components of the atmosphere alone can be calculated accurately. The MODIS spectral bands will be chosen in the atmospheric windows, where molecular absorption is weak. McClatchey *et al.* (1971) and Kneizys *et al.* (1983) give methods for calculating atmospheric transmission. Well developed radiative transfer models exist for calculating molecular and aerosol scattering (Lenoble, 1977). Since aerosols are always present in the atmosphere, the molecular scattering should not be considered independent of light scattered by aerosols, when the aerosol optical density is large on either the path from the ground to the sun or to a satellite.

The difficulties in making atmospheric corrections are caused by aerosols, since their optical properties are difficult to estimate during satellite observations: their properties are not known accurately and they are variable. The aerosol optical parameters are their optical thickness, single scattering albedo, and scattering phase matrix. The scattering phase matrix, which accounts for the polarization properties of scattered light, is required instead of just the phase functions, if any of the following three conditions apply:

1. The MODIS radiometer is sensitive to polarization
2. The polarization of light reflected from plants is measured
3. Accurate atmospheric corrections are calculated for atmospheres containing moderate amounts of haze

Some idea of the accuracy required for the aerosol optical parameters can be given for two atmospheric states and observations near the nadir direction. Assume that the surface reflectance will be measured with an accuracy of 0.01. A rather common state is one where the aerosol optical thickness is 0.2, its albedo of single scattering is 0.96, and the surface reflectance is 0.1. The required accuracy of the optical thickness is 0.1, and an accurate value of the single-scattering albedo is unimportant. This implies that atmospheric corrections are not required for near-nadir observations, if the aerosol optical thickness is less than 0.2 (Schowengerdt and Slater, 1979). To take another example, consider the problem of dense haze (an optical thickness of 0.6) that is common in such places as the eastern United States during the summer, or the Sahara region. The optical thickness is still an important parameter, but now the radiance is sensitive to the aerosol single-scattering albedo, which has to be specified with an accuracy of 0.02, when the surface is bright (r = 0.4) (Fraser and Kaufman, 1985). The reflectance measured at a satellite, however, depends on both the optical thickness and the single-scattering albedo when the zenith angle at the ground of a ray from the ground to either a satellite or the sun is large.

The aerosol optical properties are a function of wavelength, but the correlation of the same parameter at two different wavelengths is generally good. The aerosol optical thickness can vary from hundredths to values large enough to obliterate surface features. Usually, the visible optical thickness range over land is 0.05 to 1.0. The aerosol single-scattering albedo ranges from 0.5 in some urban environments to 0.99 in rural environments (Shettle and Fenn, 1979). The scattering phase matrix depends on molecular scattering and on aerosol size, composition, and shape. This matrix has large variations (Sekera, 1957).

The small amount of experimental data indicates that the spatial gradients of aerosol parameters may be important when moderate to dense haze is present. The vertical profiles of the parameters are important for calculating the transfer of radiant energy from outside to inside the instantaneous field-of-view (IFOV); but this adjacency effect is significant for IFOVs smaller than that of MODIS (Kaufman, 1984). The vertical profiles become more important with increasing amounts of haze and large polar angles from the point of observation to either the sun or satellite. The horizontal gradients of the optical parameters depend on the locations of

sources such as cities, forest fires, agricultural burnings, and dust storms. The smallest significant scale seems to be about the depth of the mixed boundary layer (about 1 km) (Stull and Eloranta, 1984). Since the aerosols are frequently hygroscopic, their optical properties depend on the relative humidity, which changes diurnally.

Two general approaches have been used or considered for making atmospheric corrections to the radiances measured from satellites. One approach is essentially empirical, whereas the other involves computations with radiative transfer models. In either case, analyses can be simplified by accounting for the variation in flux of solar radiant energy incident at the point of observation by ratioing the spectral radiance to the solar spectral irradiance. Then atmospheric effects can be reduced by ratioing the normalized radiances in the various bands. This method is most successful when the radiance is strongly dominated by light reflected from the ground. Another empirical method is to make a principal component analysis of the normalized radiances in the various bands (Lambeck, 1977). The components with information about the surface parameters tend to be independent of atmospheric effects. Such empirical methods, however, do not have general applications.

The other approach utilizing radiative transfer models requires specification of the aerosol optical properties, which is difficult to do. The accuracy of the computed radiance is not restricted by the numerical methods, but by the agreement between the models of the atmosphere and its true state on the occasion of satellite observations. In addition to calculating the atmospheric transmission and path radiance, the modulation transfer function of the atmosphere can be calculated, and applied to the Fourier transform of the measured radiances, in order to find the Fourier transform of the surface reflectance (Kaufman, 1984). Atmospheric correction procedures may complicate processing of satellite measurements so much that corrections will be made only on limited sets of measurements.

When atmospheric corrections are computed with radiative transfer models, only climatological data on aerosol optical parameters will be available (Shettle and Fenn, 1979) unless special efforts are made to measure the optical parameters. The climatological data are always incomplete and also extremely sparse for some regions of the world. More accurate data will have to be derived from measurements made by satellite radiometers themselves, such as MODIS and LASA. The cost and manpower required are too great for making auxiliary measurements from the ground or aircraft, except during special experiments. Methods are being developed to measure the optical thickness and scattering phase function, and albedo of single scattering from satellite data (Slater, 1980; Fraser *et al.*, 1984; Fraser and Kaufman, 1985).

APPENDIX B: ATMOSPHERIC CORRECTIONS OVER OCEANS

The Coastal Zone Color Scanner (CZCS), a precursor of MODIS, utilizes an algorithm that corrects for the atmosphere and determines chlorophyll concentrations in ocean waters with little or no suspended sediment. This algorithm will, with some improvements, be used by MODIS. The Nimbus-7/CZCS is a scanning radiometer that views the ocean in six coregistered spectral bands, five in the visible and near infrared (443, 520, 550, 670, and 750 μm), and the sixth, a thermal infrared band (10.5 to 12.5 μm). The sensor has an active scan of 78° centered on nadir, and a field-of-view of 0.0495°, which, from a nominal height of 955 km, produces a ground resolution of 825 m at nadir. The satellite is in a sun-synchronous orbit with ascending node near local noon. The sensor is equipped with provision for tilting the scan plane ±20° from nadir in 2° increments along the satellite track, in order to minimize the influence of direct sunglint (the contribution to the sensor radiance from photons that were specularly reflected from the sea surface without interacting with the atmosphere).

The CZCS provides estimates of the near-surface concentration of phytoplankton pigments (defined to be chlorophyll-α and its associated phaeopigments) by measuring the spectral radiance backscattered out of the ocean (Gordon and Morel, 1983). This radiance scattered out of the ocean and reaching the top of the atmosphere comprises only a small portion of the total radiance measured at the sensor. In general the sensor radiance L_t at wavelength (λ) can be decomposed into $L_t(\lambda)$, the radiance due to photons that never penetrated the sea surface, and $t(\lambda)L_w(\lambda)$, the radiance due to photons that were backscattered out of the water (the water-leaving radiance) and diffusely transmitted to the top of the atmosphere, i.e.:

$$L_t(\lambda) = L_t(\lambda) + t(\lambda)L_w(\lambda).$$

All of the information relating to the oceanic constituents, such as the chlorophyll concentration, is contained in $L_w(\lambda)$, which is usually an order of magnitude smaller than $L_t(\lambda)$.

Schemes for extracting $L_w(\lambda)$ from $L_t(\lambda)$ are referred to as "atmospheric correction" algorithms. To facilitate the discussion of these, it is often more convenient to work with reflectance, rather than radiance. We define the reflectance according to:

$$\rho = \pi L/F_o\cos\theta_o,$$

where L is the radiance in the given viewing direction, F_o is the extraterrestrial solar irradiance, and θ_o is the solar zenith angle. With this normalization for L, ρ determined at the top of the atmosphere would be the albedo of the ocean-atmosphere system if L were independent of the viewing angle. (Note that this is just a normalization of the radiance to the extraterrestrial solar irradiance, and has no other significance.)

The CZCS signal is eight-bit digitized aboard the spacecraft. The reflectance corresponding to one digital count for the least-sensitive gain (1) and the most sensitive gain setting (4) is given in Table B.1. (The near infrared band at 750 nm has Landsat MSS sensitivity and is not used in oceanic studies except as a land/cloud discriminator.) In practice the gain is set based on the mean value of the solar zenith angle for a given set of scenes, i.e., for small zenith angles Gain 1 is used, and for very large angles Gain 4 is used. Thus, the red band (670 nm) saturates at an ocean-atmosphere reflectance about 0.06, i.e., 6 percent.

The correction algorithm as it is presently being used is most easily understood by considering only single scattering (Gordon *et al.*, 1983). In this approximation, ignoring direct sunglint and assuming that the sea surface is flat, the reflectance measured by the sensor $\rho_t(\lambda)$ can be divided into its components: $\rho_r(\lambda)$ the contribution arising from Rayleigh scattering; $\rho_a(\lambda)$ the contribution arising from aerosol scattering; and $t(\lambda)\rho_w(\lambda)$ the contribution from the water-leaving radiance diffusely transmitted to the top of the atmosphere; i.e.:

$$\rho_t(\lambda) = \rho_r(\lambda) + \rho_a(\lambda) + t(\lambda)\rho_w(\lambda). \qquad (1)$$

Typical values of ρ_r, ρ_a, and ρ_w are given in Table B.2.

The values of ρ_r and ρ_a correspond to points near the center of the scan (there is considerable limb brightening ρ_r), and the ρ_a values correspond to an aerosol optical thickness at 670 nm of about 0.1 (ρ_a varies considerably with the specific properties of the aerosol, e.g., for a given optical thickness it can vary by more than a factor of two depending on the aerosol model used in the computations). The values of ρ_w are given for both high and low pigment

Table B.1. Reflectance for One CZCS Digital Count

λ (nm)	Gain 1	Gain 4
443	0.00075	0.00036
520	0.00053	0.00025
520	0.00042	0.00020
670	0.00024	0.00011

Table B.2. Typical Values of ρ_r, ρ_a, and ρ_w

λ (nm)	ρ_r	ρ_a	ρ_w	
			C ≅ 0.03	C ≅ 1
443	0.10	0.015	0.035	0.0008
520	0.05	0.013	0.008	0.010
550	0.04	0.012	0.005	0.015
670	0.02	0.010	0.0001	0.002

C is the chlorophyll concentration in mg/m^3.

concentrations (this is the significant range of variation); however, there are water types (called Morel Case 2 waters) for the most part in coastal areas for which $\rho_w \approx 0.05$ to 0.07 and rather featureless for the spectral range $450 < \lambda < 600$ nm, and ≈ 0.01 near 670 nm. In most situations of interest, the pigment concentration is determined from the ratio of reflectances: $\rho_w(440)/\rho_w(550)$ at low chlorophyll concentrations; and $\rho_w(520)/\rho_w(550)$ for high pigment concentrations. There is no generally accepted method of extracting the pigment concentration from CZCS-measured $\rho_w(\lambda)$ for the Morel Case 2 waters mentioned above. Thus, the data in Table B.2 suggest that we need to extract ρ_w from ρ_t to within about 0.0001 in order to obtain a useful estimate of ρ_w, under most conditions for two of the three bands 443 nm, 520 nm, and 550 nm.

ρ_r and ρ_a in Equation 1 are given by

$$\rho_x = \frac{\omega_x(\lambda)\,\tau_x(\lambda)T(\lambda)p_x(\theta,\theta_o,\lambda)}{4\cos\theta\cos\theta_o} \qquad (2)$$

where

$$p_x(\theta,\theta_o,\lambda) = \{P_x(\theta_-,\lambda) + [\rho(\theta) + \rho(\theta_o)] \times P_x(\theta_+,\lambda)\}.$$

and $\cos\theta_\pm = \pm\cos\theta_o\cos\theta + \sin\theta_o \sin\theta \cos(\phi - \phi_o)$. θ_o and ϕ_o are, respectively, the solar zenith and azimuth angles, θ and ϕ are the zenith and azimuth angles of a vector from the point on the sea surface under examination (pixel) to the sensor. $\rho(\theta)$ is the Fresnel reflectance of the interface for an incident angle θ, $P_x(\theta,\lambda)$ is the scattering phase function of component x (x = r or a) at λ, $\omega_x(\lambda)$ the single-scattering albedo of x ($\omega_r = 1$), and $\tau_x(\lambda)$ the optical thickness of x. $T(\lambda)$ is the two-way transmittance through the ozone layer, i.e.,

$$T = \exp[-\tau_{oz}(1/\cos\theta + 1/\cos\theta_o)],$$

where τ_{oz} is the ozone optical thickness. The term involving θ_- in Equation 2 provides the contribution owing to photons that are backscattered from the atmosphere without interacting with the sea surface. The term involving θ_+ account for those photons that are scattered in the atmosphere toward the sea surface (sky radiance) and then specularly reflected from the surface into the field-of-view of the sensor ($\rho(\theta)$ term), as well as photons that are first specularly reflected from the sea surface and then scattered by the atmosphere into the field-of-view of the sensor ($\rho(\theta_o)$ term). If the assumption of a flat surface is relaxed, these terms involving ρ become integrals over solid angle of essentially the product of the reflectance, the phase function, and the surface-slope probability density function.

$t(\lambda)$ is the diffuse transmittance of the atmosphere between the sea surface and the sensor. It is given by:

$$t(\lambda) = \exp[-(\tau_r/2 + \tau_{oz})/\cos\theta]t_a(\lambda), \qquad (3)$$

where

$$t_a(\lambda) = \exp[-(1 - \omega_a(\lambda)F(\lambda))\,\tau_a(\lambda)/\cos\theta],$$

and F is the probability that a photon scattered by the aerosol will be scattered through an angle less than 90°. The upper limit to the factor $(1 - \omega_a(\lambda)F(\lambda))$ is about 1/6, so t_a depends only weakly on the aerosol optical thickness. The rationale for using the diffuse transmittance rather than the direct transmittance is to account for the fact that when the sensor is viewing a given pixel, some of the radiance it receives originates from neighboring pixels. The only unknowns in these equations (other than ρ_w) are ω_a, τ_a, and the aerosol scattering phase function.

Examinations of CZCS imagery in the red band over low chlorophyll waters ($\rho_w(670) \approx 0$) shows that the aerosol reflectance is dependent on position. This means that knowing the aerosol reflectance (or even the aerosol phase function and optical thickness) at one point in an image *does not* provide sufficient information to compute the aerosol reflectance everywhere in the image. This dependence of $\rho_a(\lambda)$ on position is believed to be due to variations in the aerosol optical thickness, implying that such variations must, at least implicitly, be taken into account in any atmospheric correction scheme.

From Equation 2 it is seen that:

$$\rho_a(\lambda_2)/\rho_a(\lambda_1) = \epsilon(\lambda_2,\lambda_1)\,[T(\lambda_2)/T(\lambda_1)], \qquad (4)$$

where

$$\epsilon(\lambda_2,\lambda_1) = \frac{\omega_a(\lambda_2)\tau_a(\lambda_2)p_a(\theta,\theta_o,\lambda_2)}{\omega_a(\lambda_1)\tau_a(\lambda_1)p_a(\theta,\theta_o,\lambda_1)} \qquad (5)$$

The quantity of $\epsilon(\lambda_2,\lambda_1)$ is of central importance in the atmospheric correction procedure, because for a given aerosol type, defined here to be a given refractive index and normalized particle size distribution, $\epsilon(\lambda_2,\lambda_1)$ is independent of the aerosol concentration. To the extent that variations in $\rho_a(\lambda)$ are due only to variations in aerosol concentration (or optical thickness), $\epsilon(\lambda_2,\lambda_1)$ will be nearly independent of position within an image.

Equations 1 and 2 are rigorously correct in the limit that the slant paths $\tau_r/\cos\theta$, $\tau_r/\cos/\theta_o$, $\tau_a/\cos\theta$, and $\tau_a/\cos\theta_o$ all approach zero. Although Equation 2 provides a poor estimate of $\rho_a(\lambda)$ for values of $\tau_a(\lambda)$ where multiple scattering becomes important, multiple scattering computations show that Equation 1 is still approximately valid even for large optical thicknesses, as long as the radiometer is viewing the ocean sufficiently far from the center of the glitter pattern (Gordon *et al.*, 1983), a condition normally ensured by the glint-avoidance procedure on the CZCS. Deschamps *et al.* (1983) have derived a correction to Equation 1 which significantly increases the accuracy; however, the simpler Equation 1 is sufficient for the CZCS. Also, in this case the $\epsilon(\lambda_2,\lambda_1)$ value given by Equation 5 is only an approximation and multiple scattering introduces a weak dependence of $\epsilon(\lambda_2,\lambda_1)$ on concentration (Gordon *et al.*, 1983).

In what follows, it is assumed that $\epsilon(\lambda_2,\lambda_1)$ is constant* even in the presence of a horizontally inhomogeneous aerosol. This is equivalent to assuming a constant aerosol type. Combining Equations 1 and 5 we have:

$$t(\lambda_i)\,\rho_w(\lambda_i) = \rho_t(\lambda_i) - \rho_r(\lambda_i) - S(\lambda_i,\lambda_4)\,[\rho_t(\lambda_4) - \rho_r(\lambda_4) - t(\lambda_4)\,\rho_w(\lambda_4)]; \quad (6)$$

for i = 1, 2, and 3, where the indices i = 1, 2, 3, and 4 refer to the four visible CZCS bands in order of increasing wavelength, and

$$S(\lambda_i,\lambda_4) = \epsilon(\lambda,\lambda_4)\,\frac{T(\lambda_i)}{T(\lambda_4)}.$$

Equations 6 are 3 in number but there appear to be 11 unknowns, $t(\lambda_i)$ for i = 1 to 4, $S(\lambda_i,\lambda_4)$ for i = 1 to 3, and $\rho_w(\lambda_i)$ for i = 1 to 4. However, for a given aerosol type the three $S(\lambda_i,\lambda_4)$'s can be determined everywhere once they are determined at one position in the image, reducing the number of unknowns to eight. Also, $t(\lambda_i)$ is unknown only because the aerosol optical thickness is required for the computation of $t_a(\lambda_i)$. In most cases of practical interest, $t_a(\lambda_i)$ can be set to unity because the entire algorithm will break down for other reasons before τ_a becomes large enough to influence significantly the results through its effect on $t_a(\lambda_i)$. Thus, $t(\lambda_i)$ can be taken to be known, and there are in fact only four unknowns in the three Equations 6. To close the system and enable a solution, an additional equation must be included. Smith and Wilson (1981) use an empirical equation of the form

$$f(\rho_w(\lambda_1),\,\rho_w(\lambda_3),\,\rho_w(\lambda_4)) = 0, \quad (7a)$$

while Gordon *et al.* (1983) used

$$t(\lambda_4)\,\rho_w(\lambda_4) = 0 \quad (7b)$$

which can be shown to be satisfactory for pigment concentrations $\lesssim 1$ mg/m^3. The key to effecting a solution to Equations 6 and 7 is the determination of $\epsilon(\lambda_i,\lambda_4)$, which provides $S(\lambda_i,\lambda_4)$.

In the initial application of this algorithm to CZCS imagery (Gordon *et al.*, 1980), the $S(\lambda_i,\lambda_4)$ were determined from ship measurements of $\rho_w(\lambda)$ at a single location in the image. This reliance on surface measurements was, however, unsatisfying, and a technique was sought that would enable determination of $S(\lambda_i,\lambda_4)$ from satellite measurements alone. The concept of clear water reflectance (CWR) provides the basis for such a determination. Gordon and Clark (1981) have shown that for phytoplankton pigment concentrations (C) less than about 0.25 mg/m^3 the reflectance corresponding to the water-leaving radiance in the green, yellow, and red CZCS bands can be written:

$$\rho_w(\lambda) = [\rho_w(\lambda)]_N \cos\theta_o \times \exp\,[-(\tau_r/2 + \tau_{oz})/\cos\theta_o]; \quad (8)$$

where $[\rho_w]_N$, the reflectance corresponding to the normalized water-leaving radiance is 0.0084, 0.0051, and less than 0.0001 for 520, 550, and 670 nm, respectively. Thus, if a region of image for which C < 0.25 mg/m^3 can be located, equations 6 and 8 can be used to determine $\epsilon(520,670)$, $\epsilon(550,670)$, and $\epsilon(670,670)$. $\epsilon(443,670)$ can then be estimated by extrapolation, since the model calculations below show that $\epsilon(\lambda_i,\lambda_4)$ is a smooth function of λ_i. To automate this procedure, it is assumed for convenience that:

$$\epsilon(\lambda_i,\lambda_4) = (\lambda_i/\lambda_4)\,n(\lambda_i) \quad (9)$$

and then $\epsilon(\lambda_i,\lambda_4)$ is determined from:

$$n(\lambda_i) = [n(\lambda_2) + n(\lambda 3)]/2. \quad (10)$$

An important aspect of this algorithm is that no surface measurements of either $\rho_w(\lambda)$ or any properties of the aerosol are required to affect the atmospheric corection with this scheme.

*The assumption that $\epsilon(\lambda_2,\lambda_1)$ is independent of position is required for the CZCS only because there are too few spectral bands available to enable determination of ϵ at each pixel. For newly proposed sensors, e.g., the Ocean Color Imager (OCI) and MODIS, additional spectral bands in the near infrared will facilitate this determination and the constant ϵ assumption will not be needed.

APPENDIX C: MODIS INSTRUMENT PANEL STATEMENT OF WORK

1. Clarify and refine the science and measurement objectives outlined in the Science and Mission Requirements Working Group Report for the Moderate-Resolution Imaging Spectrometer (MODIS).
2. Specify detailed observational requirements.
3. Define characteristics of a candidate instrument and alternative approaches including:
   (a) typical observing scenarios
   (b) operating characteristics and requirements
   (c) data acquisition, processing, and interpretation strategies
   (d) refined definition of spectral bands, resolutions, and sensitivities
   (e) requirements for correlative data for image correction, calibration, and interpretation
   (f) appropriate use of array detector technology and selectable spectral bands
   (g) onboard processing opportunities and requirements
   (h) strategy for on-orbit servicing
   (i) determination of which instrument functions can be integrated into a common optical train versus which require separate hardware implementation
4. Coordinate with ongoing studies and development of related instruments.
5. Make recommendations to the Earth Science and Applications Division/NASA Headquarters and to the Eos Project on the feasibility, development timing, limiting technologies, and possible follow-on definition and development activities of this instrument.
6. Produce an interim oral report in October 1984 and a written study report by March 1985.

REFERENCES

Abbott, M.R., and P.M. Zion, Satellite observations of phytoplankton variability during an upwelling event, *Cont. Shelf. Res.*, *4*, 661, 1985.

Abbott, M.R., T.M. Powell, and P.J. Richardson, The relationship of environmental variability to the spatial patterns of phytoplankton biomass in Lake Tahoe, *J. Plankton Res.*, *4*, 927, 1982.

Abrams, M.J., J. Conel, and H. Lang, The joint NASA/Geosat test case study: Final report, *AAPG Special Publication*, in press, 1985.

Barker, J.L., (Ed.), LANDSAT-4 science characterization early results, *NASA Conference Publication 2355*, 3, 1985.

Bennett, A.F., and K.L. Denman, Phytoplankton patchiness: Interferences from particle statistics, *J Mar. Res.*, *43*, 307, 1985.

Bernstein, R., Report on the Toga Workshop on sea surface temperature and net surface radiation, 71 pp., ICSU/WMO, 1984.

Brown, O.B., R.H. Evans, J.W. Brown, H.R. Gordon, R.C. Smith, and K.S. Baker, Phytoplankton blooming off the U.S. east coast: A satellite description, *Science*, *229*, 163, 1985.

Butler, D.M., *et al.*, Earth Observing System: Science and Mission Requirements Working Group Report, *NASA TM 86129*, 1984.

Campbell, J.W., and W.E. Esaias, Spatial patterns in temperature and chlorophyll on Nantucket Shoals, from airborne remote sensing data, May 7-9, 1981, *J. Mar. Res.*, *43*, 139, 1985.

Chahine, M.T., N.L. Evans, V. Gilbert, and R.D. Haskins, Requirements for a passive IR advanced moisture and temperature sounder, *Appl. Opt.*, *23*, 979, 1984.

Chang, S.H., and W. Collins, Confirmation of the airborne biogeophysical mineral exploration technique using laboratory methods, *Econ. Geol.*, *78*, 723, 1983.

Charney, J.G., W.G. Quirk, C.S. Hsien, and J. Kornfield, A comparative study of albedo change on drought in semi-arid regions, *J. Atmos. Sci.*, *34*, 1366, 1977.

Colwell, R.N., (Ed.), Spectral transmissivity of clouds of various thickness, in *Manual of Remote Sensing*, 2nd ed., Figure 5-30, American Society of Photogrammetry, Falls Church, VA, 1983.

Courel, M., Etude de l'evolution recente des milieux saheliens a' paitio des mesures fouries pou les satellites, published Ph.D. Thesis, University of Paris, 1985.

Cox, S.C., (Ed.), The multispectral imaging science working group: Final Report, *NASA Conference Publication 2260*, 3.20, 1983.

Curran, R.J., Proposal for a cloud climatology and radiation budget experiment for Space Lab-2, 53 pp., Submitted to the Office of Planning and Program Integration, December 1976.

Curran, R.J., The cloud radiation experiment as the climate related component of a GLAS aircraft cloud-top experiment, 40 pp., NASA Proposal submitted to the Office of Space Science and Applications, June 1982.

Denman, K.L., Predictability of the marine planktonic ecosystem, in *The Predictability of Fluid Motions*, edited by G. Holloway and B.J. West, p. 601, American Institute of Physics, NY, 1983.

Denman, K.L., Covariability of chlorophyll and temperature in the sea, *Deep Sea Res.*, *23*, 539, 1976.

Denman, K.L., and T.M. Powell, Effects of physical processes on planktonic ecosystems in the coastal ocean, *Oceanogr. Mar. Biol. Ann. Rev.*, *22*, 125, 1984.

Deschamps, P.Y., M. Herman, and D. Tanre, Modeling of the atmospheric effects and its application to the remote sensing of ocean color, *Appl. Opt.*, *22*, 3751, 1983.

DeVooys, C.G.N., Primary production in aquatic environments, in *Scope 13, The Global Carbon Cycle*, edited by B. Bolin, E.T. Degans, S.S. Kempe, and P. Ketner, p. 259, J. Wiley, 1979.

Eppley, R.W., E. Stewart, M.R. Abbott, and U. Heyman, Estimating ocean primary production from satellite chlorophyll: Introduction to regional differences and statistics for the Southern California bight, *J. Plankton Res.*, *7*, 57, 1985.

Eppley, R.W., Estimating phytoplankton growth rates in the Central Oligotrophic Oceans, in *Primary Productivity in the Sea*, edited by P.G. Falkowski, p. 213, Plenum Press, NY, 1980.

Eppley, R.W., and B.J. Peterson, Particulate organic matter flux and planktonic new production in the deep ocean, *Nature, 282*, 677, 1979.

Esaias, W.E., Remote sensing of oceanic phytoplankton: Present capabilities and future goals, in *Primary Productivity in the Sea*, edited by P.J. Falkowski, p. 321, Plenum Press, NY, 1980.

Fraser, R.S., and Y.J. Kaufman, The relative importance of aerosol scattering and absorption in remote sensing, *IEEE Trans. Geosci. Remote Sens., GE-23*, 625, 1985.

Fraser, R.S., Y.J. Kaufman, and R.L. Mahoney, Satellite measurements of aerosol mass and transport, *Atmos. Environ., 18*, 2577, 1984.

Fung, I.Y., C.J. Tucker, and K.C. Prentice, Applications of AVHRR vegetation index to study atmosphere-troposphere exchange and CO_2, *J. Geophys. Res.*, in press, 1986.

Gatlin, J.A., R.J. Sullivan, and C.J. Tucker, Considerations of and improvements to large-scale vegetation monitoring, *IEEE Trans. Geosci. Remote Sens., GE-22*, 496, November 1984.

Goetz, A.F.H., B.N. Rock, and L.C. Rowan, Remote sensing for exploration: An overview, *Econ. Geol., 78*, 573, 1983.

Gordon, H.R., D.K. Clark, J.L. Mueller, and W.A. Hovis, Phytoplankton pigments from the Nimbus-7 coastal zone color scanner: Comparisons with surface measurements, *Science, 210*, 63, 1980.

Gordon, H.R., and D.K. Clark, Clear water radiances for atmospheric correction of coastal zone color scanner imagery, *Appl. Opt., 20*, 299, 1981.

Gordon, H.R., D.K. Clark, J.W. Brown, O.B. Brown, R.H. Evans, and W.W. Broenkow, Phytoplankton pigment concentrations in the Middle Atlantic bight: Comparison of ship determinations and CZCS estimates, *Appl. Opt., 22*, 20, 1983.

Gordon, H.R., and A.Y. Morel, *Remote Assessment of Ocean Color for Interpretation of Satellite Visible Imagery: A Review*, 114 pp., Springer-Verlag, NY, 1983.

Goward, S.N., D.G. Dye, and C.J. Tucker, North American vegetation patterns observed by NOAA-7 AVHRR, *Vegetation*, in press, 1985.

Griggs, M., and L.L. Stowe, Measurements of aerosol optical parameters from satellites, in *Proceedings of the International Radiation Symposium*, Perugia, Italy, August 21-28, 1984.

Gurney, R.J., J.P. Ormsby, and D.K. Hall, A comparison of remotely-sensed surface temperature and biomass estimates for aiding evapotranspiration determination in Central Alaska, in *Proceedings of the Permafrost: Fourth International Conference*, 1983.

Halem, M., and J. Susskind, Findings of a joint NOAA/NASA sounder comparison: (1) AMTS vs. HIRS-2, (2) physical vs. statistical retrievals, in *Advances in Remote Sensing Methods*, A. Deepak, publisher, in press, 1984.

Hansen, J., D. Johnson, and A. Lacis, Climate impact of increasing atmospheric carbon dioxide, *Science, 231*, 957, 1981.

Harries, J.E., D.T. Llwellyn-Jones, P.J. Minnett, R.W. Saunders, and A.M. Zavody, Observations of sea surface temperature for climate research, *Phil. Royal Soc. London, A309*, 381, 1983.

Harris, G.P., Temporal and spatial scales in phytoplankton ecology: Mechanisms, methods, models, and management, *Can. J. Fish. Aquat. Sci., 37*, 877, 1980.

Hayes, L., The current use of TIROS-N series of meteorological satellites for land cover studies, *Int. J. Remote Sens., 6*, 35, 1985.

Hayward, T.L., and E.L. Venrick, Relationship between surface chlorophyll, integrated chlorophyll and integrated primary production, *Mar. Biol., 69*, 247, 1982.

Heimburg, K.F., L.H. Allen, and W.C. Huber, Evapotranspiration estimates based on surface temperature and net radiation: Development of remote sensing methods, *Florida Water Resour. Res. Ctr., 66*, University of FL, Gainesville, FL, 1982.

Holligan, P.M., M. Viollier, D.S. Harbour, P. Camus, and M. Champagne-Phillipe, Satellite and ship studies of coccolithophore production along a continental shelf edge, *Nature, 304*, 339, 1983.

Hovis, W.A., The Nimbus-7 coastal zone color scanner (CZCS) program, in *Oceanography From Space*, edited by J.F.R. Gower, p. 213, Plenum Press, NY, 1981.

Huck, F.O., R.E. Davis, C.L. Fales, R.M. Aherron, R.F. Ardvini, and R.W. Samms, Study of remote sensor spectral responses and data processing algorithms for feature classification, *Opt. Eng., 23*, 650, 1984.

Huyer, A., Coastal upwelling in the California current system, *Prog. in Oceanogr., 12*, 259, 1983.

ICSU/WMO/IOC, Large-scale experiments in the WCRP, Volume 1, 121 pp., *WCRP Publ. Series No. 1*, WMO, Geneva, Switzerland, 1983.

Justice, C.O., J.P. Malingreau, and J.U. Hielkema, The application of satellite remote sensing techniques for monitoring natural vegetation, crops and rainfall, in *Proceedings of the Workshop on Early Warning Systems in Asia and the Pacific Region*, UN/FAO, Rome, 1984.

Justice, C.O., J.R.G. Townshend, B.N. Holben, and C.J. Tucker, Analysis of the phenology of global vegetation using meteorological satellite data, *Int. J. Remote Sens.*, in press, 1985.

Kaufman, Y.J., Atmospheric effects on remote sensing of surface reflectance, *Soc. Phot.-Opt. Instru. Eng.*, *475*, 20, 1984.

Kidwell, K.B., NOAA polar orbital data users guide (TIROS-N, NOAA-6, 7, 8), NOAA National Climate Center, 2-5, Washington, DC, 1984.

Kiefer, D.A., Fluorescence properties of natural phytoplankton populations, *Mar. Biol.*, *22*, 263, 1973.

Kneizys, F.X., E.P. Shettle, W.O. Gallery, J.H. Chetwynd, Jr., L.W. Abreu, J.E.A. Selby, S.A. Clough, and R.W. Fenn, Atmospheric transmittance/radiance: Computer code LOWTRAN 6, *AFGL-TR-8-3-0187*, 200 pp., AFGL, Hanscom AFB, MA, 1983.

Koblentz-Mishke, O.J., V.V. Volkovinsky, and J.G. Kabanova, Plankton primary production of the world ocean, in *Scientific Exploration of the Southern Pacific*, edited by W.S. Wooster, p. 183, National Academy of Sciences, 1970.

Labovitz, M.L., E.J. Masuoka, R. Bell, A.W. Siegrist, and R.F. Nelson, The application of remote sensing to geobotanical exploration for metal sulfides, *Econ. Geol.*, *78*, 750, 1983.

Lambeck, R.F., Signature extension preprocessing for Landsat MSS data, 74 pp., Environmental Research Institute of Michigan, Ann Arbor, MI, 1977.

Laurs, R.M., P.C. Fiedler, and D.R. Montgomery, Albacore tuna catch distributions relative to environmental features observed from satellites, *Deep Sea Res.*, *31*, 1085, 1984.

Lenoble, J., Standard procedures to compute atmospheric radiative transfer in scattering atmosphere, 125 pp., NCAR, Boulder, CO, 1977.

Mackas, D.L., K.L. Denman, and M.R. Abbott, Plankton patchiness: Biology in the physical vernacular, *Bull. Mar. Sci.*, *37*, 652, 1985.

Malingreau, J.P., G. Stevens, and L. Fellows, Remote sensing of forest fires: Kalimantan and North Borneo in 1982-83, *Ambio*, *14*, 314, 1985.

Matson, M., S.R. Schneider, B. Aldridge, and B. Satchwell, Fire detection using the NOAA series of satellites, *NOAA/NESDIS TR 7*, Washington, DC, 1984.

McCarthy, J.J., Measuring oceanic primary productivity, in *Proceedings of a Global Ocean Flux Study*, p. 151, National Academic Press, Washington, DC, 1984.

McClatchey, R.A., R.W. Fenn, J.E.A. Selby, F.E. Volz, and J.S. Garing, Optical properties of the atmosphere, 85 pp., *AFCRL-7102-79*, AFCRL, Hanscom AFB, MA, 1971.

McElroy, J.H., and S.R. Schneider, Utilization of NASA's space station program for operational Earth observations, *NOAA/NESDIS TR 12*, Washington, DC, 1984.

Mintz, Y., J. Susskind, J. Dorman, and G. Walker, Global fields of transpiration and soil moisture as derived from TIROS-N satellite measurements, in preparation, 1985.

Mitchell, G., and D.A. Kiefer, Determination of absorption and fluorescence excitation spectra for phytoplankton, in *Marine Phytoplankton and Productivity*, edited by O. Holm-Hansen, L. Bolis, and R. Gilles, p. 157, Springer-Verlag, 1984.

Morel, A., and L. Prieur, Analysis of variations in ocean color, *Limnol. and Oceangr.*, *22*, 709, 1977.

National Academy of Sciences (NAS), *Global tropospheric chemistry: A plan for action*, p. 3-49, National Academic Press, 1984.

National Academy of Sciences (NAS), Global ocean flux study: in *Proceedings of a Workshop*, 360 pp., National Academic Press, 1984.

National Oceanic and Atmospheric Administration (NOAA), *Global Vegetation Index Users Guide*, SDSD/NESDIS, 27 pp., National Climate Data Center, Washington, DC, 1986.

Norwine, J., and D.H. Greegor, Vegetation classification based on AVHRR satellite imagery, *Remote Sens. Environ.*, *13*, 69, 1983.

O'Reilly, J.E., and D.A. Busch, Phytoplankton primary production on the northwestern shelf, *Rapp. P.-V. Reun. Cons. Perm. Int. Explor. Mer., 183*, 255, 1984.

Otterman, J., Satellite and field studies of man's impact on the surface in arid regions, *Tellus, 33*, 68, 1981.

Peterson, D.L., J.G. Lawless, P. Matson, J.D. Aber, P. Vitousek, and S. Running, Biogeochemical cycling in terrestrial ecosystems, in *Proceedings of the 36th Congress of the IAF*, Stockholm, Sweden, 1985.

Platt, T., and A.W. Herman, Remote sensing of phytoplankton in the sea: Surface-layer chlorophyll as an estimate of water-column chlorophyll and primary production, *Int. J. Remote Sens., 4*, 343, 1983.

Platt, T., and D.V. Subba Rao, Primary production of marine microphytes, in *Photosynthesis and Productivity in Different Environments*, International Biological Programme 3, edited by J.P. Cooper, p. 249, Cambridge University Press, 1975.

Richards, F., and P. Arkin, On the relationship between satellite derived cloud cover and precipitation, *Mon. Wea. Rev., 109*, 1081, 1981.

Richardson, A.J., J.H. Everitt, and H.W. Gausssman, Radiometric estimation of biomass and nitrogen content of alicia grass, *Remote Sens. of Environ., 13*, 179, 1983.

Rock, B.N., Mapping of deciduous forest cover using simulated Landsat DTM data, *International Geoscience Remote Sensing in Proceedings of the Symposium*, 5, 3.1, 1982.

Rock, B.N., and J.E. Vogelmann, Stress assessment and spectral characterization of suspected acid deposition damage in red spruce (Picea rubens) from Vermont, *Amer. Soc. Photogrammetry Tech. Prog.*, 1985a.

Rock, B.N., Remote detection of geobotanical anomalies associated with hydrocarbon microseepage using Thematic Mapper Simulator (TMS) and Airborne Imaging Spectrometer (AIS) data, in *Remote Sensing for Geologic Mapping, 18*, edited by Teleki and Weber, p. 299, International Union of Geological Sciences, 1985b.

Running, S.W., Microclimate control of forest productivity: Analysis by computer simulation of transpiration photosynthesis balance in different environments, *Agric. and Forest Meteor., 32*, 267, 1984.

Running, S.W., D.L. Peterson, M.A. Spanner, and K.B. Teuber, Remote sensing of coniferous forest leaf area, *Ecology*, in press, 1985.

Ryther, J.H., Photosynthesis and fish production in the sea, *Science, 166*, 72, 1969.

Schneider, S.R., S.R. McGinnis, Jr., and J.A. Gatlin, Use of NOAA/AVHRR visible and near-infrared data for land remote sensing, 48 pp., *NOAA TR NESS 84*, Washington, DC, 1981.

Schowengerdt, R.A., and P.N. Slater, MRS literature survey of atmospheric corrections, 52 pp., *NAS5-25606*, NASA/GSFC, Greenbelt, MD, 1979.

Schwalb, A., The TIROS-N/NOAA-A to G satellite series, 73 pp., *NOAA TM NESS 95*, Washington, DC, 1982.

Sekera, Z., Polarization of Skylight, in *Handbuch der Physik, 48*, p. 288, 1957.

Shafer, O., Simple infrared telescope with stray-light rejection, *SPIE, 304*, 171, 1981.

Shettle, E.P., and R.W. Fenn, Models for the aerosols of the lower atmosphere and the effects of humidity variations on their optical properties, 94 pp., *AFGL-TR-79-0214*, AFGL, Hanscom AFB, MA, 1979.

Slater, P.N., MRS "Proof-of-Concept" on atmospheric corrections using an orbitable, pointable imaging system, 80 pp., *NAS5-25606-TR-1653*, NASA/GSFC, Greenbelt, MD, 1980.

Smith, R.C., and W.H. Wilson, Bio-optical research in the southern California bight, in *Oceanography from Space*, edited by J.F.R. Gower, p. 281, Plenum Press, NY, 1981.

Smith, R.C., R.W. Eppley, and K.S. Baker, Correlation of primary production as measured aboard ship in southern California coastal waters and as estimated from satellite chlorophyll images, *Mar. Biol., 66*, 281, 1982.

Soer, G.J.R., Estimation of regional evapotranspiration and soil moisture conditions using remotely-sensed crop surface temperatures, *Remote Sens. Environ., 9*, 27, 1980.

Spanner, M.A., K.W. Tuber, W. Ecevedo, S.W. Running, D.L. Peterson, D.H. Card, and D.A. Mouat, Remote sensing of the leaf area index of temperate coniferous forests, in *Proceedings of the 10th International Symposium on Machine Processing of Remotely-Sensed Data*, p. 362, Purdue University, Lafayette, IN, 1984.

Spencer, R.W., D.W. Martin, B.B. Hinton, and J.A. Weinman, Satellite microwave radiances correlated with radar rain rates over land, *Nature*, *4*, 141, 1983.

Steele, J.H., (Ed.), *Spatial Pattern in Plankton Communities*, 470 pp., Plenum Press, NY, 1978.

Steeman-Nielsen, E., The use of radioactive carbon (C^{14}) for measuring organic production in the sea, *J. du Cons.*, *18*, 117, 1952.

Stull, R.B., and E.W. Eloranta, Boundary layer experiment-1983, *Bull. Amer. Meteor. Soc.*, *65*, 450, 1984.

Susskind, J.J., J. Rosenfield, D. Reuter, and M.T. Chahine, Remote sensing of weather and climate parameters from HIRS-2/MSU on TIROS-N, *J. Geophys. Res.*, *89D*, 4677, 1984.

Tarpley, J.D., S.R. Schneider, and R.L. Money, Global vegetation indices from NOAA-7 meteorological satellite, *J. Climate Appl. Meteor.*, *23*, 491, 1984.

Townshend, J.R.G., and C.J. Tucker, Objective assessment of AVHRR data for land cover mapping, *Int. J. Remote Sens.*, *5*, 492, 1984.

Tucker, C.J., C. Vanpraet, E. Boerwinkle, and A. Gaston, Satellite remote sensing of total dry matter accumulation in the Senegalese Sahel, *Remote Sens. Environ.*, *13*, 461, 1983.

Tucker, C.J., B.N. Holben, and T.E. Goff, Intensive forest clearing in Rondonia, Brazil as detected by satellite remote sensing, *Remote Sens. Environ.*, *15*, 255, 1984a.

Tucker, C.J., J.A. Gatlin, and S.R. Schneider, Monitoring vegetation in the Nile Delta with NOAA-6 and NOAA-7 AVHRR, *Photogram. Eng. Remote Sens.*, *50*, 53, 1984b.

Tucker, C.J., J.R.G. Townshend, and T.E. Goff, African land cover classification using satellite data, *Science*, *227*, 110, 1985a.

Tucker, C.J., J.U. Hielkema, and J. Roffey, Satellite remote sensing monitoring in desert locust breeding areas, *Int. J. Remote Sens.*, *6*, 127, 1985b.

Tucker, C.J., Remote sensing of leaf water content in the near infrared, *Remote Sens. of Environ.*, *10*, 23, 1980.

Turco, R.P., O.B. Toon, T.P. Ackerman, J.B. Pollack, and C. Sagan, Nuclear winter: Global consequences of multiple nuclear explosions, *Science*, *222*, 1283, 1983.

Waring, R. H., Estimating forest growth and efficiency in relation to canopy leaf area, *Adv. Ecol. Res.*, *13*, 327, 1983.

Woods, J.D., Satellite monitoring of the ocean for global climate research, *Phil. Trans. of the Royal Soc. London, A-309*, 337, 1983.

Wolfe, W.L., and G.J. Zissis, (Eds.), Calculated change in bulk reflectance of ocean water with increasing concentration of phytoplankton, in *The Infrared Handbook*, Figure 3-124, Environmental Research Institute of Michigan, Ann Arbor, MI, 1978.